UNIVERSIDADE FEDERAL DO RIO GRANDE DO SUL

CENTRO DE BIOTECNOLOGIA

PROGRAMA DE PÓS-GRADUAÇÃO EM BIOLOGIA CELULAR E MOLECULAR

EXPRESSÃO DE *BMI1* E ATIVAÇÃO DE ERK COLABORAM NA MANUTENÇÃO DO FENÓTIPO INDIFERENCIADO EM CÉLULAS DE MEDULOBLASTOMA

Mariane da Cunha Jaeger

Novembro de 2018.

UNIVERSIDADE FEDERAL DO RIO GRANDE DO SUL

CENTRO DE BIOTECNOLOGIA

PROGRAMA DE PÓS-GRADUAÇÃO EM BIOLOGIA CELULAR E MOLECULAR

EXPRESSÃO DE *BMI1* E ATIVAÇÃO DE ERK COLABORAM NA MANUTENÇÃO DO FENÓTIPO INDIFERENCIADO EM CÉLULAS DE MEDULOBLASTOMA

Mariane da Cunha Jaeger

Tese submetida ao Programa de Pós-Graduação em Biologia Celular e Molecular da Universidade Federal do Rio Grande do Sul como requisito parcial para a obtenção do grau de Doutor em Ciências.

Orientador: Rafael Roesler

Novembro de 2018.

INSTITUIÇÕES E FONTES FINANCIADORAS

Este trabalho foi desenvolvido no Laboratório de Câncer e Neurobiologia do Centro de Pesquisa Experimental do Hospital de Clínicas de Porto Alegre, sob orientação do Dr. Rafael Roesler e no Instituto Blizard da *Barts and London School of Medicine and Dentistry* da Universidade *Queen Mary University of London*, sob supervisão da Dra. Silvia Marino.

A aluna recebeu bolsa de doutorado do Conselho Nacional de Desenvolvimento Científico e Tecnológico (CNPq) e bolsa de doutorado sanduíche da Coordenação de Aperfeiçoamento de Pessoal de Nível Superior (CAPES; Código de Financiamento 001).

O trabalho recebeu financiamento do Conselho Nacional de Desenvolvimento Científico e Tecnológico (CNPq; processo 409287/2016-4 para Rafael Roesler), do Instituto do Câncer Infantil (ICI), do PRONON/Ministério da Saúde (Processo 25000.162.034/2014-21), e do Fundo de Incentivo a Pesquisa do Hospital de Clínicas de Porto Alegre (FIPE/HCPA).

“Todas as vitórias ocultam uma abdicação.”

Simone de Beauvoir

AGRADECIMENTOS

Aos que fizeram a jornada possível: Prof. Rafael Roesler por me aceitar como aluna e aos Colegas de laboratório pelo convívio quase diário;

Aos que fizeram a jornada me fortalecer: Profa Silvia Marino, por me ensinar a reconhecer meu trabalho; Xinyu por me ajudar a aprimorar meus conhecimentos e as amigas Loredana e Barbara por serem exemplos de força.

Aos que trilharam parte da jornada comigo: Henrique, Tiarlos e Marília, pelos momentos de descontração, pelas risadas, pelos papos sérios (ou não), mas, principalmente, pela companhia quando tudo familiar estava longe.

Aos que me aconselharam e ajudaram durante a jornada: Carol B. de Farias e Carolina Nor, por toda a parceria dentro e fora do laboratório; Everaldo, por todas as conversas durante meu intervalo para o chá; e Meg, por todo apoio e conhecimento compartilhado.

Aos que me motivaram durante a jornada: Eduarda Ghisleni, Sophia Andreola, Marco A. e Paula Cardoso, por me recordarem sempre o motivo da jornada; e a Clévia e a Juliana, por me permitirem participar de suas jornadas.

Aos que estiveram comigo desde os primeiros passos da jornada: Carla, Daniel, Andressa, Káren, Cícero, Susana e Marina, pela amizade, que começou nos anos de Biomed mas ja é para a VIDA (sempre meus VIPs).

Aos que renovaram minhas energias durante minha jornada: Isabela e Henrique, por serem meus pedacinhos de felicidade.

E principalmente para aqueles que independente da jornada estão sempre comigo: Eliane, Marco, Caroline, Carine e Marcele por sempre me apoiarem, me motivarem a ser melhor e, principalmente, por serem exemplos incríveis.

A todos vocês que contribuíram para a realização dessa tese, meu MUITO OBRIGADA!

ÍNDICE

INTRODUÇÃO.....**10**

1.1MEDULOBLASTOMA……..10

1.2 EPIGENÉTICA E O CÓDIGO DE HISTONAS……...14

1.3 CÉLULAS TRONCO TUMORAIS……...21

1.4 BMI1……..24

1.5 SINALIZAÇÃO DE ERK EM MB……...26

1.6 HIPÓTESE GERAL……...27

1.7 OBJETIVOS……...28

CAPÍTULO I – HDAC and ERK inhibitors cooperate to reduce viability and stemness phenotype in medulloblastoma cells.....**29**

CAPÍTULO I – Resultados adicionais.....**60**

CAPÍTULO II – Convergence of BMI1 and CHD7 on ERK signalling in medulloblastoma.....**64**

CAPÍTULO II – Resultados adicionais.....**79**

DISCUSSÃO GERAL.....**84**

CONCLUSÃO.....**86**

REFERÊNCIAS.....**87**

Lista de Abreviaturas

ABC – do inglês *ATP-binding cassete*

BMI1 – do inglês *B-lymphoma Moloney murine leukemia virus insertion region-1*

CHD7 – do inglês *Chromodomain helicase DNA binding gene 7*

CSC – do inglês *Cancer stem cells* (células tronco tumorais)

EMT – do inglês *Epithelial-to-mesenchymal transition* (transição epitélio-mesenquima)

ERK – do inglês *Extracellular signal–regulated kinases*

HAT – Histona acetil-transferase

HDAC – Histona deacetilase

MB – Meduloblastoma

NaB – do inglês *sodium butyrate* (butirato de sódio)

PTM – do inglês *post-translational modification* (modificações pós-tradução)

SAHA – do inglês *Suberoylanilide hydroxamic acid* (ácido hidroxâmico suberoilanilida)

SCID – do inglês *Severe combined immunodeficient* (imunodeficiência severa combinada)

SNC – Sistema nervoso central

WNT – Wingless

SHH – Sonic hedgehog

Lista de Figuras

Figura 1. Subgrupos moleculares de meduloblastoma.....**12**

Figura 2. Código de histonas.....**16**

Figura 3. Acetilação de histonas.....**18**

Figura 4. Inibidores de histona deacetilases.....**19**

Figura 5. Modelo de células tronco tumorais.....**23**

Resumo

Meduloblastoma (MB), um tumor cerebral prevalentemente infantil, compreende um grupo de tumores com diferentes subtipos moleculares e prognósticos. Esses tumores apresentam alterações em vias de sinalização importantes para o desenvolvimento do cerebelo. Recentemente, estudos genômicos mostraram a importância de fatores epigenéticos para a formação e manutenção de MB. Esses fatores, que regulam processos associados a pluripotência, contribuem para a indução de um fenótipo mais indiferenciado e mais agressivo. Essas células indiferenciadas, as células tronco tumorais (CSC), são identificadas por marcadores como *CD133*, pela capacidade de formar esferas não aderentes em culturas livres de soro fetal bovino e pela tumorigenicidade. CSC participam nos processos iniciais do tumor, na progressão, na metástase e na recidiva tumoral. Muitos desses processos podem ser explicados pelo fenótipo indiferenciado, ou seja, pela modulação de mecanismos associados a células tronco normais. A ativação de ERK, por exemplo, importante durante o desenvolvimento do cerebelo, está aumentada em biópsias de MB comparada ao tecido normal do cérebro e regula processos como crescimento e migração nesse tumor. O objetivo dessa tese foi avaliar o impacto da modulação epigenética no fenótipo indiferenciado e, consequentemente, na manutenção de células de MB humano. No capítulo I, destaca-se que a inibição de histonas deacetilases (HDACs) por butirato de sódio (NaB) e consequente aumento na acetilação de histonas é capaz de diminuir marcadores de pluripotência de células de MB-SHH e MB-não-WNT/SHH. A ativação da via de ERK contribui para esse efeito e a inibição dessa via intensifica o efeito antiproliferativo de NaB, provavelmente por também modulador a capacidade "tromco". No capítulo II, ressalta-se a importância da ativação de ERK no MB-Grupo 4. Tumores desse subgrupo com a assinatura gênica específica $BMI^{high}/CHD7^{low}$ apresentam um fenótipo de maior malignidade (alta proliferação e indiferenciados) que está relacionado a ativação aumentada da sinalização de ERK. Juntos, os dados dessa tese demonstram que o fator epigenético BMI1 e a ativação da via de sinalização de ERK estão envolvidos na manutenção de um fenótipo indiferenciado em células tumorais de MB, fortalecendo as evidências de que eles devem ser considerados potenciais alvos terapêuticos nesse tumor.

Palavras-chave: meduloblastoma; epigenética; BMI1; sinalização de ERK

Abstract

Medulloblastoma (MB), a prevalent type of childhood brain cancer, comprises a tumor group with different molecular subtypes and outcomes. These tumors present modifications in essential pathways in cerebellar development. Recently, integrative genomics studies showed the importance of epigenetic factors to the formation and maintenance of MB. These factors support the malignant and undifferentiated cellular phenotype by regulation of pluripotency-associated process. These cells, named cancer stem cells (CSC), are identified by expression of the marker *CD133*, by their ability to form non-adherent spheres in fetal bovine serum free medium and by their tumorigenicity. CSCs participate in tumor initiation process, progression, metastasis and relapse. Most of these processes are explained by stemness phenotype derived from modulation of mechanisms associated to normal stem cell. ERK signaling, for example, wich is important for cerebellar development, is upregulated in MB biopsies compare to normal brain. In MB, ERK activation also modulates processes such as growth and migration. The aim of this thesis was to evaluate the impact of epigenetic modulation on the stemness phenotype and, consequently, on the maintenance of human MB cells. In chapter I, it is noteworthy that the inhibition of histone deacetylases (HDACs) by sodium butyrate (NaB) and the consequent increase in histone acetylation is able to decrease stem cell markers in MB-SHH and MB-non-WNT / SHH cells. ERK pathway activation contributes to this effect and the inhibition of this pathway enhances the antiproliferative effect of NaB, probably by modulating stemness. In chapter II, we higlighted the importance of ERK activation in MB-Group 4. Tumors in this subgroup harbouring the specific genetic signature $BMI^{high}/CHD7^{low}$ have a higher malignancy (high proliferation and undifferentiated status) phenotype that is related to increased activation of ERK signaling. Together, data from this thesis demonstrate that the epigenetic factor BMI1 and the activation of ERK signaling are involved in maintaining an undifferentiated phenotype in MB tumor cells, supporting the view they should be considered as potential therapeutic targets in this tumor type.

Keywords: medulloblastoma; epigenetics; *BMI1*; ERK signaling

INTRODUÇÃO

"*Children are not little adults.*" [1]

Tumores pediátricos compreendem um conjunto de mais de 100 neoplasias que são biologicamente e geneticamente diferentes daquelas encontradas em adultos (ADAMSON *et al*., 2014). Eles apresentam, em média, menos mutações somáticas que tumores adultos, e essas alterações ocorrem com alta frequência em genes que codificam proteínas envolvidas na regulação epigenética (DOWNIN *et al.*, 2012; HUETHER *et al*., 2014).

Embora seja considerada uma doença rara, o câncer pediátrico é a principal causa de morte em crianças no mundo. No Brasil, assim como em países desenvolvidos, tumores são a primeira causa de morte por doença na população de 0-19anos e, considerando causas de morte gerais, é superado apenas pelo número de mortes por causas externas (INCA, 2016; STELIAROVA-FOUCHER, *et al*., 2017). Entre os tumores pediátricos, tumores do sistema nervoso central (SNC) são o segundo tipo de câncer mais prevalente, depois das leucemias, entretanto são os que possuem as maiores taxas de mortalidade e morbidade (GROB & LEVY, 2017). No mundo, aproximadamente 20% dos tumores infantis dessa classe são diagnosticados como meduloblastoma (MB) (LEECE *et al*., 2017; SCHWALBE *et al*., 2017).

1.1MEDULOBLASTOMA

MB, um câncer embrionário maligno do cerebelo, é um tumor do SNC prevalentemente infantil, com uma incidência cerca de 10x maior em crianças do que em adultos. A maioria dos casos, aproximadamente 70-80%, ocorrem em pacientes com faixa etária de 0-14anos (ROBLES *et al.,* 2015; TULLA *et al.,* 2015; FAIRLEY *et al.*, 2016; KHANNA *et al*., 2017).

O tratamento dessa doença consiste em ressecção cirúrgica, radioterapia (em crianças maiores de 3 anos) e quimioterapia e apresenta uma taxa de cura variável de acordo com características clínicas do paciente como idade e status metastático (BARTLETT *et al*., 2013). Devido à adição de quimio- e radioterapia ao tratamento

cirúrgico padrão e a melhora nas técnicas cirúrgicas e de radioterapia, as taxas de sobrevida tem aumentado consideravelmente ao longo das últimas décadas, passando de 22% em 1950 para 50% na década de 80 e alcançando até 80% nos dias de hoje para a maioria dos pacientes. Porém, uma parcela dos pacientes considerada de alto risco (menores de 3 anos e/ou com doença disseminada) apresenta taxa de sobrevida livre de doença em 5 anos de 60-65% e pacientes que apresentam recaídas possuem um prognóstico ainda pior, com taxa de sobrevida livre de doença menor que 10% (RAMASWAMY & TAYLOR, 2017; BAUTISTA *et al*., 2017).

Apesar de eficaz para a maioria dos pacientes, o tratamento atual apresenta inúmeros efeitos colaterais de longo prazo. Perda auditiva, deficiências neurológicas, neuroendócrinas e psicológicas são alguns danos que impedem que muitos pacientes tenham uma vida independente mesmo depois de curados (MILLARD *et al.*, 2016). Além disso, tumores secundários como glioblastomas e leucemias acometem 3-5% dos sobreviventes de MB (PACKER *et al.*, 2013). Uma melhor classificação dos pacientes considerando características da biologia tumoral, além dos fatores utilizados na prática clínica, pode contribuir para a escolha de tratamento (como uso ou não de radioterapia e dose administrada) e, consequentemente, para uma diminuição das morbidades associadas a ele (HOLGADO *et al.*, 2017).

De acordo com a última classificação para tumores do SNC da Organização Mundial da Saúde, MB é um tumor embrionário altamente maligno (grau IV) que compreende um grupo de diferentes neoplasias que podem ser classificadas de acordo com sua histologia e/ou perfil molecular (LOUIS *et al.,* 2016). Até 2016, o MB era categorizado em 4 grupos histológicos (Clássico, Desmoplásico/Nodular, MB com Extensa Nodularidade e MB de Grande Células/Anaplásico), os quais já refletiam a heterogeneidade dessa doença (LOUIS *et al.*, 2007). A classificação mais recente mantém a divisão histopatológica e inclui uma divisão baseada em características moleculares, subdividindo-os em: MB-WNT, MB-SHH/*TP53*wt, MB-SHH/*TP53*mut e MB não-WNT/SHH (provisoriamente divididos em Grupo 3 e Grupo 4). Esses grupos moleculares divergem nos perfis de expressão gênica, nos padrões histológicos e nas características clínicas. (NORTHCOTT *et al.*, 2012a, LOUIS, *et al.,* 2016) (**Figura1**).

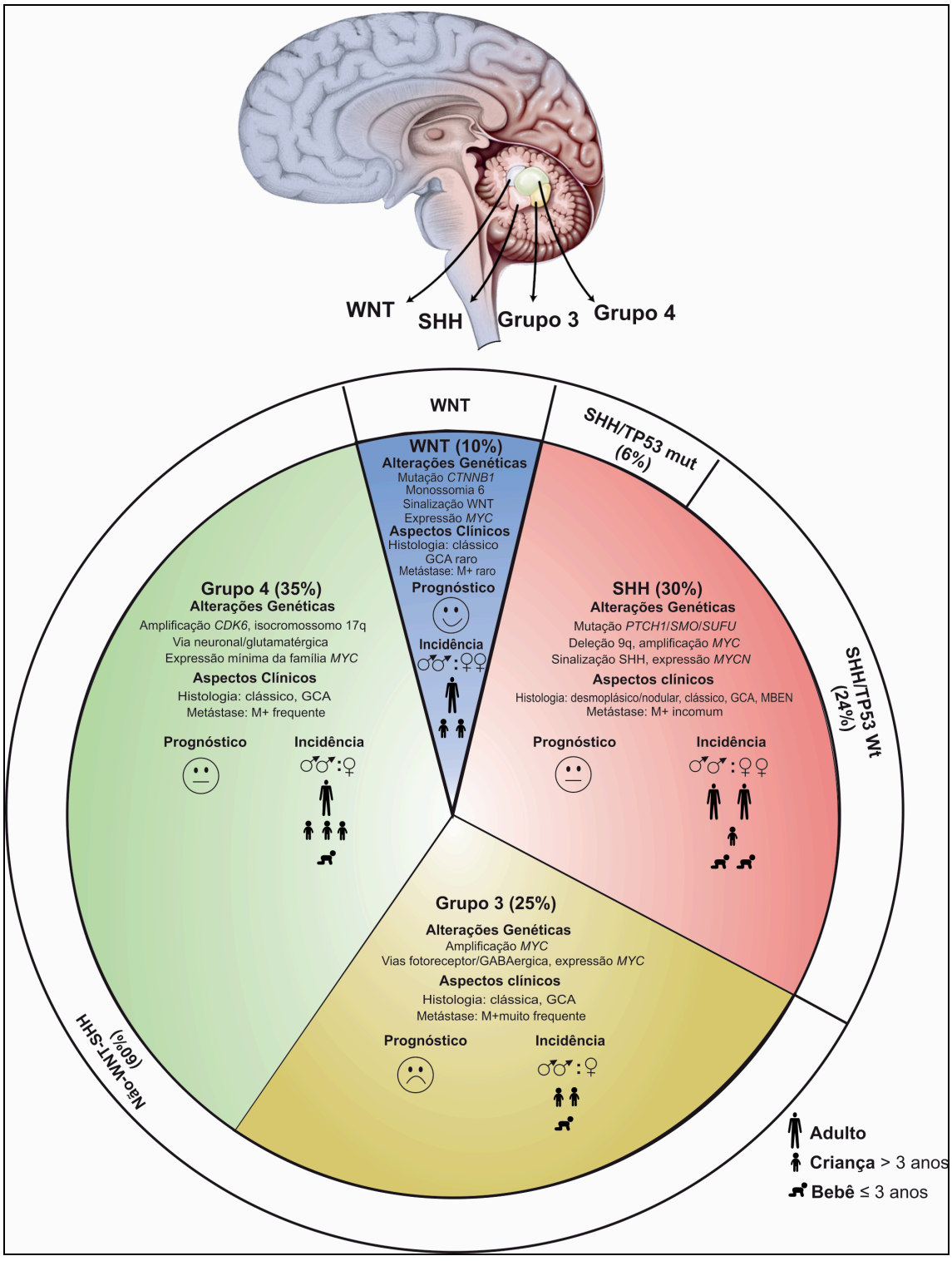

Figura 1. Características dos subgrupos moleculares de meduloblastoma. O gráfico apresenta frequência, alterações genéticas e características clínicas e demográficas dos quatro subtipos moleculares de meduloblastoma. A borda externa do gráfico representa a classificação da Organização Mundial da Saúde para esse tumor com suas respectivas frequências. Abreviaturas: GCA, Grande Células/Anaplásico; MBEN, meduloblastoma com Extensa Nodularidade; M+, metástase positiva ao diagnóstico; SHH, sonic hedgehog. Adaptado de Northcott *et al.*, 2012a e Louis, *et al*., 2016.

O MB-WNT ocorre em 10% dos pacientes, possui o melhor prognóstico (com índice de cura superior a 90%) e raramente apresenta metástases (KOOL *et al.,* 2012; PICKLES *et al.,* 2017). Esses tumores estão associados a mutações no gene *CTNNB1* (gene que codifica a proteína beta-catenina) ou, com menos frequência, em outros componentes da via de sinalização WNT, como *APC*, gene supressor tumoral envolvido na Síndrome de Turcot, que predispõe a MB. Essas alterações levam a uma ativação constitutiva da sinalização WNT, com o acúmulo de beta-catenina no núcleo e ativação de genes relacionados à progressão do ciclo celular, apoptose e diferenciação. Monossomia do cromossomo 6 está presente em cerca de 85% dos casos de MB-WNT e tem sido proposto como marcador para diagnóstico desse subgrupo juntamente com a avaliação de beta-catenina nuclear por imunohistoquímica. Embora já utilizado, 10-15% dos pacientes MB-WNT não são identificados por esse método de diagnóstico (ELLISON *et al*., 2005; Taylor *et al*., 2012; NORTHCOTT *et al.*, 2012a, NORTHCOTT *et al.*, 2012b; NORTHCOTT *et al.*, 2017).

O MB-SHH ocorre em 30% dos casos, possui prognóstico variável e metástases ao diagnóstico são incomuns (KOOL *et al.,* 2012; PICKLES *et al.,* 2017). Esses tumores contem mutações em diferentes fatores da via de sinalização SHH, como *PTCH1* (gene supressor tumoral envolvido na Síndrome de Gorlin, que predispõe a MB), *SUFU*, *SMO, GLI1* e *GLI2*. A via SHH, constitutivamente ativa nesse subgrupo, é importante no desenvolvimento do cerebelo, onde controla a proliferação de células precursoras granulares. Alterações somáticas em genes codificadores de proteínas envolvidas com modulação de acetilação de histonas (como *CREBBP*, *KATB6B*, *EP300* e *BRPF1*) tem uma representação maior em MB-SHH do que nos outros subgrupos. Alterações estruturais como deleções no cromossomo 9q e 10q e amplificação em *MYCN* e *GLI2* estão presentes nesse subgrupo. Aproximadamente 21% dos pacientes MB-SHH tem mutações em *TP53* (MB-SHH/*TP53*mut) o que confere a eles um pior prognóstico. Taxa de sobrevida em 5 anos caem de 81% em pacientes MB-SHH/*TP53*wt para 50% em pacientes MB-SHH/*TP53*mut (TAYLOR *et al.*, 2012; NORTHCOTT *et al.*, 2012a, NORTHCOTT *et al.*, 2012b; ZHUKOVA *et al*., 2013; NORTHCOTT *et al.*, 2017).

O MB não-WNT/SHH são provisoriamente divididos em Grupo 3 e Grupo 4, os quais ainda não possuem uma composição molecular claramente demarcada como os subgrupos MB-WNT e MB-SHH. Eles representam 20% e 40% dos casos de MB respectivamente. O MB Grupo 3 apresenta o pior prognóstico (sobrevida livre de doença em 5 anos menor que 50%) e frequentemente apresenta metástase ao diagnóstico, enquanto o MB Grupo 4 tem um prognóstico intermediário (sobrevida livre de doença em 5 anos de 70%) e as metástases ocorrem em cerca de um terço dos pacientes (KOOL *et al.,* 2012; PICKLES *et al.,* 2017). Esses grupos raramente apresentam mutações somáticas em regiões codificadoras e as poucas mutações identificadas são associadas com remodeladores da cromatina e modificadores de histonas. O gene *SMARCA4* é o que se apresenta mais mutado nos MB Grupo 3 (11%), enquanto mutações no gene *KDM6A*, que codifica uma demetilase de histona, ocorrem em MB Grupo 4 (12%). MB não-WNT/SHH tem grande instabilidade cromossomal, com inúmeras variações estruturais. Algumas dessas variações são específicas, como amplificação de *MYC* ou *OTX2* em Grupo 3 e deleções em *KDM6A* no Grupo 4, e outras são comuns aos dois grupos, como isocromossomo 17q (i17q). MB não-WNT/SHH apresentam alterações nas vias de sinalização associadas a manutenção de células tronco, diferenciação neuronal e neurogênese, com o Grupo 3 superexpressando genes relacionados ao desenvolvimento da retina e o Grupo 4 genes envolvidos na diferenciação e desenvolvimento neuronal. Apesar de terem transcriptomas mais similares entre si do que os outros subtipos de MB, Grupo 3 e 4 apresentam perfis de metilação de DNA diferentes, confirmando que eles representam entidades moleculares distintas (TAYLOR *et al.*, 2012; NORTHCOTT *et al.*, 2012a, NORTHCOTT *et al.*, 2012b; NORTHCOTT *et al.*, 2017, CAVALLI *et al.,* 2017).

Os recentes estudos genômicos em MB, além de confirmarem sua divisão molecular em no mínimo quatro subtipos, evidenciaram a importância de fatores epigenéticos para a patogênese desse tumor (HUETHER *et al.,*2014, CAVALLI *et al.*, 2017).

1.2 EPIGENÉTICA E O CÓDIGO DE HISTONAS

Epigenética é o estudo de mudanças na função gênica que podem ser herdáveis mitótica e/ou meioticamente e que não envolvem modificações na sequência de DNA. Os

mecanismos epigenéticos alteram a estrutura da cromatina e funcionam em conjunto com o DNA para estabilizar programas transcricionais que definem a identidade de cada tipo celular (BERGER *et al.*, 2009; ALLIS & JENUWEIN, 2016).

A cromatina, a forma no qual o DNA é empacotado dentro da célula eucariótica, é formada por unidades funcionais denominadas nucleossomos. Esses são compostos por um octâmero de proteínas histonas (H2A, H2B, H3 e H4), que são envoltas por aproximadamente 147 pares de bases do DNA. As variações nos componentes do nucleossomo, nas proteínas que se ligam a ele (incluindo aquelas que reconhecem histonas modificadas e chaperonas) e em remodeladores da cromatina dependentes de ATP afetam a estrutura da cromatina, mantendo-a menos condensada e transcricionalmente ativa (a eucromatina) ou altamente condensada e inativa (a heterocromatina). Esse grau de compactação definido por mudanças no nucleossomo é resultado de eventos epigenéticos, como a metilação do DNA e as diferentes modificações pós-tradução (PTM) que ocorrem nas histonas (LUGER *et al.*, 2012 BRIEN, *et al.*, 2016).

As histonas são proteínas que apresentam uma estrutura globular e uma região N-terminal mais flexível (a "cauda" da histona), a qual é exposta na superfície do nucleossomo e está sujeita a diversas modificações covalentes. Essas PTM incluem, entre outras, acetilação, fosforilação, metilação, ubiquitinação e ADP-ribosilação, e agem sequencialmente ou em combinação para formar o "código de histonas". Esse código regula padrões funcionais e distintos de transcrição, reparo do DNA e replicação através de proteínas que adicionam a marca epigenética as histonas (*writers*), proteínas que retiram a marca (*erasers*) e proteínas que reconhecem as modificações (*readers*). Uma das PTM mais estudadas é a acetilação de resíduos de lisina da cauda das histonas (STRAHL & ALLIS, 2000; JENUWEIN & ALLIS, 2001; TURNER, 2002; KOUZARIDES, 2007; ALLIS & JENUWEIN, 2016) (**Figura 2**).

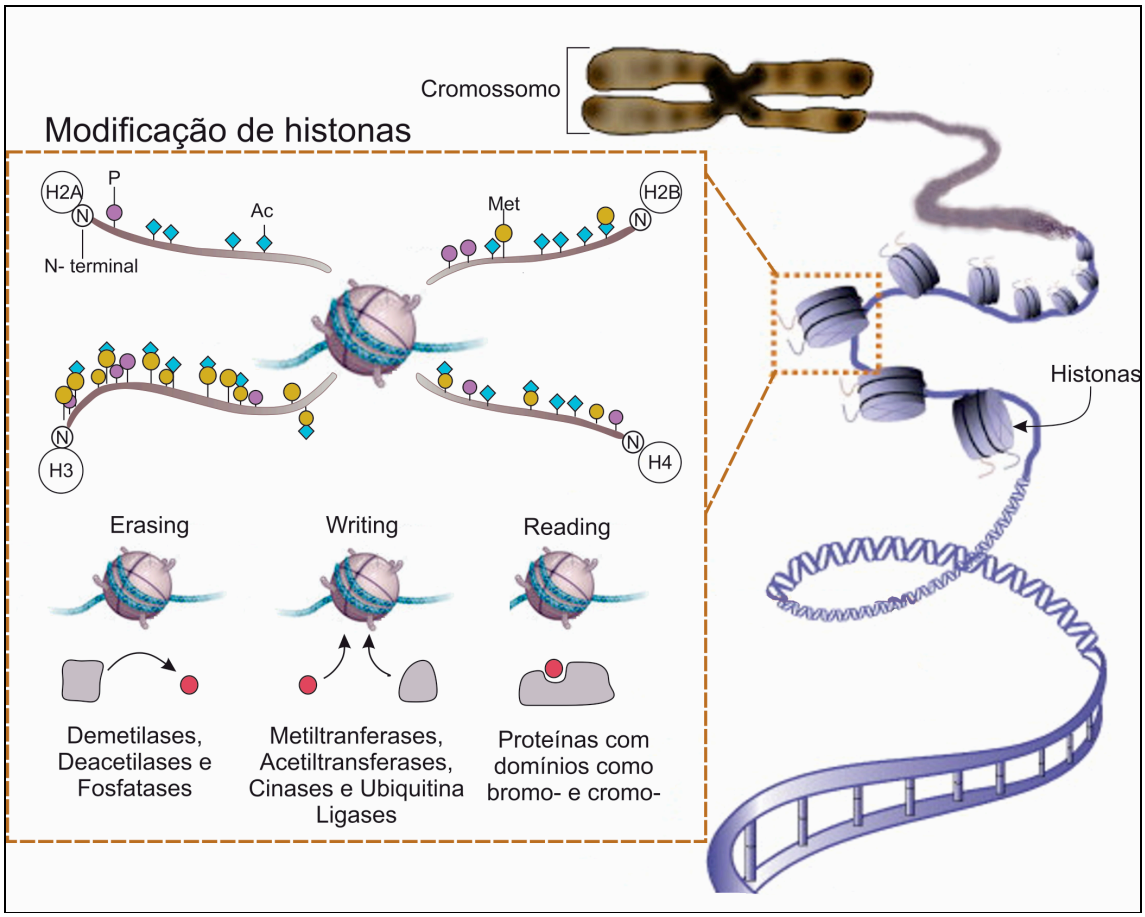

Figura 2. Código de histonas. Modificação pós-tradução de histonas é um dos mecanismos de regulação epigenética. Essas alterações pós-tradução covalentes ocorrem na região N-terminal das histonas H3, H4, H2A, e H2B. Esse processo envolve enzimas que adicionam (writer), retiram (eraser) ou interpretam (reader) as modificações. Adaptado de Sawan *et al*. (2008) e Helin & Dhanak (2013).

A primeira modificação descrita para as histonas foi a acetilação (PHILLIPS, 1963), processo regulado por dois tipos de enzimas: as histonas acetiltransferases (HATs) e as histonas deacetilases (HDACs). As HATs funcionam como *writers* e catalisam a transferência de um grupo acetil, originado do cofator acetil-CoA, para resíduos de lisina da cauda das histonas. Esse processo altera a carga da proteína, o que resulta em uma interação eletrostática menor com o DNA, um maior relaxamento da estrutura de empacotamento e um maior acesso de fatores de transcrição e da RNA polimerase. Além de presentes no núcleo (HATs tipo A), onde estão envolvidas com a regulação da expressão gênica, HATs estão presentes no citoplasma (HATs do tipo B) onde acetilam diferentes proteínas, inclusive histonas sintetizadas que serão direcionadas para o núcleo. As HATs nucleares podem ser agrupadas ainda em várias famílias de acordo com a

homologia de sequência e as características estruturais e funcionais. Essas famílias apresentam domínios diferentes que são reconhecidos por proteínas, as quais atuam como cofatores e determinam a especificidade de substrato e de gene-alvo das HATs (ROTH *et al.,* 2001; KIMURA *et al.,* 2005; LEE & WORKMAN, 2007; SCHENEIDER *et al*., 2013).

Em oposição ao efeito das HATs e atuando como *erasers*, as enzimas HDACs removem o grupamento acetil das lisinas da cauda das histonas, restaurando sua carga positiva, estabilizando a arquitetura da cromatina e dificultando a transcrição gênica. Além disso, promovem o estabelecimento e a disponibilidade de resíduos de lisina que podem ser alvos de diferentes PTM, como metilação e ubiquitinação. Em humanos, HDACs são divididas em quatro classes de acordo com sua homologia com HDACs de leveduras, localização celular e atividade enzimática e, assim como as HATs, HDACs podem ser encontradas em complexos formados por proteínas que regulam sua atividade enzimática (BOLDEN *et al*., 2006; COHEN *et al*., 2011; SETO & YOSIDA, 2014).

O desequilíbrio entre atividade de HATs e HDACs, assim como alterações em fatores regulatórios ou complexos de remodeladores da cromatina que reconhecem resíduos acetilados (*readers*), resulta em uma mudança no padrão de acetilação das histonas. Essa mudança tem o potencial de afetar a estrutura e integridade do genoma, interromper programas de expresssão gênica normais, e, assim, contribuir com o surgimento de patologias como o câncer **(Figura 3)**. A hipoacetilação em genes supressores tumorais, por exemplo, pode silenciá-los ou reduzir seus níveis de expressão, contribuindo para o processo tumoral (COHEN *et al*., 2001; DELCUVE *et al*., 2012; CERBO & SCHENEIDER, 2013). Diferentes tipos de neoplasias apresentam alteração no nível global de acetilação de histonas, principalmente perda de acetilação na lisina 16 da histona H4 (H4K16ac) (FRAGA *et al*., 2005). Essa hipoacetilação pode ser explicada pela atividade aberrante de HDACs, dado que a superexpressão dessas enzimas é observada em diferentes neoplasias (WITT *et al.*, 2009). Em MB, diversas isoformas específicas de HDACs são diferencialmente expressas, sendo a superexpressão de HDAC 5 e 9 correlacionadas com um pior prognóstico clínico (MILDE *et al.,* 2010). Apesar de alterações em outros componentes envolvidos na acetilação também participarem em eventos oncogênicos (como mutações em componentes do complexo N-CoR em MB-

SHH), a inibição de HDACs é uma das estratégias terapêuticas estudadas para reverter mudanças epigenéticas associadas ao câncer (JOHNSTONE, 2002).

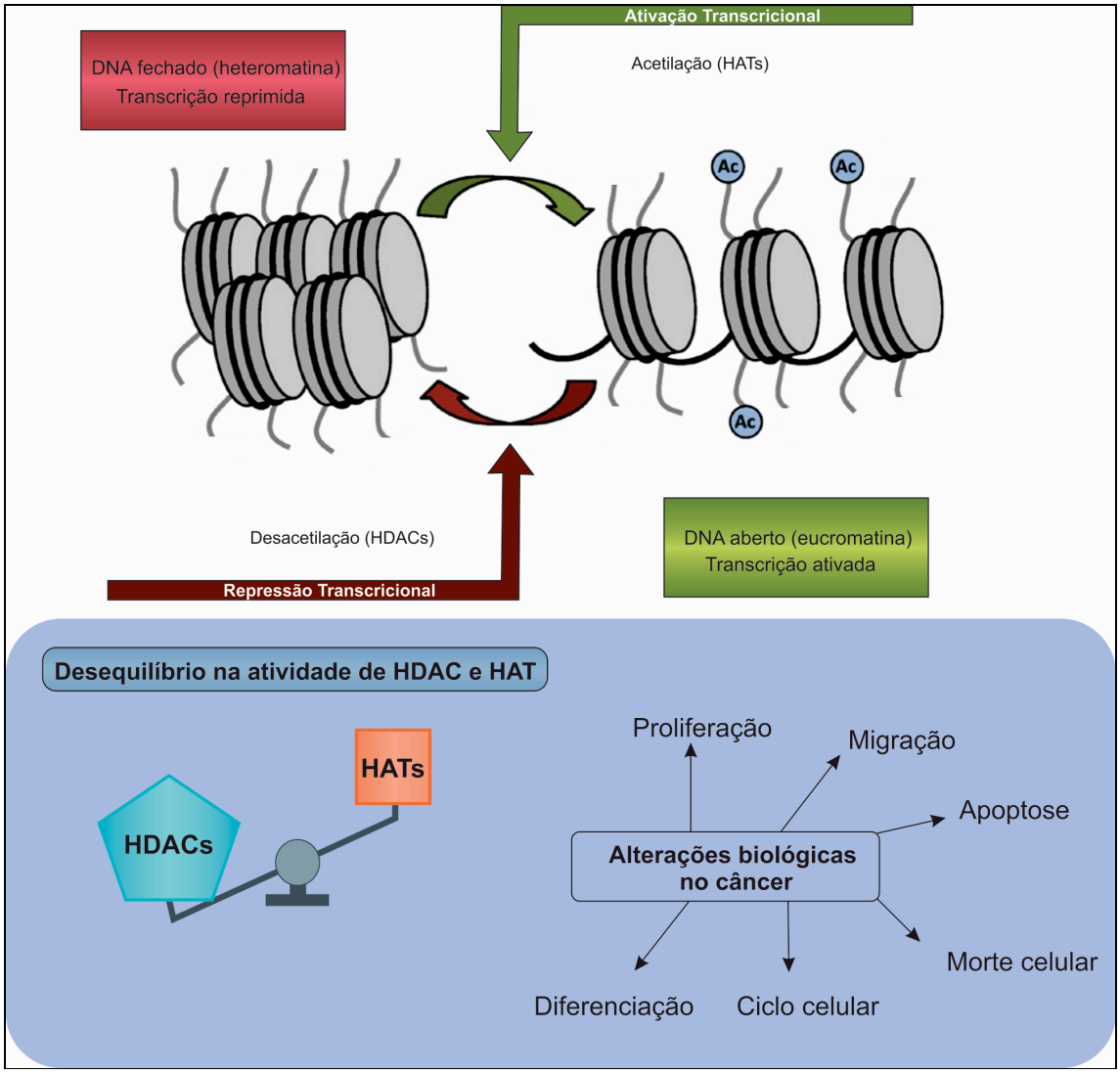

Figura 3. Acetilação de histonas. O perfil de acetilação de histonas é determinado pela ação das enzimas histonas acetiltransferases (HATs) e as histonas deacetilases (HDACs). Histonas acetiladas são correlacionadas com a ativação da expressão gênica e histonas deacetiladas com a repressão gênica. O desequilíbrio na ação das enzimas HATs e HDACs, como uma maior ativação de HDACs, promove alterações em processos biológicos envolvidos em câncer. Adaptado de Shalome A. Bassett & Matthew P. G. Barnett, (2014) e Katherine Ververis *et al.* (2013).

Inibidores de HDAC (HDACis) são compostos químicos (naturais ou sintéticos) que causam uma hiperacetilação de histonas no nucleossomo, resultando na expressão de um grupo específico de genes que podem levar a parada do ciclo celular, apoptose e/ou diferenciação. Eles são classificados de acordo com a estrutura química em ácidos

hidroxâmicos, ácidos alifáticos de cadeia curta, benzamidas, tetrapeptídeos cíclicos e inibidores de sirtuínas. Eles podem atuar em apenas alguns tipos de HDACs (inibidores seletivos para isoformas) ou contra todos os tipos (pan-inibidores) e os genes afetados são dependentes do tipo celular, sendo as células tumorais muito mais sensíveis aos HDACis do que as células normais. Apesar de, de forma geral, histonas acetiladas serem correlacionadas com ativação da transcrição gênica, um número similar de genes são reprimidos e induzidos após tratamento com HDACis. Essas mudanças na expressão de genes afetam diferentes processos correlacionados a carcinogênese, inclusive a diferenciação celular **(Figura 4)** (KRETSOVALI *et al*., 2012; BISWAS & RAO, 2017; ECKSCHLAGER *et al.*, 2017; WEST & JONSTONE, 2017).

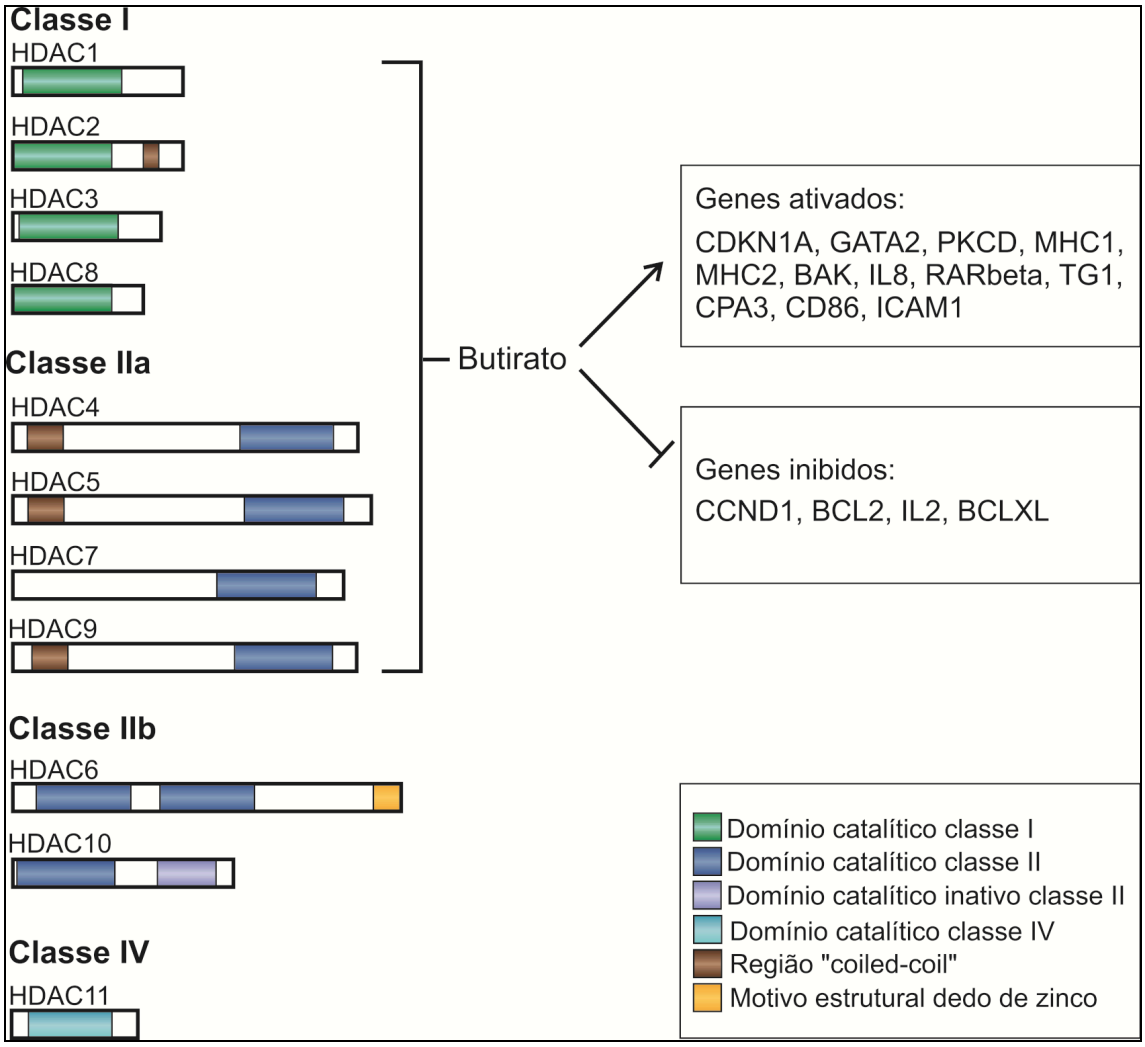

Figura 4. Classes de histonas deacetilases inibidas por butirato de sódio. Histonas deacetilases são divididas em 4 classes, sendo as classes I e IIA alvos da ação do Butirato de sódio. Esse inibidor já foi descrito regular genes envolvidos em diversos processos biológicos, como ciclo celular e apoptose. Adaptado de Bolden *et al*. (2006) e Blank (2015).

HDACis já foram descritos como agentes indutores de diferenciação em linhagens de célula tumorais como câncer de colon (WANG *et al.*, 2014), de mama (MUNSTER *et al*., 2001), neuroblastoma (FRUMM *et al*., 2013), sarcoma de Ewing (SOUZA *et al*., 2018) entre outros, com a diferenciação sendo avaliada por parâmetros como morfologia, parada do ciclo celular na fase G1 e marcadores de desenvolvimento/diferenciação tecido-específico (MARKS *et al.,,* 2000; GOTTLICER *et al*., 2001). Em células de MB, o efeito antiproliferativo do HDACi fenilbutirato é acompanhado por uma mudança morfológica das células, uma parada no ciclo celular em G0/G1 e um aumento na expressão do marcador de diferenciação glial *GFAP* e neuronal *SYN*, sugerindo a indução de um fenótipo mais diferenciado. Experimentos *in vivo* demonstraram que após tratamento com 3 mM de fenilbutirato por 28 dias há uma redução tumoral e um tempo de latência mais curto na formação de tumores em camundongos SCID. A hiperacetilação da histona H4 é importante para determinar a resposta à droga e os genes associados com um fenótipo mais diferenciado, tais como *GFAP*, *SYN*, receptores GABAérgicos e dopaminérgicos, são identificados em células tratadas (LI *et al.*, 2004). Nor e colaboradores demostraram que outro HDACi, butirato de sódio (NaB), além de induzir diferenciação é capaz de diminuir a formação de esferas de células de MB, um modelo de cultura para enriquecimento de células com fenótipo mais indiferenciado (células tronco tumorais – CSC) (NOR *et al*., 2013). NaB é um inibidor de HDAC classe I e IIa que possui a capacidade de modular a expressão de genes relacionados a pluripotência em células tronco normais e pode ser usado para estudar a reprogramação desses genes em CSC (CANANI *et al*., 2012).

A acetilação e outras PTM de histonas funcionam como um código e assim, a alteração promovida por HDACis podem levar a modificações em outros elementos importantes para a interpretação do código. Diferentes HDACis testados em células tumorais e não tumorais induzem uma aumento na metilação de H3K4 (NIGHTINGALE *et al.*, 2007) e NaB, em câncer de mama, reduz a expressão de *BMI1*, gene que codifica uma proteína do complexo PRC1 envolvida na auto-renovação e proliferação de células tronco normais e tumorais (BOMMI *et al*., 2010).

1.3 CÉLULAS TRONCO TUMORAIS

Células tronco tumorais (CSC) é o termo que define uma população tumoral distinta de células com habilidade de auto renovação e capacidade de repopulação clonal, ou seja, gerar os diferentes tipos celulares que constituem um tumor (REYA *et al*., 2001). Essas células são nomeadas assim devido a suas propriedades "tronco" (*stemness*) similares às observadas em células tronco de tecidos normais, as quais incluem extensa habilidade de auto renovação (simétrica e assimetricamente) e capacidade de diferenciação. CSC são capazes de iniciar um tumor, característica experimentalmente demonstrada pela capacidade de um número limitado dessas células, quando injetadas em um ambiente ortotópico *in vivo*, originarem um tumor composto por diferentes tipos celulares (CSC e não-CSC) e similar fenotipicamente ao tumor parental (KRESO &.DICK, 2014).

CSC foram inicialmente identificadas e caracterizadas em leucemia mielóide aguda humana (LMA) utilizando o conhecimento sobre células-tronco hematopoiéticas. Nesse tumor hematológico foi possível observar que a população de células transplantadas em camundongos NOD/SCID capaz de originar e recapitular a leucemia original era aquela que apresentava um perfil de marcadores de superfície específico de células imaturas da medula (CD34+CD38-). Além disso, células com outros perfis (CD34- ou CD34+CD38+) não apresentavam a mesma capacidade (LAPIDOT *et al*., 1994). Em tumores sólidos, a presença de CSC só foi observada quase dez anos depois, quando, utilizando estratégia similar, elas foram identificadas em câncer de mama (AL HAJJ *et al.*, 2003). Desde então, CSC, também conhecidas como células iniciadoras de tumores, foram identificadas em tumores sólidos de diversos órgãos, incluindo SNC (SINGH *et al.*, 2003), fígado (MA *et al.*, 2007), ovário (ZHANG *et al.*, 2008), próstata (COLLINS *et al.*, 2005), pulmão (ERAMO *et al.,* 2008), melanoma (FANG *et al.*, 2005), pâncreas (LI et al., 2007) e cólon (O'BRIEN *et al.*, 2006), com cada tipo tumoral apresentando diferentes marcadores de superfície. Em MB, CSC são identificadas pela expressão de marcadores de células tronco neurais como *CD133*, *BMI1* e *Nestina*, pela capacidade de formar esferas não aderentes em culturas livres de soro fetal bovino e pela tumorigenicidade (HEMMATI *et al*., 2003; SINGH *et al*., 2004;).

Atualmente, é amplamente aceito que CSC participam nos processos iniciais do tumor, na progressão, na metástase e na recidiva tumoral, produto de células resistentes a

terapia (PEITZSCH *et al*., 2017). Alguns dos mecanismos moleculares presentes em CSC e responsáveis por suas propriedades tem sido descritos em diferentes tipos tumorais. A resistência de CSC à quimioterápicos, por exemplo, é resultado da alta expressão de transportadores de efluxo de drogas como membros da família de transportadores ABC (*ATP-binding cassete*), que incluem ABCG2, MDR1 e MRP1 (BEGICEVI & FALASCA, 2017). A resistência de CSC à terapia convencional, principalmente à radioterapia, também pode ser explicada por mecanismos que protegem as CSC do dano ao DNA induzido pelo tratamento como: regulação do status do ciclo celular, aumento da capacidade de reparo ao DNA e prevenção de dano ao DNA por uma eficiente redução de espécies reativas de oxigênio (COJOC *et al.*, 2014).

Em meduloblastoma, observa-se uma relação entre resistência à terapia e o fenótipo indiferenciado. Células de MB tolerantes à radioterapia, por exemplo, apresentam propriedades de células tronco como a habilidade de iniciar e recapitular o tumor parental e, comparada as células parentais, células radiorresistentes tem uma expressão aumentada do transportador ABCG2, um dos mecanismos descritos para CSC (INGRAM et al., 2013). Também células expressando altos níveis de marcadores de células tronco tumorais, como *CD133, Sox-2, Bmi1* e *Nestin*, são radioresistentes quando comparadas as células parentais (YU *et al.*, 2010).

Em relação a capacidade metastática, CSC podem migrar do sítio primário e se estabelecer em um novo nicho onde originam um tumor heterogêneo. Análises de células únicas mostram que células metastáticas em estádios iniciais possuem padrão de expressão de células tronco (COJOC *et al.*, 2014; LAWSON *et al*, 2015). Em diferentes tumores, CSC estão envolvidas no processo de transição epitélio-mesenquima (EMT), no qual células epiteliais aderentes adquirem o fenótipo de células mesenquimais migratórias tumorais (MITRA *et al*., 2015). CSC expressam fatores de transcrição indutores de EMT como *TWIST, SNAIL* e *SLUG*, assim como células em processo de EMT apresentam uma similaridade com CSC quando comparadas com células que não estão em EMT. Essas observações indicam que CSC podem migrar e são provavelmente as responsáveis por iniciar o processo de metástase (BACCELLI & TRUMPP, 2012; SHIOZAWA *et al*., 2013). No modelo de formação de esferas, CSC de MB apresentam elevada expressão de *MMP-9* e *MT1- MMP*, os quais estão envolvidos nos processos de invasão celular e

metástase (ANNABI *et al*., 2008). Assim como para resistência, há uma diminuição conjunta da capacidade invasiva de células e de marcadores de pluripotência em MB (GONG *et al.,* 2018).

Além dos mecanismo acima citados, a repopulação de CSC após ou durante a terapia antitumoral pode ser atribuída à ativação de vias de sinalização essenciais na homeostase do tecido adulto e desenvolvimento embrionário (COJOC *et al*., 2014). O conjunto desses programas moleculares que governam e mantem o estado indiferenciado das CSC define a característica *stemness* dessas células (KRESO & DICK, 2014). Em modelo mais recente da hipótese de CSC, o modelo de plasticidade de CSC, diferentes células podem adquirir o fenótipo indiferenciado, com as CSC representando um estado celular e não necessariamente uma população estática **(Figura 5).** Nesse modelo, características como *stemness* e plasticidade de CSC são determinados por fatores intrínsicos e extrínsicos, como regulação epigenética e, consequentemente, modulação em vias de sinalização associadas a auto-renovação e diferenciação (LI & LATERRA, 2012; PRASETYANTI & MEDEMA, 2017). As Proteínas do Grupo Policombo, por exemplo, são moduladores epigenéticos que participam da homeostase de células tronco normais e que também atuam na atividade de *stemness* nas CSC (SAUVAGEAU & SAUVAGEAU, 2010).

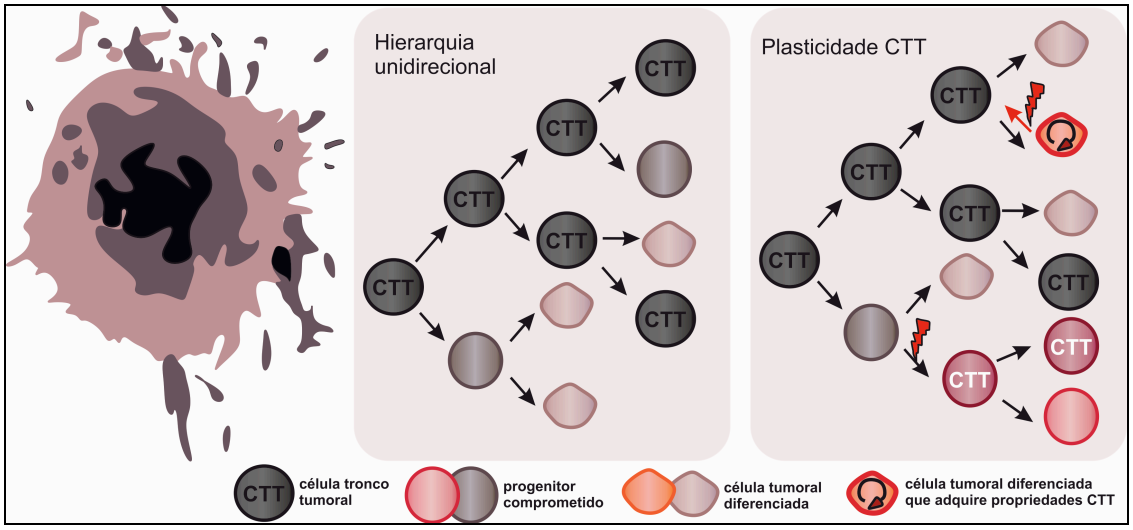

Figura 5. Modelos de CSC. O modelo de CSC original (hierarquia unidirecional) define que apenas CSC são capazes de recapitular o tumor parental. No modelo de platicidade de CSC, células tumorais tem a habilidade dinâmica bidirecional de converter seu fenótipo de um estado não-CSC para um estado de CSC e vice e versa. Assim, *stemness* e a plasticidade de CSC são determinados por fatores intrínsecos e extrínsecos, que podem ser estímulos do microambiente tumoral ou mudanças epigenéticas (representados como raios vermelhos na figura). Assim, não-CSC podem servir como um reservatório de CSC durante a tumorigênese. Adaptado de PRASETYANTI & MEDEMA, 2017.

1.4 BMI1

BMI1 (*B-cell-specific Moloney murine leukemia virus insertion site 1*) é um componente do complexo de regulação epigenética *Polycomb Repressive Complex 1* (PRC1) (CAO *et al.*, 2005). A proteína do Grupo Policombo codificada por *BMI1* apresenta um domínio "dedo de zinco" conservado na região N-terminal e um motivo "hélice-volta-hélice" central e, apesar de ser um componente regulatório central do PRC1, nenhuma atividade enzimática intrínseca de BMI1 é conhecida (CAO *et al.*, 2005; LI *et al*., 2006). Em conjunto com outras proteínas que formam PRC1, BMI1 modula a estrutura da cromatina e regula a transcrição de vários genes importantes envolvidos no desenvolvimento, ciclo celular, resposta a dano do DNA, senescência, regulação de células tronco e auto renovação celular (SIMON & KINGSTON, 2009; BHATTACHARYA *et al*., 2015).

Além de suas ações fisiológicas, BMI1 atua em diversos processos associados a tumorigênese e está superexpresso em vários tipos de neoplasias como câncer de pulmão, câncer de ovário, câncer de mama, leucemia mielóide aguda e crônica e gliomas (WANG *et al*., 2015). Em neoplasias oriundas de diferentes tecidos, uma assinatura baseada em genes regulados por BMI1 define um perfil de maior malignidade e pior prognóstico correlacionado com um menor intervalo para doença recorrente, presença de metástase e menores taxas de respostas à terapia (GLINSKY *et al.*, 2005; LI *et al*., 2010). Esse perfil está relacionado, em parte, a repressão do locus *INK4a/ARF* por BMI1 e, consequentemente, inibição das vias supressoras tumorais p16INK4A/RB e p14ARF/MDM2/p53 relacionadas a auto-renovação e controle do ciclo celular (JACOBS *et al*., 1999; BRACKEN *et al*., 2007). BMI1, mesmo na ausência do locus *INK4a/ARF*, controla a proliferação, adesão e diferenciação em modelo animal de glioma, demonstrando que ele atua em outros processos associados a genes diferentes de *Ink4a/Arf* (BRUGGEMAN *et al.*, 2007).

BMI1 interfere em processos associados ao fenótipo de CSC como na EMT induzida por Twist1 (YANG *et al.,* 2010), na invasão e metástase por alterar a expressão de metaloproteinases MMP-2 e MMP-9 (LI *et al*, 2013) e na quimioresistência por regular a expressão do tranportador ABC ABCG2 (SU *et al.,* 2015) e prevenir dano de DNA

causado por espécies reativas de oxigênio (WANG *et al*, 2011). Esses processos corroboram com o papel funcional de BMI1 em CSC (BAKHSHINYAN *et al*., 2017).

Em MB, *BMI-1* tem a expressão aumentada em todos os subgrupos moleculares, com níveis mais altos detectados no MB-Grupo 4, seguido por MB-Grupo3, MB-SHH e MB-WNT (BEHESTI *et al.,* 2013). Assim como em outros tumores, maior expressão gênica de *BMI1* está associada com uma diminuição na sobrevida de pacientes (ZAKRZEWSKA *et al.,* 2011), provavelmente por sua ação em induzir a auto renovação de células tronco neurais e a proliferação de progenitores granulares do cerebelo, possíveis células de origem do MB (LEUNG *et al*., 2004; SUTTER *et al.*, 2010).

Vários processos tumorais em MB são modulados por BMI1. A diminuição nos níveis dessa proteína, por exemplo, reduz a proliferação de células de MB por dois mecanismos distintos: indução de apoptose e mudança no estado redox intracelular e consequente inibição da senescência celular (WIEDERSCHAIN *et al.*, 2007; VENKATARAMAN *et al*., 2010). BMI-1 também altera a expressão de genes envolvidos nos processos de remodelamento da matrix extracelular, adesão celular e nas vias de sinalização TGF, WNT, VEGF e AKT (WIEDERSCHAIN *et al*., 2007), importantes no processo de migração. De fato, *knockdown* de BMI1 reduz a ativação da via de BMPs (*bone morphogenetics proteins*), membros da via de sinalização de TGFb, restringindo a migração celular (MERVE *et al*., 2014).

Um número importante de reguladores do desenvolvimento e fatores de diferenciação são modulados por BMI1 em MB, sugerindo a atuação dele na manutenção de um fenótipo indiferenciado e na inibição de indução de progamas de diferenciação (WIEDERSCHAIN *et al*., 2007). Corroborando com essa hipótese, CSC de MB apresentam níveis mais elevados de *BMI1* do que células tronco neurais e a sua redução inibe a auto-renovação e a capacidade tumorigênica dessas células (WANG *et al*., 2012; MANORANJAN *et al.,* 2013). Além disso, demonstrou-se que crescimento de MB-Grupo 4 e MB-SHH é dependente de BMI1, uma vez que *knockdown* de seu transcrito resultou na redução do crescimento e invasão tumoral em modelo de xenotransplante (MERVE *et al.,* 2014) e camundongos duplo negativos para BMI1 não formavam tumores em modelo animal para desenvolvimento de meduloblastoma dirigido por ativação da via Hedgehog (MICHAEL *et al*., 2008).

Apesar de essencial para a manutenção de diferentes subtipos moleculares de MB, a expressão aumentada de *BMI1* em células tronco neurais ou progenitores granulares do cerebelo não é suficiente para induzir a formação de MB (BEHESTI *et al*., 2013; YADIRGI *et al.*, 2011). Entretanto, em camundongos com deleção em *TP53*, a expressão aumentada de BMI1 é capaz de induzir tumores, embora com uma frequência muito baixa, indicando a necessidade de eventos oncogênicos adicionais para que BMI1 induza a formação de MB (BEHESTI *et al*., 2013).

1.5 SINALIZAÇÃO DE ERK EM MB

Similar ao observado para a expressão de BMI1, a ativação de ERK está aumentada em biópsias de MB comparada ao tecido normal do cérebro e contribui para a proliferação das células desse tumor (WANG *et al.,* 2001; WLODARSKI *et al*., 2006). A ativação dessa via também contribui para o processo de migração celular em MB, com inibição de ERK reduzindo a capacidade invasiva tumoral (YUAN *et al.*, 2010). Essas observações estão de acordo com estudo prévio que demonstra um aumento nos níveis de membros da cascata de ativação RAS/ERK em MB metastáticos (MACDONALD *et al.*, 2001).

A atividade da via de ERK é importante para a sobrevida de progenitores cerebelares (KENNEY & ROWITCH, 2000), o que possibilita que essa sinalização esteja relacionada a manutenção de CSC em MB. Chow e colaboradores mostraram que a ativação de ERK influencia na capacidade de células de MB formarem neuroesferas. Tumores que formavam esferas independente de estímulo de fatores de crescimento (EGF e bFGF) apresentavam alta ativação de ERK em comparação a tumores que dependiam de fatores de crescimento ou tumores incapazes de formar esferas. Células provenientes de tumores com alta ativação de ERK e, consequentemente, formadores de neuroesferas independente de fatores de crescimento, apresentaram maior potencial tumorigênico e letalidade (CHOW *et al.,* 2014). Esses resultados sugerem uma relação entre a sinalização de ERK e CSC de MB.

1.6 HIPÓTESE GERAL

Visto que:

- A formação e manutenção de MB tem sido associada a desregulação em fatores epigenéticos (ROUSSEL & STRIPAY, 2018);

- Esses fatores regulam a diferenciação neural e o desenvolvimento do cerebelo humano (QURESHI & MEHLER, 2013) e, quando alterados, contribuem para a indução de um fenótipo indiferenciado de CSC e para MB mais agressivos (HUANG *et al*., 2016);

- CSC em MB tem expressão aumentade de *BMI1*, um potente regulador de células tronco neurais, que apesar de ser essencial na formação e manutenção de MB, não é capaz de sozinho formar tumores (BEHESTI *et al*., 2013);

- A sinalização de ERK, envolvida no desenvolvimento do cerebelo, tem ativação aumentada em MB mestastáticos (MACDONALD *et al.*, 2001), característica atribuída a plasticidade de CSC, o que sugere sua participação na propriedade *stemness* dessas células;

- Moduladores da cromatina são propostos como como indutores de diferenciação em tumores (SHARMA *et al*., 2010).

A hipótese desse trabalho é que alterações epigenéticas são responsáveis pela formação e manutenção de MB por induzirem um fenótipo *stemness* através da expressão de *BMI1* e ativação da via de sinalização de ERK.

1.7 OBJETIVOS

Avaliar o impacto da modulação epigenética no fenótipo indiferenciado e, consequentemente, na manutenção de células de MB humano.

Objetivos específicos:

CAPÍTULO I

i. Determinar a expressão de marcadores de *stemness CD133* e *BMI1* e a modulação da via de sinalização de ERK após a inibição da acetilação de histonas em células de MB;
ii. Avaliar o efeito da inibição da acetilação de histonas e da sinalização de ERK na proliferação de células de MB;
iii. Determinar a expressão de marcadores de *stemness CD133* e *BMI1* após a inibição da sinalização de ERK;
iv. Avaliar o efeito da inibição de ERK na formação de CSC de MB;

CAPÍTULO II

i. Avaliar a proliferação *in vitro* de célula primária de MB-Grupo 4 com alta expressão de BMI1 após knockdown do gene modificador da cromatina identificado em screening de mutagênese insercional (gene *CHD7*);
ii. Avaliar a proliferação de xenotransplantes de MB-Grupo 4 com alta expressão de BMI1 após knockdown de *CHD7*;
iii. Determinar a expressão *in vitro* e *in vivo* de marcadores de diferenciação;
iv. Determinar mecanismo(s) molecular(es) responsáveis pelo fenótipo de células de MB-Grupo 4 com o alta expressão de *BMI1* e expressão reduzida de *CHD7*.

CAPÍTULO I: HDAC and MAPK/ERK Inhibitors Cooperate to Reduce Viability and Stemness Phenotype in Medulloblastoma

Autores: Mariane da Cunha Jaeger [1,2] • Eduarda Chiesa Ghisleni [1] • Paula Schoproni Cardoso [1] • Marialva Siniglaglia [1,2] • Tiago Falcon [3] • André T. Brunetto [1,2] • Algemir L. Brunetto [1,2] Caroline Brunetto de Farias [1,2] • Michael D. Taylor [4,5,6,7] • Carolina Nör [4,5] • Vijay Ramaswamy [4,8] • Rafael Roesler [1,9]

Periódico: Molecular Neurobiology

Status: manuscrito em preparação

HDAC and MAPK/ERK Inhibitors Cooperate to Reduce Viability and Stemness Phenotype in Medulloblastoma

Mariane da Cunha Jaeger [1,2] • Eduarda Chiesa Ghisleni [1] • Paula Schoproni Cardoso [1] • Marialva Siniglaglia [1,2] • Tiago Falcon [3] • André T. Brunetto [1,2] • Algemir L. Brunetto [1,2] Caroline Brunetto de Farias [1,2] • Michael D. Taylor [4,5,6,7] • Carolina Nör [4,5] • Vijay Ramaswamy [4,8] • Rafael Roesler [1,9]

[1] Cancer and Neurobiology Laboratory, Experimental Research Center, Clinical Hospital (CPE-HCPA), Federal University of Rio Grande do Sul, Porto Alegre, RS, Brazil

[2] Children's Cancer Institute, Porto Alegre, RS, Brazil

[3] Bioinformatics Core, Experimental Research Center, Clinical Hospital (CPE-HCPA), Porto Alegre, RS, Brazil

[4] The Arthur and Sonia Labatt Brain Tumour Research Centre, The Hospital for Sick Children, Toronto, ON, Canada

[5] Developmental and Stem Cell Biology Program, The Hospital for Sick Children, Toronto, ON, Canada

[6] Department of Laboratory Medicine and Pathobiology, University of Toronto, Toronto, ON, Canada

[7] Division of Neurosurgery, The Hospital for Sick Children, Toronto, ON, Canada

[8] Division of Haematology/Oncology, The Hospital for Sick Children, Toronto, ON, Canada

[9] Department of Pharmacology, Institute for Basic Health Sciences, Federal University of Rio Grande do Sul, Porto Alegre, RS, Brazil

Correspondence: Rafael Roesler

Department of Pharmacology, Institute for Basic Health Sciences, Federal University of Rio Grande do Sul, Rua Sarmento Leite, 500 (ICBS, Campus Centro/UFRGS), 90050-170 Porto Alegre,RS, Brazil.

Telephone: +5551 33083183; fax: +5551 33083121.

E-mail: rafaelroesler@hcpa.edu.br

Abstract

Medulloblastoma (MB), which originates from embryonic neural stem cells (NSCs) or neural precursors in the developing cerebellum, is the most common malignant brain tumor of childhood. Recurrent and metastatic disease is the principal cause of death and may be related to resistance within cancer stem cells (CSCs). Chromatin state is involved in maintaining signaling pathways related to stemness, and inhibition of histone deacetylase enzymes (HDAC) has emerged as a therapeutic tool to target this specific cell population across many tumors. Here, we observed changes in the stemness phenotype induced by HDAC inhibition in MB cells. We treated two human MB cell lines with the HDAC inhibitor (HDACi) sodium butyrate (NaB). Increased acetylation mediated by NaB reduced MB cell viability and expression of stemness markers *BMI1* and *CD133*. In addition, activation of extracellular-regulated kinase (ERK) signaling was also decreased after treatment with NaB. We went on to use the mitogen-activated protein kinase kinase (MEK) inhibitor U0126 to explore the role of the mitogen-activated protein kinase (MAPK)/ERK pathway in the stemness phenotype. MEK inhibition reduced the expression of the stemness markers and, when combined with NaB, the antiproliferative effect was enhanced. Inhibition of MAPK/ERK activity hindered MB neurosphere formation, supporting the possibility that this pathway is involved in regulating stemness in MB. These results suggest that combining HDAC and MAPK/ERK inhibitors may be more effective in reducing MB proliferation than single-drug treatments, through modulation of the stemness phenotype of MB cells.

Keywords Medulloblastoma ● Histone deacetylase ● BMI1 ● Stemness ● Cancer stem cell ● Brain tumor

Introduction

Medulloblastoma (MB), the most common malignant pediatric brain tumor, likely arises from genetic and epigenetics abnormalies during cerebellar development [1]. Integrative genomic, epigenomic and transcriptional analyses have shown that MB is not a single tumor type. Instead, it is comprised of at least four molecular subgroups: Wingless (WNT), Sonic hedgehog (SHH), Group 3 and Group 4, that also have distinct demographic, clinical, and prognostic features [2]. The WHO 2016 classification of central nervous system (CNS) tumors divides MB in WNT-MB, SHH-MB/*TP53* wild type, SHH-MB/*TP53* mutated, Group 3 and Group 4 [3]. This molecular identification of MB subgroups has resulted in several clinical trials of subgroup specific therapies, however, except for de-escalation of therapy for WNT patients, there are a paucity of new treatment options for most patients. Specifically, the long-term neurocognitive sequelae of therapy affect the life quality of MB survivors while patients with recurrent and metastatic disease usually succumb to their disease [4, 5].

According to the cancer stem cell (CSC) hypothesis, recurrence and metastasis in some tumor types may arise from a specific tumor cell subpopulation, the CSC, a distinct population of cells presenting stem cell-like properties such as clonal long-term repopulation and self-renewal capacity [6, 7]. In some cancers, including CNS tumors, CSCs drive tumor initiation and progression and are able to recapitulate the phenotype of the tumor from which they were derived [8]. In MB, CSCs are identified by the expression of neural stem cell (NSC) markers such as *CD133*, *BMI1*, *Nestin* and *Sox2*, by their capacity to form neurospheres *in vitro*, and by tumorigenicity in animal xenograft models

[8, 9]. These highly tumorigenic cells display features including stemness, therapeutic resistance, and invasion [10-14].

Given that a failure in maturation of cerebellar progenitor cells is likely at the origin of MB, and the resistance characteristics presented by CSCs may be responsible for therapeutic failure, modulation of cellular differentiation may be seen as a relevant strategy. In this context, epigenetic modulators have emerged as an exciting therapeutic avenue, particularly histone deacetylase inhibitors (HDACis) [15, 16]. HDACs are enzymes that control, in a balance with histone acetyltransferases (HATs), histone acetylation regulating chromatin state. HDACis promote the acetylation of histones and non-histone proteins, modify gene expression profiles, and regulate many biological processes involved in tumor homeostasis, such as apoptosis, cell-cycle arrest, angiogenesis, and differentiation [16]. HDACi play a role as differentiation inducers in several childhood cancers including neuroblastoma [17], Ewing sarcoma [18] and MB [19]. In MB, the antiproliferative effect of HDACi is accompanied by morphological changes, cell cycle arrest, increased expression of glial and neuronal markers, and reduced tumorigenicity [20-25]. We have previously shown that sodium butyrate (NaB), a class I and IIa HDACi, decreases neurosphere formation in MB cultures [23]. Using different HDACis, a recent study found a similar effect on neurosphere survival, even in the absence of significant changes in the expression of the stemness marker *CD133* [24].

Given that the stemness phenotype is proposed as a poor prognostic marker in many cancer types including MB [26, 27] and the effects of HDACi in regulating stemness are still not fully understood, the aim of this study was to investigate how NaB influences aspects of the stemness phenotype of MB cells. We examined the expression of *BMI-1*, a

potent inducer of NSC self-renewal and neural progenitor proliferation during cerebellar development [28], and activation of extracellular-regulated kinase (ERK), which plays a role in maintenance of pluripotency in normal human stem cells [29], in MB cells after treatment with NaB.

Materials and Methods

Cell Culture

Human Daoy (HTB186™) and D283 Med (HTB185™) MB cells were obtained from the American Type Culture Collection (ATCC, Rockville, USA). Cells were maintained in tissue culture flasks at 37 °C with humidified atmosphere and 5 % CO_2. The culture medium, which was changed every 2/3 days, was prepared with DMEM (Gibco, Grand Island, USA), 1% penicillin and streptomycin (Gibco), supplemented with 10 % fetal bovine serum (Gibco), with the pH adjusted to 7.4.

Treatments and Cell Viability

MB cells were seeded at 18.000 cells/well in 24 wells plates. After 24 h, cells were treated with the HDAC inhibitor NaB (Sigma-Aldrich, St. Louis, USA) alone or in combination with the MEK1/2 inhibitor U0126 (12.5 or 25 μM, Sigma-Aldrich). The NaB doses used in Daoy (0.25, 1.0, or 2.5 mM) and D283 (0.5, 2.5, or 5.0 mM) cells were chosen in agreement with a protocol previously described [23]. Forty-eight hours after treatment, cells were trypsinized and counted in a Neubauer chamber with trypan blue (10 μl dye to each 10 μl cell suspension) for viability measurement.

Histone H3 Acetylation

Cells treated for 48 h with NaB were lysed with a lysis solution buffer and acetylation of H3 was measured with PathScan® Acetylated Histone H3 Sandwich enzyme-linked immunosorbent assay (ELISA) Kit (Cell Signaling Technology, Danvers, USA) according to the manufacturer's instructions. Colorimetric signals were measured by spectrophotometric determination (OD450 nm) on Biochrom® Anthos Zenyth 200 Microplate Reader.

Gene Expression Correlation and Enrichment Analysis

We analyzed data from 763 MB samples [30] to detect genes significantly correlated ($p < 0.05$) with both *CD133* or *BMI1* expression and to perform enrichment analysis of the correlated genes using the R2: Genomics Analysis and Visualization Platform (http://r2.amc.nl). KEGG results and Gene Ontology Biological Process pathways were checked again and plotted using the R software environment v.3.4.4 [31] and the R package pathfindR v.1.2.1 [32] considering as significantly enriched pathways those with FDR < 0.05 in the function *run_pathfindR*. This function requires as input a dataset containing the gene identification (we used the HUGO symbol) the log fold change and corrected p-value of their expression to perform the cut-off. Here, we replaced the fold change for the r (correlation) value and the p-value for the p-value of this correlation. Thus, we could indicate those up- or downcorrelated genes with either *BMI1* or *CD133*.

Reverse Transcriptase Polymerase Chain Reaction (RT-qPCR)

The mRNA expression of stemness markers was analysed by RT-qPCR. Total RNA was extracted from MB cells using SV Total RNA Isolation System kit (Promega, Madison, USA), in accordance with the manufacturer's instructions and quantified in NanoDrop

(Thermo Fisher Scientific, Waltham, USA). The cDNA was obtained using GoScript Reverse System (Promega) according to the manufacturer's instructions. The mRNA expression levels of target genes (*BMI1* and *CD133*) were quantified using PowerUp SYBR Green Master Mix (Thermo Fisher Scientific.) The primers used for RT-qPCR amplification were designed according to the corresponding GenBank and are shown in Table 1. Expression of β-actin was measured as an internal control.

Western Blot

Cells were lysed after NaB treatment with 1X Lysis Buffer (Cell Lysis Buffer 10X, Cell Signaling Technology), and protein was quantified using the Bradford protein assay (Thermo Scientific). For blotting, 20 µg of protein were separated by SDS-PAGE and transferred to a PVDF membrane. After 1h with blocking solution (5%BSA in TTBS), the membrane was incubated overnight at 4 °C with primary antibodies against BMI1 (1:1000; Cell Signaling), Phospho-p44/42 MAPK (pErk1/2, 1:2000; Cell Signaling), p44/42 MAPK (Erk1/2, 1:1000; Cell Signaling) and β-actin (1:2000; Santa Cruz Biotechnology) as protein control. Incubation of primary antibodies was followed by incubation with the secondary antibody (1:2000; Sigma Aldrich) for 2 h. Chemoluminescence was detected using ECL Western Blotting substrate (Pierce, Thermo Scientific) and analyzed using ImageQuant LAS 500 (GE Healthcare Life Sciences, Little Chalfont, UK). Immunodetection signal were analyzed using ImageJ (National Institutes of Health, Bethesda, USA).

Neurosphere Formation

Neurosphere formation was used as an established experimental assay to evaluate cancer stem cell proliferation [23,33]. Daoy and D283 cells were dissociated with trypsin-EDTA

into a single cell suspension and seeded at 500 cells/well in 24-well low-attachment plates. The cells were cultured in serum-free sphere-induction medium, containing DMEM/F12 supplemented with 20 ng/ml epidermal growth factor (EGF, Sigma-Aldrich), 20 ng/ml basic fibroblast growth factor (Sigma-Aldrich), B-27 supplement 1X (Gibco), N-2 supplement 0.5X (Gibco), 50 μg/ml bovine serum albumin (Sigma Aldrich), and antibiotics during 7 days as previously described [23]. The ERK inhibitor U0126 was added in the first day after plating cells with the sphere-induction medium. Spheres photomicrographs were captured 7 days after treatment under an inverted phase microscope (Leica Microsystems, Mannheim Germany) at×10 magnification.

Statistics

Data are shown as mean ± standard deviation (SD). Statistical analysis was performed by one-way analysis of variance (ANOVA) followed by Tukey post-hoc tests for multiple comparisons. Experiments were replicated at least three times; *P* values under 0.05 were considered to indicate statistical significance. The GraphPad Prism 6 software (GraphPad Software, San Diego, USA) was used for analyses.

Table 1. Forward and reverse primers used for RT-qPCR amplification

Gene	Primer sense	Primer anti-sense
ACTB	5'- AAA CTG GAA CGG TGA AGG TG -3'	5'- AGA GAA GTG GGG TGG CTT TT -3'
BMI1	5′- TGC TTT GTG GAG GGT ACT TC -3'	5'- GTC TGG TCT TGT GAA CTT GGA -3'
CD133	5' GGC AAA TCA CCA GGT AAG AAC-3'	5'- AAC GCC TTG TCC TTG GTA G-3′

Results

HDAC Inhibition Impairs MB Cell Viability

Direct cell quantification after 48-h treatment with escalating doses of NaB confirmed a significant reduction in cell viability of both Daoy and D283 relative to vehicle. Consistently with a previous report [23], Daoy cells presented a somewhat higher sensibility to NaB than D283 cells. A dose of 2.5 mM reduced viability to 41.7% of control levels in Daoy cells ($P<0.0001$), whereas the same dose decreased D283 cell viability to 71% of control levels ($P<0.0001$). Lower doses of NaB, namely 0.25 mM in Daoy and 0.5 mM in D283 cells, did not significantly change cell numbers **(Fig. 1a)**.

In order to evaluate a biochemical indicator of efficacy, histone H3 acetylation was measured by ELISA in cells treated for 48 h. The effective doses of NaB (1.0 and 2.5 mM in Daoy, and 2.5 and 5.0 mM in D283) induced 2.42-fold and 3.03-fold increases (Daoy, $P < 0.0001$) and 2.5-fold and 5.7-fold increases (D283, $P = 0.005$ and $P < 0.0001$, respectively) in the levels of acetylated H3 compare to controls **(Fig. 1b)**. Notably, the levels of acetylated H3 were inversely correlated to the effect on cell viability.

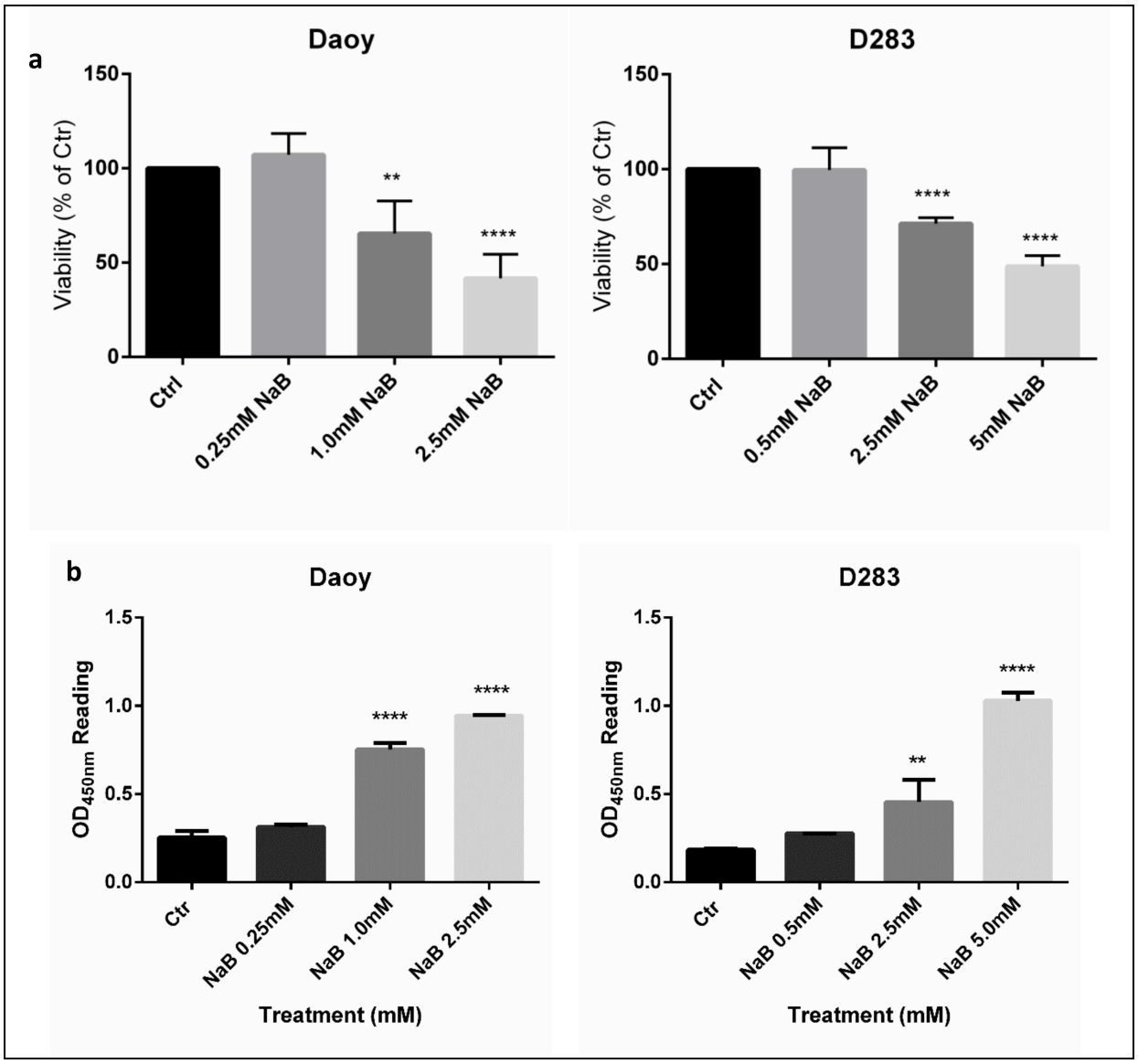

Fig. 1. HDAC inhibition hinders the viability of MB cells. **a** Daoy and D283 cells were treated with different concentrations of NaB, and the number of living cells was quantified using trypan blue exclusion assays. **b** H3 acetylation was determined by ELISA. Results represent the mean ± SD. of three independent experiments. ** $P < 0.01$; **** $P < 0.0001$ compared to controls (Ctr).

HDAC Inhibition Reduces the Expression of Stemness Markers and ERK Activation in MB Cells

To elucidate whether NaB could suppress MB viability by modulating the stemness phenotype, expression of *BMI1* and *CD133* was analyzed after 48 h of NaB treatment. The

both marks are expressed in all molecular subgroups of MB as observed in Cavalli et al. (2017) samples **(Fig. 2a)**. Experiments using RT-qPCR showed a reduction in mRNA levels of stemness markers *BMI1* and *CD133***.** In Daoy cells, mRNA expression of *BMI1* was reduced in cells treated with the higher dose of NaB (2.5 mM; $P = 0.0007$), whereas all doses of NaB (0.25, 1.0, and 2.5 mM) reduced *CD133* expression compared to controls (0.25 mM, $P = 0.018$; 1 mM, $P = 0.01$; 2.5 mM, $P = 0.0006$). In D283 cells, both doses that were effective when used in cell counting experiments (2.5 and 5 mM) reduced *BMI1* expression (2.5 mM, $p = 0.0017$; 5 mM, $P < 0.0001$), and *CD133* expression was reduced by all doses (0.5 mM, $P = 0.0198$; 2.5 mM and 5 mM, $P < 0.0001$) **(Fig. 2b)**.

The reduction in protein levels of BMI1 was confirmed after 24 h of NaB treatment in both cell lines at any dose capable of significantly impairing cell viability. After a 48-h treatment, Daoy cells maintained a consistent reduction in BMI1 protein levels compared to controls, and a significant reduction was found in D283 cells treated with the highest dose (5 mM) compared to controls ($P = 0.0023$) **(Fig. 2c)**.

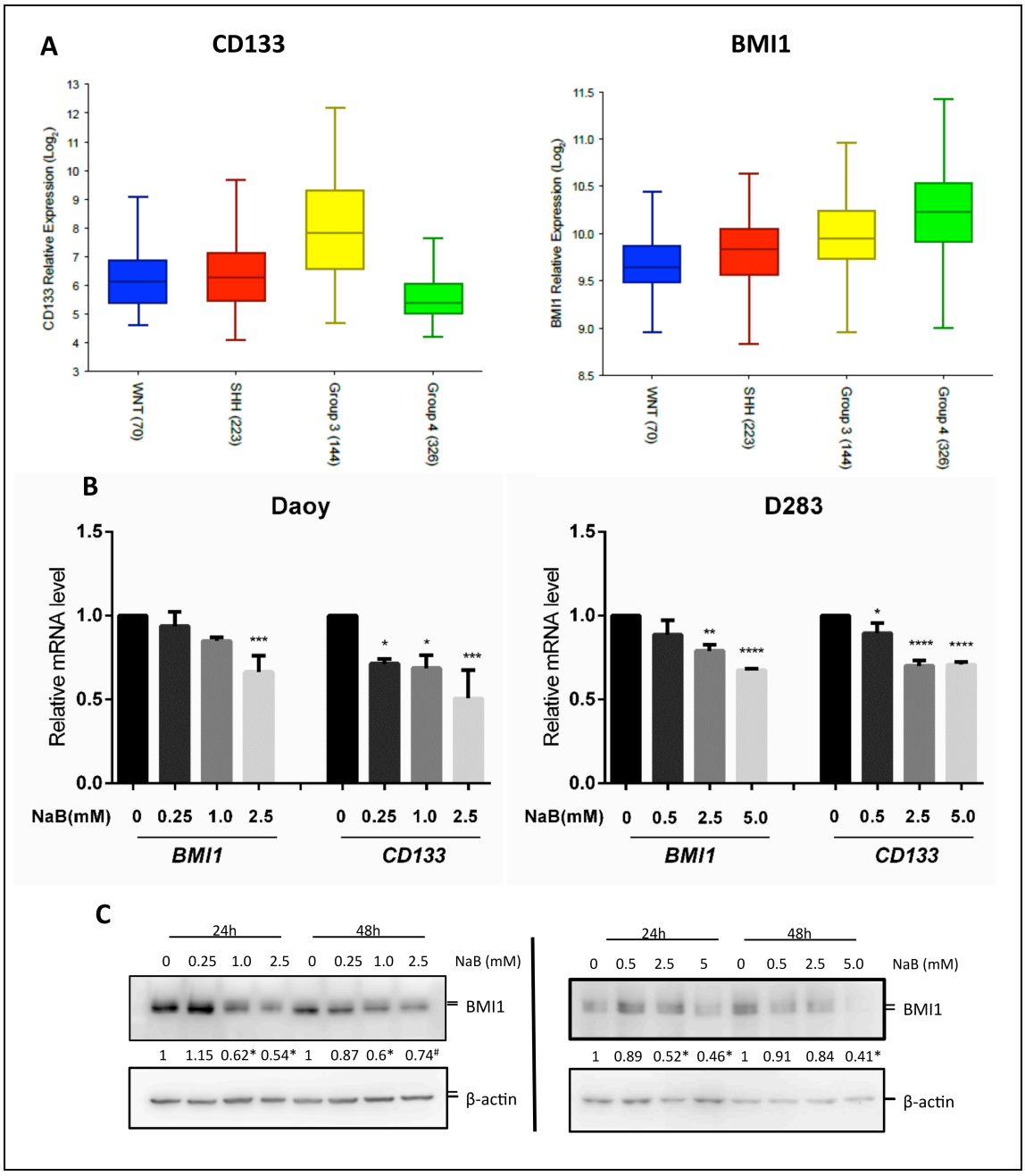

Fig. 2. HDAC inhibition reduces stemness in MB cells. **a** Representative boxplot of *CD133* and *BMI1* expression in the medulloblastoma molecular subgroups from Cavalli *et al.* **b** Relative mRNA levels of stemness markers were determined in control and NaB-treated Daoy and D283 MB cells by RT-qPCR using primers specific for *BMI1* and *CD133* as described in Materials and Methods. **c** Daoy and D283 cells were treated with different concentrations of NaB for 24 or 48h, cells were then harvested and the expression of BMI1 and β-actin (loading control) was determined by Western blot analysis. The relative expression of BMI1 (24 or 48 h), were determined by densitometric analysis of signals normalized for the corresponding β-actin signal. The analysis was performed using Image J software (NIH, Bethesda, MD). Results represent the mean ± SD of three independent experiments; * $P < 0.05$; ** $P < 0.01$; *** $P < 0.001$; **** $P < 0.0001$ compared to controls (Ctr).

MAPK/ERK signaling regulates normal CNS development. The enrichment analysis of the genes significantly correlated with *CD133* or *BMI1* expression showed MAPK signaling or associated pathways (like Neurotrophin and Erb signaling) as the most enriched process **(Fig. 3a)**. To investigate the status of the MAPK/ERK pathway in the MB cells after treatment with NaB, Western blotting was performed. NaB at any dose led to a decrease in ERK pathway activation measured by ERK phosphorylation in both cell lines after 48 h. Even in non-effective doses (0.25 mM in Daoy and 0.5 mM in D283 cells), a reduction of about 20% was observed, whereas doses that significantly affect cell viability reduced ERK activation in both cell lines *P*s < 0.0001) **(Fig. 3b, c)**.

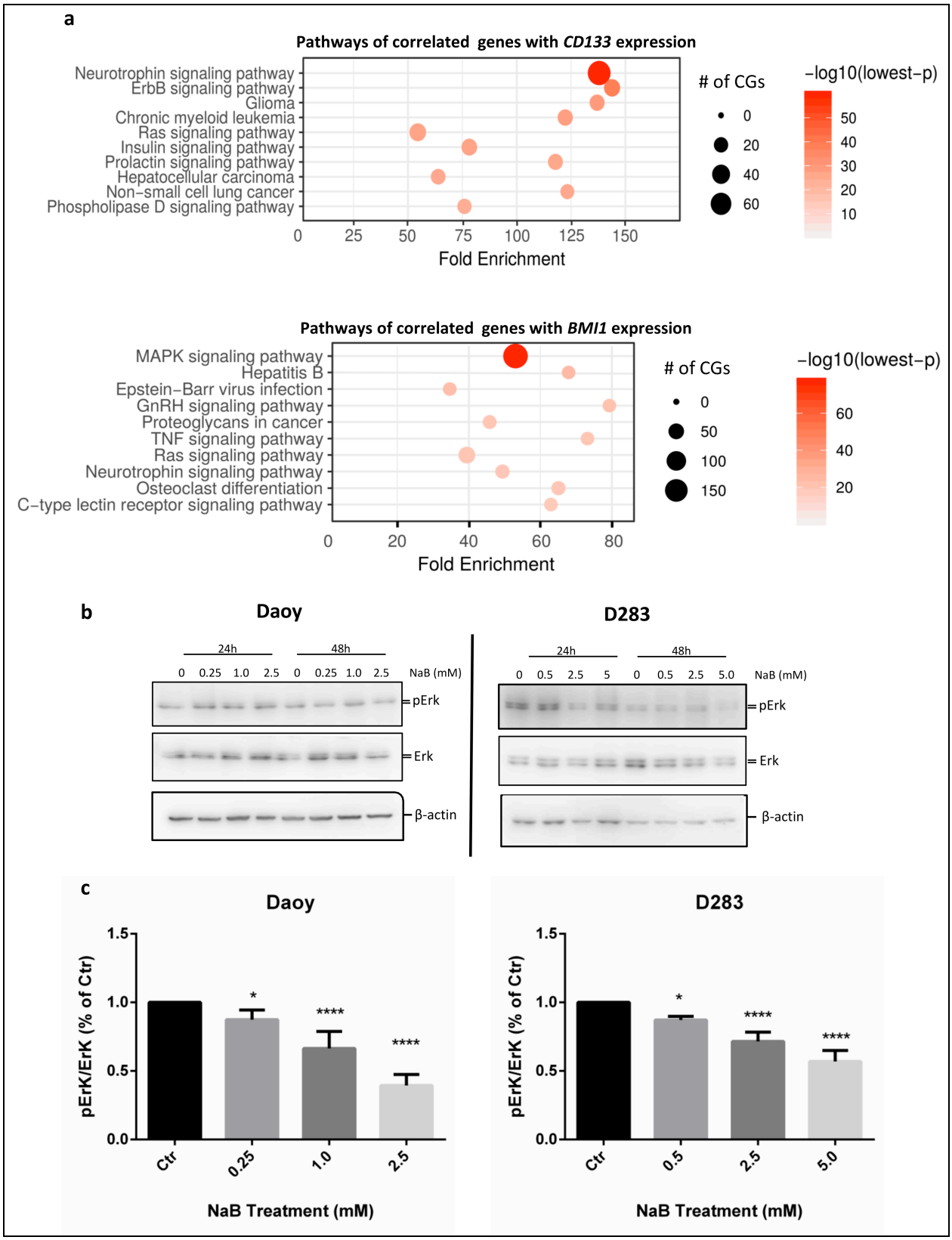

Legend of figure 3 on the next page.

Fig. 3. HDAC inhibition reduces ERK activation in MB cells. **a** Balloon plot of the 10 most representative KEGG pathways of *CD133* or *BMI1* correlated genes. # of CGs: number of correlated genes. Large circles indicate higher number of correlated genes. A darker color indicates a more significant *P* value **b** Daoy and D283 cells were treated with different concentrations of NaB for 24 or 48 h, cells were then harvested and the expression ERK, pERK and β-actin (loading control) was determined by Western blot analysis. The relative expression of ERK and p-ERK (48 h) were determined by densitometric analysis of signals normalized for the corresponding β-actin signal. The analysis was performed using Image J software (NIH, Bethesda, MD). Results represent the mean ± SD of three independent experiments; * $P < 0.05$; ** $P < 0.01$; *** $P < 0.001$; **** $P < 0.0001$ compared to controls (Ctr).

HDAC and MAPK/ERK Inhibition Cooperate to Reduce MB Growth

To determine the effect of ERK inhibition on stemness markers in MB cells, mRNA expression of *BMI1* and *CD133* was measured after 48 h of treatment with the MEK1/2 inhibitor U0126 (12.5, or 25 μM). *CD133* expression decreased significantly after treatment in both cell lines (Daoy, $P = 0.0001$ and $P < 0.0001$; D283, $P = 0.02$ and $P < 0.0001$). Reductions in *BMI1* were observed in both cell lines (Daoy, 12.5 μM, $P = 0.0094$; 25 μM, $P = 0.0016$; D283, 25 μM, $P = 0.0436$) **(Fig. 4a)**.

Given that there is a possible relationship between the stemness phenotype and cell viability, cell counting after treatment with U0126 with or without NaB was performed. U0126 (25 μM) significantly reduced MB cell viability (Daoy, $P = 0.0008$; D283, $P < 0.0001$). Combined treatment of the highest dose of U0126 (25 μM) plus NaB (1.0 or 2.5 mM in Daoy and 2.5 or 5 mM in D283) produced more robust inhibition of cell proliferation than either inhibitor alone at the same doses in both cell lines. **(Fig. 4b)**.

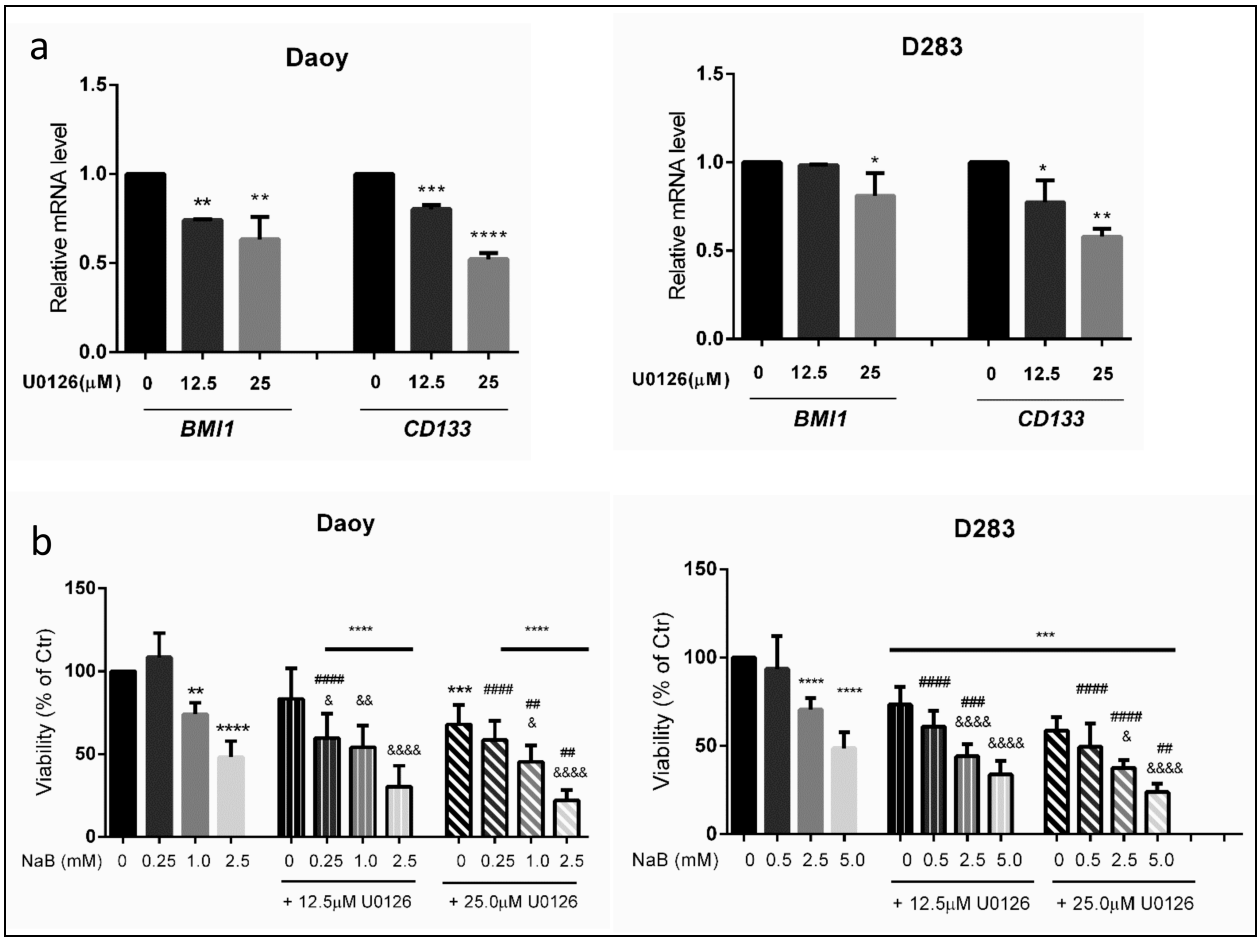

Fig. 4. Inhibition of HDAC and ERK impairs MB cell proliferation. **a** Relative mRNA levels of stemness markers were determined in control and U0126 -treated Daoy and D283 MB cells by RT-qPCR, using primers specific for *BMI1* and *CD133*. **b** Daoy and D283 cells were treated with different concentrations of NaB alone or in combination with the ERK inhibitor U0126, and the number of living cells were quantified using trypan blue exclusion assays. Results represent the mean ± SD of three independent experiments; * $P < 0.5$; ** $P < 0.01$; *** $P < 0.001$; **** $P < 0.0001$ compared to controls (Ctr); $^{\#}P < 0.05$; $^{\#\#}P < 0.01$; $^{\#\#\#}P < 0.001$; $^{\#\#\#\#}P < 0.0001$ compared to respective NaB dose; $^{\&}P < 0.05$; $^{\&\&\&\&}P < 0.0001$ compared to respective U0126 dose.

MAPK/ERK Inhibition Hinders the Expansion of Putative MB CSCs

A neurosphere assay was performed to investigate the formation of MB CSCs. First, the mRNA expression of *CD133* and *BMI1* was measured to confirm enrichment of stemness after sphere formation. Expression of both markers was increased in neurospheres compared to monolayer cultures. After 7 days of culturing cells in appropriated medium for expansion of stem cells, *BMI1* expression was increased 1.68-fold in Daoy ($P = 0.0006$) and to 2.0-fold in D283 ($P = 0.0028$) cells, while *CD133*

expression increased 2.89-fold in Daoy ($P = 0.0005$) and to 2.36-fold in D283 ($P < 0.0001$) cells in comparison to controls **(Fig. 5a)**. After MAPK/ERK inhibition (12.5 or 25 μM), cells were unable to form neurospheres **(Fig. 5b)**. These results suggest an essential role of ERK signalling in MB stem cell formation.

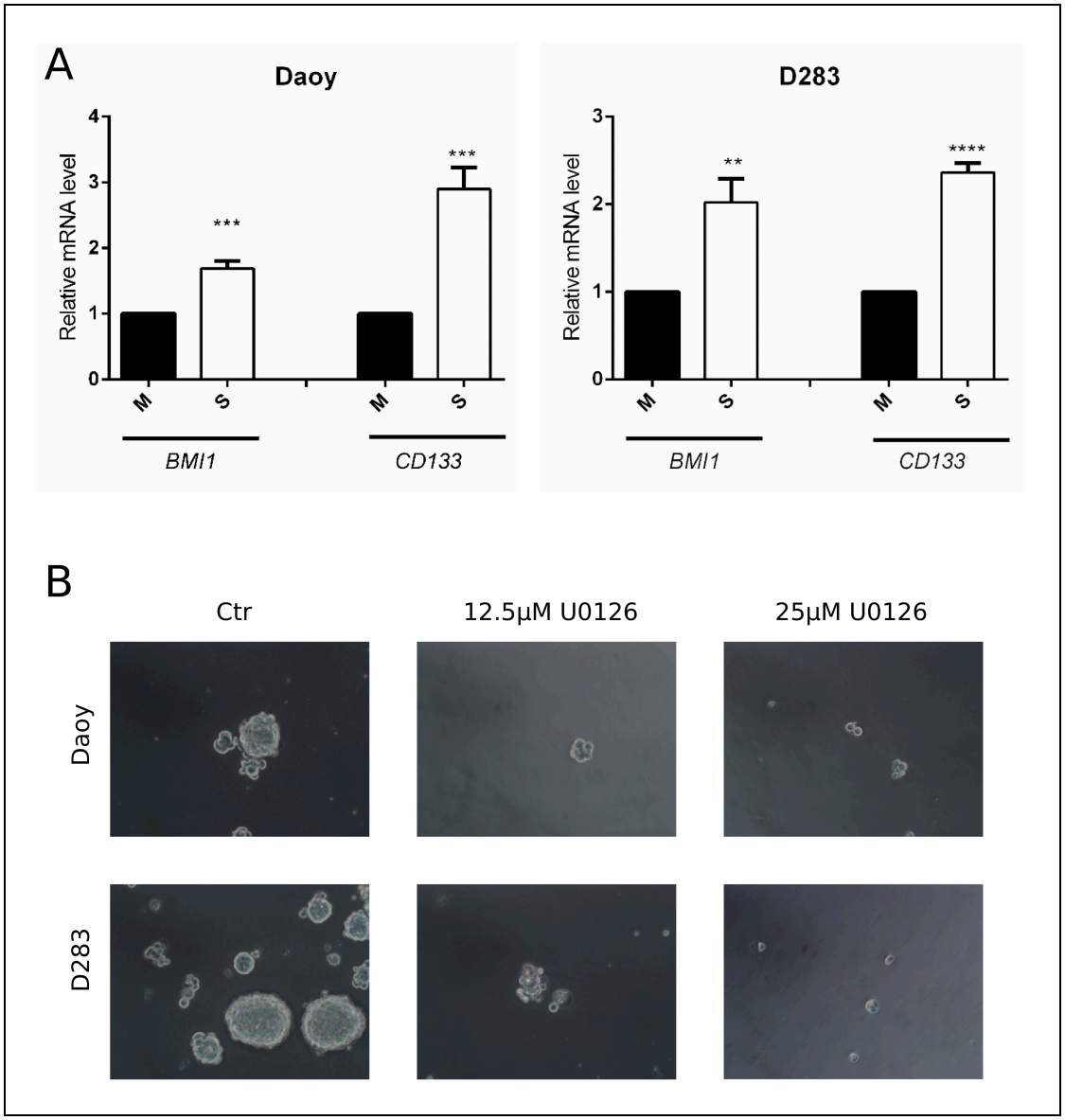

Fig. 5. ERK inhibition avoid MB stem cell formation. **a** Daoy and D283 cells were cultured in medium specific for stem cell expansion during 7 days for enrichment of neurospheres. Relative mRNA levels of stemness markers were determined in monolayer (M) and sphere (S) cultures by RT-qPCR using primers specific for *BMI1* and *CD133* as described in Materials and Methods. **b** Representative photomicrographs of neurospheres after 7 days of induction in the absence (Ctr) or presence of the ERK inhibitor U0126 (12.5 or 25 μM) in the first day of induction. Results represent the mean ± SD of three independent experiments; ** $P < 0.01$; *** $P < 0.001$; **** $P < 0.0001$ compared to controls.

Discussion

MB is a pediatric brain tumor featuring a high frequency of mutations in epigenetic modifier genes [34,35]. Deregulation in epigenetic programming has been linked to tumorigenesis, possibly through induction of a stemness phenotype [36]. Histone acetylation status is related to cancer stemness regulation, and HDAC inhibition constitutes an important therapeutic strategy to induce differentiation in CSCs [37].

We have previously shown responsiveness of human MB cells and putative MB CSCs to NaB [23]. Here, we used the same compound to investigate the influence of HDAC inhibition on maintenance of a stemness phenotype of MB. We confirmed that the effect of NaB is associated with its capability to increase histone acetylation. We have also shown a reduction in markers of stemness and inhibition of MAPK/ERK signalling. Moreover, HDAC and MEK1/2 inhibitors cooperate to reduce viability in MB cells and, as with HDACi, MAPK/ERK inhibition hinders neurosphere formation.

Expression of *CD133* and *BMI1* was significantly decreased after NaB treatment. CD133, also called Prominin-1, is the most used marker to isolate and to identify brain tumor CSCs [38]. BMI1 is a polycomb group protein overexpressed in MB [28] and present in CSC [39]. Patients with metastatic MB show higher levels of *CD133* and a worse prognostic when compared with non-metastatic patients [40]. *In vitro* characterization of CD133-positive cells demonstrates that they present increased migration and invasion capabilities and higher expression of stemness-associated genes compared to the parental cell line. In addition, CD133-positive, but not CD133-negative cells, are invasive *in vivo* [41, 42]. These functional features of CD133-positive cells are associated with a stemness genetic signature. The volume of xenografted tumors is reduced

by treatments that inhibit the expression of stemness-related genes such as *SOX2*, *Nestin*, *Nanog*, *Oct4* and *BMI1* [42, 43]. BMI-1, another marker of poor outcomes in MB [43], is also involved in tumor invasion, as indicated by evidence that BMI1 knockdown in MB cells decreases infiltration of xenotransplants [44].

We observed a decrease in phosphorylated ERK (pERK) in MB cells after NaB treatment. Components of the ERK pathway are up-regulated in metastatic MB, and pharmacological inhibition of ERK decreases migration of MB cells [45]. In carcinoma and sarcoma cell lines, ERK reduces the stem-like characteristics of tumor cells [46]. In our study, ERK inhibition reduced the expression level of stemness markers and enhanced the antiproliferative effect of NaB. In agreement with our results, Ozaki and colleagues have shown an increase in HDACi-induced cell death after specific inhibition of the ERK pathway by the generation of reactive oxygen species [47, 48]. Although our study has not evaluated the mechanisms mediating functional interactions between HDAC and ERK inhibitors, our findings suggest that both types of compounds are involved in stemness modulation.

The influence of ERK activity in regulating the stemness phenotype was showed in a neurosphere model [49]. Expansion of neurospheres resulted in an enrichment of the stemness phenotype in cell cultures, as indicated by increased levels of *CD133* and *BMI1* content in comparison with a monolayer culture. We found that pharmacological inhibition of ERK impairs MB neurosphere formation. The role of ERK signaling was already described in other tumor stem-like cells [50,51]. In embryonal rhabdomyosarcoma stem-like cells, the inhibition of ERK decrease sphere formation, induce myogenic differentiation, and reduce tumorigenicity *in vivo* [50]. In glioblastoma CSCs, ERK inhibition also limited the capacity to form tumors in nude mice and promote cell

differentiation. Consistently with our results, ERK inhibition of glioblastoma CSCs reduces the expression of stemness markers, including *BMI1* [51].

In MB, Chow and collegues showed differential ERK signalling activation and neurosphere formation capability in MB cells from spontaneous tumors obtained from Patched (Ptch)+/- mice [52]. Tumors that were able to form neurospheres independently of the presence of growth factors (EGF and basic fibroblast growth factor) had a higher activation of the ERK pathway compared to those tumors dependent on growth factors or not capable of forming spheres. Interestingly, tumors derived from growth factors independent neurospheres cells presented higher tumorigenicity potential and lethality [52].

In summary, our results provide evidence indicating that HDAC inhibition can modulate the stemness phenotype, by reducing the expression of stemness markers *CD133* and *BMI1*, and decreasing ERK activity, in MB. Combined inhibition of HDAC and ERK signaling was more effective in reducing MB cell viability than single-drug treatments. To our knowledge, this is the first report to indicate that ERK inhibition impairs MB CSC formation/survival. We suggest the combination of HDAC and ERK inhibitors as an experimental therapeutic approach in MB, which should be further investigated with the use of additional experimental approaches such as *in vivo* models.

Acknowledgements

This research was supported by the National Council for Scientific and Technological Development (CNPq; grant numbers 409287/2016-4 and 303276/2013-4 to

R.R. and graduate fellowship to MCJ); PRONON/Ministry of Health, Brazil (number 25000.162.034/2014-21); the Children's Cancer Institute (ICI); the Coordination for the Improvement of Higher Education Personnel (CAPES - Finance Code 001); the Clinical Hospital institutional research fund (FIPE/HCPA). T.F. is supported by Programa Nacional de Pós-Doutorado (PNPD) CAPES/HCPA (Process number: 88887.160608/2017-00). C.N. is supported by the National Council for Scientific and Technological Development (CNPq: grant number 201001/2014-4) and the William Donald Nash fellowship from the Brain Tumour Foundation of Canada. V.R. is supported by operating funds from the Canadian Institutes for Health Research, the American Brain Tumour Association, and the Brain Tumour Foundation of Canada.

References

1. Wang J, Wechsler-Reya RJ (2014) The role of stem cells and progenitors in the genesis of medulloblastoma. Exp Neurol 260: 69-73.

2. Taylor MD, Northcott PA, Korshunov A, Remke M, Cho YJ, Clifford SC, Eberhart CG, Parsons DW, et al. (2012) Molecular subgroups of medulloblastoma: the current consensus. Acta Neuropathol 123: 465-472.

3. Louis DN, Perry A, Reifenberger G, von Deimling A, Figarella-Branger D, Cavenee WK, Ohgaki H, Wiestler OD, et al. (2016) The 2016 World Health Organization Classification of Tumors of the Central Nervous System: a summary. Acta Neuropathol 131: 803-820.

4. Schwalbe EC, Lindsey JC, Nakjang S, Crosier S, Smith AJ, Hicks D, Rafiee G, Hill RM, et al. (2017) Novel molecular subgroups for clinical classification and outcome prediction in childhood medulloblastoma: a cohort study. Lancet Oncol 18: 958-971.

5. Sabel M, Fleischhack G, Tippelt S, Gustafsson G, Doz F, Kortmann R, Massimino M, Navajas A, et al. (2016) Relapse patterns and outcome after relapse in standard risk medulloblastoma: a report from the HIT-SIOP-PNET4 study. J Neurooncol 129: 515-524.

6. Peitzsch C, Tyutyunnykova A, Pantel K, Dubrovska A (2017) Cancer stem cells: The root of tumor recurrence and metastases. Semin Cancer Biol 44: 10-24.

7. Kreso A, Dick JE (2014) Evolution of the cancer stem cell model. Cell Stem Cell 14: 275-291.

8. Singh SK, Hawkins C, Clarke ID, Squire JA, Bayani J, Hide T, Henkelman RM, Cusimano MD, et al. (2004) Identification of human brain tumour initiating cells. Nature 432: 396-401.

9. Hemmati HD, Nakano I, Lazareff JA, Masterman-Smith M, Geschwind DH, Bronner-Fraser M, Kornblum HI (2003) Cancerous stem cells can arise from pediatric brain tumors. Proc Natl Acad Sci U S A 100: 15178-15183.

10. Hambardzumyan D, Becher OJ, Rosenblum MK, Pandolfi PP, Manova-Todorova K, Holland EC (2008) PI3K pathway regulates survival of cancer stem cells residing in the perivascular niche following radiation in medulloblastoma in vivo. Genes Dev 22: 436-448.

11. Annabi B, Rojas-Sutterlin S, Laflamme C, Lachambre MP, Rolland Y, Sartelet H, Beliveau R (2008) Tumor environment dictates medulloblastoma cancer stem cell expression and invasive phenotype. Mol Cancer Res 6: 907-916.

12. Lu KH, Chen YW, Tsai PH, Tsai ML, Lee YY, Chiang CY, Kao, CL, Chiou SH, et al. (2009) Evaluation of radiotherapy effect in resveratrol-treated medulloblastoma cancer stem-like cells. Childs Nerv Syst 25: 543-550.

13. Yu CC, Chiou GY, Lee YY, Chang YL, Huang PI, Cheng YW, Tai LK, Ku HH, et al. (2010) Medulloblastoma-derived tumor stem-like cells acquired resistance to TRAIL-induced apoptosis and radiosensitivity. Childs Nerv Syst 26: 897-904.

14. Liu J, Chi N, Zhang JY, Zhu W, Bian YS, Chen HG (2015) Isolation and characterization of cancer stem cells from medulloblastoma. Genet Mol Res 14: 3355-3361.

15. Klonou A, Spiliotakopoulou D, Themistocleous MS, Piperi C, Papavassiliou AG (2018) Chromatin remodeling defects in pediatric brain tumors. Ann Transl Med 6: 248.

16. Ververis K, Hiong A, Karagiannis TC, Licciardi PV (2013) Histone deacetylase inhibitors (HDACIs): multitargeted anticancer agents. Biologics 7: 47-60.

17. Frumm SM, Fan ZP, Ross KN, Duvall JR, Gupta S, VerPlank L, Suh BC, Holson E, et al. (2013) Selective HDAC1/HDAC2 inhibitors induce neuroblastoma differentiation. Chem Biol 20: 713-725.

18. Souza BK, da Costa Lopez PL, Menegotto PR, Vieira IA, Kersting N, Abujamra AL, Brunetto AT, Brunetto AL, et al. (2018) Targeting histone deacetylase activity to arrest cell growth and promote neural differentiation in Ewing sarcoma. Mol Neurobiol 55: 7242-7258.

19. Li XN, Parikh S, Shu Q, Jung HL, Chow CW, Perlaky L, Leung HC, Su J, et al. (2004) Phenylbutyrate and phenylacetate induce differentiation and inhibit proliferation of human medulloblastoma cells. Clin Cancer Res 10: 1150-1159.

20. Sonnemann J, Kumar KS, Heesch S, Muller C, Hartwig C, Maass M, Bader P, Beck JF (2006) Histone deacetylase inhibitors induce cell death and enhance the susceptibility to ionizing radiation, etoposide, and TRAIL in medulloblastoma cells. Int J Oncol 28: 755-766.

21. Spiller SE, Ditzler SH, Pullar BJ, Olson JM (2008) Response of preclinical medulloblastoma models to combination therapy with 13-cis retinoic acid and suberoylanilide hydroxamic acid (SAHA). J Neurooncol 87: 133-141.

22. Marino AM, Sofiadis A, Baryawno N, Johnsen JI, Larsson C, Vukojevic V, Ekstrom TJ (2011) Enhanced effects by 4-phenylbutyrate in combination with RTK inhibitors on proliferation in brain tumor cell models. Biochem Biophys Res Commun 411: 208-212.

23. Nor C, Sassi FA, de Farias CB, Schwartsmann G, Abujamra AL, Lenz G, Brunetto AL, Roesler R (2013) The histone deacetylase inhibitor sodium butyrate promotes cell death and differentiation and reduces neurosphere formation in human medulloblastoma cells. Mol Neurobiol 48: 533-543.

24. Yuan J, Llamas Luceno N, Sander B, Golas MM (2017) Synergistic anti-cancer effects of epigenetic drugs on medulloblastoma cells. Cell Oncol (Dordr) 40: 263-279.

25. Phi JH, Choi SA, Kwak PA, Lee JY, Wang KC, Hwang DW, Kim SK (2017) Panobinostat, a histone deacetylase inhibitor, suppresses leptomeningeal seeding in a medulloblastoma animal model. Oncotarget 8: 56747-56757.

26. Glinsky GV, Berezovska O, Glinskii AB (2005) Microarray analysis identifies a death-from-cancer signature predicting therapy failure in patients with multiple types of cancer. J Clin Invest 115: 1503-1521.

27. Shats I, Gatza ML, Chang JT, Mori S, Wang J, Rich J, Nevins JR (2011) Using a stem cell-based signature to guide therapeutic selection in cancer. Cancer Res 71: 1772-1780.

28. Leung C, Lingbeek M, Shakhova O, Liu J, Tanger E, Saremaslani P, Van Lohuizen M, Marino S (2004) Bmi1 is essential for cerebellar development and is overexpressed in human medulloblastomas. Nature 428: 337-341.

29. Armstrong L, Hughes O, Yung S, Hyslop L, Stewart R, Wappler I, Peters H, Walter T, et al. (2006) The role of PI3K/AKT, MAPK/ERK and NFkappabeta signalling in the maintenance of human embryonic stem cell pluripotency and viability highlighted by transcriptional profiling and functional analysis. Hum Mol Genet 15: 1894-1913.

30. Cavalli F, Remke M, Rampasek L, Peacock J, Shih D, Luu B, Garzia L. Torchia J, et al. (2017) Intertumoral Heterogeneity within Medulloblastoma Subgroups. Cancer cell 31(6): 737-754.e6

31. R Core Team (2018). R: A language and environment for statistical computing. R Foundation for Statistical Computing, Vienna, Austria. URL <https://www.R-project.org/>.

32. Ulgen E, Ozisik O, Sezerman OU. (2018) pathfindR: An R Package for Pathway Enrichment Analysis Utilizing Active Subnetworks. bioRxiv. DOI: <https://doi.org/10.1101/272450>.

33. Zanini C, Ercole E, Mandili G, Salaroli R, Poli A, Renna C, Papa V, Cenacchi G, et al. (2013) Medullospheres from DAOY, UW228 and ONS-76 cells: increased stem cell population and proteomic modifications. PLoS One 8: e63748.

34. Robinson G, Parker M, Kranenburg TA, Lu C, Chen X, Ding L, Phoenix TN, Hedlund E, et al. (2012) Novel mutations target distinct subgroups of medulloblastoma. Nature 488: 43-48.

35. Huether R, Dong L, Chen X, Wu G, Parker M, Wei L, Ma J, Edmonson MN, et al. (2014) The landscape of somatic mutations in epigenetic regulators across 1,000 paediatric cancer genomes. Nat Commun 5: 3630.

36. Hadjimichael C, Chanoumidou K, Papadopoulou N, Arampatzi P, Papamatheakis J, Kretsovali A (2015) Common stemness regulators of embryonic and cancer stem cells. World J Stem Cells 7: 1150-1184.

37. Liu N, Li S, Wu N, Cho KS (2017) Acetylation and deacetylation in cancer stem-like cells. Oncotarget 8: 89315-89325.

38. Schonberg DL, Lubelski D, Miller TE, Rich JN (2014) Brain tumor stem cells: Molecular characteristics and their impact on therapy. Mol Aspects Med 39: 82-101.

39. Manoranjan B, Wang X, Hallett RM, Venugopal C, Mack SC, McFarlane N, Nolte SM, Scheinemann K, et al. (2013) FoxG1 interacts with Bmi1 to regulate self-renewal and tumorigenicity of medulloblastoma stem cells. Stem Cells 31: 1266-1277.

40. Raso A, Mascelli S, Biassoni R, Nozza P, Kool M, Pistorio A, Ugolotti E, Milanaccio C, et al. (2011) High levels of PROM1 (CD133) transcript are a potential predictor of poor prognosis in medulloblastoma. Neuro Oncol 13: 500-508.

41. Chen KH, Hsu CC, Song WS, Huang CS, Tsai CC, Kuo CD, Hsu HS, Tsai TH, et al. (2010) Celecoxib enhances radiosensitivity in medulloblastoma-derived CD133-positive cells. Childs Nerv Syst 26: 1605-1612.

42. Chang CJ, Chiang CH, Song WS, Tsai SK, Woung LC, Chang CH, Jeng SY, Tsai CY, et al. (2012) Inhibition of phosphorylated STAT3 by cucurbitacin I enhances chemoradiosensitivity in medulloblastoma-derived cancer stem cells. Childs Nerv Syst 28: 363-373.

43. Zakrzewska M, Zakrzewski K, Gresner SM, Piaskowski S, Zalewska-Szewczyk B, Liberski PP (2011) Polycomb genes expression as a predictor of poor clinical outcome in children with medulloblastoma. Childs Nerv Syst 27: 79-86.

44. Wang X, Venugopal C, Manoranjan B, McFarlane N, O'Farrell E, Nolte S, Gunnarsson T, Hollenberg R, et al. (2012) Sonic hedgehog regulates Bmi1 in human medulloblastoma brain tumor-initiating cells. Oncogene 31: 187-199.

45. MacDonald TJ, Brown KM, LaFleur B, Peterson K, Lawlor C, Chen Y, Packer RJ, Cogen P, et al. (2001) Expression profiling of medulloblastoma: PDGFRA and the RAS/MAPK pathway as therapeutic targets for metastatic disease. Nat Genet 29: 143-152.

46. Tabu K, Kimura T, Sasai K, Wang L, Bizen N, Nishihara, H. Taga T, Tanaka S, et al. (2010) Analysis of an alternative human CD133 promoter reveals the implication of Ras/ERK pathway in tumor stem-like hallmarks. Mol Cancer 9: 39.

47. Ozaki K, Minoda A, Kishikawa F, Kohno M (2006) Blockade of the ERK pathway markedly sensitizes tumor cells to HDAC inhibitor-induced cell death. Biochem Biophys Res Commun 339: 1171-1177.

48. Ozaki K, Kosugi M, Baba N, Fujio K, Sakamoto T, Nishihara H, Taga T, Tanaka S (2010) Blockade of the ERK or PI3K-Akt signaling pathway enhances the cytotoxicity of histone deacetylase inhibitors in tumor cells resistant to gefitinib or imatinib. Biochem Biophys Res Commun 391: 1610-1615.

49. Ishiguro T, Ohata H, Sato A, Yamawaki K, Enomoto T, Okamoto K (2017) Tumor-derived spheroids: Relevance to cancer stem cells and clinical applications. Cancer Sci 108: 283-289.

50. Ciccarelli C, Vulcano F, Milazzo L, Gravina GL, Marampon F, Macioce G, Giampaolo A, Tombolini, V (2016) Key role of MEK/ERK pathway in sustaining tumorigenicity and in vitro radioresistance of embryonal rhabdomyosarcoma stem-like cell population. Mol Cancer 15: 16.

51. Sunayama J, Matsuda K, Sato A, Tachibana K, Suzuki K, Narita Y, Shibui S, Sakurada K, et al. (2010) Crosstalk between the PI3K/mTOR and MEK/ERK pathways involved in the maintenance of self-renewal and tumorigenicity of glioblastoma stem-like cells. Stem Cells 28: 1930-1939.

52. Adamson PC, Houghton PJ, Perilongo G, Pritchard-Jones K (2014) Drug discovery in paediatric oncology: roadblocks to progress. Nat Rev Clin Oncol 11: 732-739.

CAPÍTULO I: Resultados Adicionais

Childs Nerv Syst (2016) 32:61–64
DOI 10.1007/s00381-015-2963-4

BRIEF COMMUNICATION

Viability of D283 medulloblastoma cells treated with a histone deacetylase inhibitor combined with bombesin receptor antagonists

Mariane Jaeger[1] · Eduarda C. Ghisleni[1] · Lívia Fratini[1] · Algemir L. Brunetto[1,2] · Lauro José Gregianin[3] · André T. Brunetto[2] · Gilberto Schwartsmann[1,4] · Caroline B. de Farias[1,2] · Rafael Roesler[1,5]

Received: 27 August 2015 / Accepted: 13 November 2015 / Published online: 20 November 2015

Abstract
Purpose Medulloblastoma (MB) comprises four distinct molecular subgroups, and survival remains particularly poor in patients with Group 3 tumors. Mutations and copy number variations result in altered epigenetic regulation of gene expression in Group 3 MB. Histone deacetylase inhibitors (HDACi) reduce proliferation, promote cell death and neuronal differentiation, and increase sensitivity to radiation and chemotherapy in experimental MB. Bombesin receptor antagonists potentiate the antiproliferative effects of HDACi in lung cancer cells and show promise as experimental therapies for several human cancers. Here, we examined the viability of D283 cells, which belong to Group 3 MB, treated with an HDACi alone or combined with bombesin receptor antagonists.
Methods D283 MB cells were treated with different doses of the HDACi sodium butyrate (NaB), the neuromedin B receptor (NMBR) antagonist BIM-23127, the gastrin releasing peptide receptor (GRPR) antagonist RC-3095, or combinations of NaB with each receptor antagonist. Cell viability was examined by cell counting.
Results NaB alone or combined with receptor antagonists reduced cell viability at all doses tested. BIM-23127 alone did not affect cell viability, whereas RC-3095 at an intermediate dose significantly increased cell number.
Conclusion Although HDACi are promising agents to inhibit MB growth, the present results provide preliminary evidence that combining HDACi with bombesin receptor antagonists is not an effective strategy to improve the effects of HDACi against MB cells.

Keywords Neuromedin B receptor · Gastrin-releasing peptide receptor · Sodium butyrate · Brain tumor

✉ Rafael Roesler
rroesler@terra.com.br

[1] Cancer and Neurobiology Laboratory, Experimental Research Center, Clinical Hospital (CPE-HCPA), Federal University of Rio Grande do Sul, Porto Alegre, RS, Brazil

[2] Children's Cancer Institute (ICI), Porto Alegre, RS, Brazil

[3] Department of Pediatrics, Faculty of Medicine, Federal University of Rio Grande do Sul, Porto Alegre, RS, Brazil

[4] Department of Internal Medicine, Faculty of Medicine, Federal University of Rio Grande do Sul, Porto Alegre, RS, Brazil

[5] Department of Pharmacology, Institute for Basic Health Sciences, Federal University of Rio Grande do Sul, Rua Sarmento Leite, 500 (ICBS, Campus Centro/UFRGS), Porto Alegre, RS 90050-170, Brazil

Introduction

Medulloblastoma (MB) is the most common malignant pediatric brain tumor [1] and comprises four distinct molecular subgroups [2]. Group 3 MB, characterized by amplification of *MYC*, is resistant to conventional therapy and has a particularly poor prognosis [3]. The rapidly dividing D283 MB cell line [4] has been recently characterized as a model of Group 3 MB [5].

Histone deacetylase inhibitors (HDACi) increase histone acetylation, a crucial epigenetic mechanism regulating chromatin remodeling [6]. Alterations in genes related to histone acetylation and methylation have been implicated in MB [7]. In Group 3 MB, mutations and copy number variations result in aberrant H3K27 and H3K4 histone lysine methylation patterns [8], and the HDAC2 type of class I HDAC is overexpressed [9]. HDACi reduce proliferation, promote cell

death and neuronal differentiation, and increase sensitivity to radiation and chemotherapy in MB cells in vitro [10, 11], in addition to inhibiting the in vivo growth of D283 MB in nude mice [12]. Inhibitors of class I HDACs reduce metabolic activity, cell number, and viability, with *MYC*-amplified Group 3 cell lines being particularly sensitive [9].

Emerging therapeutic targets in MB also include growth factor receptors [13]. Two types of bombesin-like peptide receptors, the neuromedin B receptor (NMBR or BB1) and the gastrin-releasing peptide receptor (GRPR or BB2), are often overexpressed in human tumors and contribute to cancer growth [14, 15]. However, the role of NMBR and GRPR in MB remains unclear.

Bombesin receptor antagonists influence the effects of HDACi in some tumor types. GRPR antagonists potentiate the inhibitory effects of HDACi on proliferation of human lung cancer cells [16]. In contrast, a stimulatory effect of a high dose of the GRPR antagonist RC-3095 on murine neuroblastoma cells is prevented by the HDACi sodium butyrate (NaB), suggesting that GRPR might interact with epigenetic mechanisms in regulating neuroblastoma cell growth [17].

The evidence reviewed above suggests that HDACi combined with bombesin receptor antagonists might display antitumor effects against Group 3 MB. Here, we report the effects of the HDACi NaB alone or combined with NMBR and GRPR antagonists on the viability of D283 MB cells in vitro.

Materials and methods

Cell culture

The D283 human MB cell line was originally obtained from the American Type Culture Collection (Rockville, MD, USA) and kindly donated by Dr. Michael D. Taylor (The Hospital for Sick Children, Toronto, Canada). Cells were grown and maintained in Dulbecco's modified Eagle's medium (DMEM; GibcoBRL, Carlsbad, USA) containing 2 % (*w*/*v*) H-glutamine and 10 % (*v*/*v*) fetal bovine serum (FBS, Sorali, Campo Grande, Brazil). Cells were kept at a temperature of 37 °C, a minimum relative humidity of 95 %, and an atmosphere of 5 % CO_2 in air.

Cell viability and treatments

Cells were seeded at 3×10^3 cells per well in DMEM/10 % FBS into 96-well plates and allowed to grow for 24 h. The medium was replaced, and NaB (5 or 7.5 mM; Sigma-Aldrich, St. Louis, USA), the NMBR antagonist BIM-23127 (0.1, 1, or 10 μM; Sigma-Aldrich, St. Louis, USA), the GRPR antagonist RC-3095 (0.01, 0.1, or 1 μM; Zentaris GmbH, Frankfurt, Germany), or the combinations of NaB with each antagonist were added to the culture. Cell counting was carried out 48 h after treatment. The medium was removed, cells were washed with Hank's Balanced Salt Solution (HBSS, Invitrogen, São Paulo, Brazil), and 50 μM of 0.25 % trypsin/EDTA solution was added to detach cells. Cell suspension was homogenized with 0.4 % Trypan blue 1:1 then immediately counted in a hemocytometer [18, 19]. Experiments were performed three times with four to six replicates for each drug concentration.

Statistics

Data are shown as mean ± standard error of the mean (SEM) number of cells. Differences between mean values were evaluated by one-way analysis of variance (ANOVA) followed by LSD post hoc tests. In all comparisons, $p < 0.05$ indicates statistical significance.

Results

NaB at 5 or 7.5 mM reduced cell counting by about 45 and 62 %, respectively, (both *p*s < 0.01). A similar pattern of results was obtained when NaB was combined with BIM-23127; at all dose combinations, a significant reduction (ranging from about 35 to about 75 %) in cell viability was observed. Treatment with BIM-23127 alone did not significantly affect cell viability (Fig. 1).

The GRPR antagonist RC-3095 at the dose of 0.1 μM induced a significant increase of about 36 % in cell number ($p < 0.05$). Treatment with NaB at either dose, as well as any combination of NaB with RC-3095, significantly inhibited cell viability, ranging from about 51 to about 44 % (all *p*s < 0.01; Fig. 2).

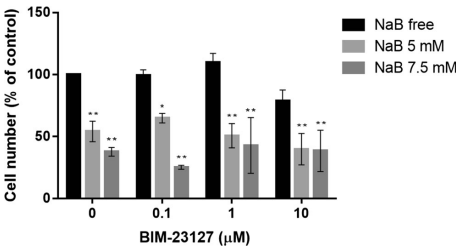

Fig. 1 Viability of D283 MB cells after treatment with an NMBR antagonist, an HDACi, or an NMBR antagonist combined with an HDACi. D283 cells were cultured and treated with BIM-23127 (0.1, 1, or 10 μM), NaB (5 or 7.5 mM), or combinations of BIM-23127 and NaB as described in Materials and Methods. Cell counting was carried out 48 h after treatment. Cell number was significantly reduced by NaB or BIM-23127 combined with NaB. Data represent the mean ± SEM of three different experiments. The mean value for control cells was taken as 100 %; **p* < 0.05 and ***p* < 0.01 compared to control cells

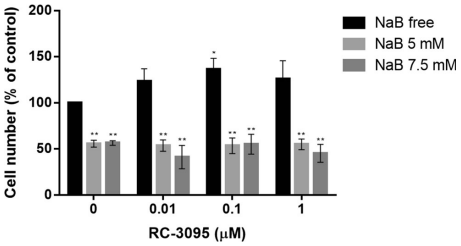

Fig. 2 Viability of D283 MB cells after treatment with a GRPR antagonist, an HDACi, or a GRPR antagonist combined with an HDACi. D283 cells were cultured and treated with RC-3095 (0.01, 0.1, or 1 μM), NaB (5 or 7.5 mM), or combinations of RC-3095 and NaB as described in Materials and Methods. Cell counting was carried out 48 h after treatment. Cell number was significantly increased by RC-3095 at 0.1 μM and significantly reduced by NaB or RC-3095 combined with NaB. Data represent the mean ± SEM of three different experiments. The mean value for control cells was taken as 100 %; $*p < 0.05$ and $**p < 0.01$ compared to control cells

Discussion

The present findings suggest that (1) the HDACi NaB reduced the viability of D283 cells; (2) neither receptor antagonist reduced cell viability; and (3) blocking NMBR or GRPR did not influence the effect of NaB, given that the reduction in cell number after treatment with combinations of NaB with receptor antagonists was similar to those of NaB alone.

The lowest dose of NaB we used (5 mM) was previously shown to be the minimal dose capable of affecting the viability of D283 cells [11]. Another limitation of the present experiments is that only one method was used to assess cell viability. The expression of both NMBR and GRPR in D283 MB cells was confirmed in previous reports [18, 19]. Although experimental therapy with NMBR and GRPR antagonists may be effective in several cancer models [14–16], its role in MB remains unclear. Previous studies have not found effects of bombesin, GRP, RC-3095, or BIM-23127 on the viability of D283 cells [18, 19]. In fact, in the present experiments, RC-3095 at an intermediate dose led to an *increase* in cell number. It is not uncommon for GRPR antagonists to display dose-response patterns in which intermediate doses are more effective than higher doses [17, 20]. Importantly, this finding suggests that, under certain conditions, GRPR antagonism can stimulate rather than inhibit MB growth.

Based on experiments using lung cancer cells [16], we hypothesized that bombesin receptor antagonists could potentiate the effects of NaB. However, all the effects we observed could be attributed to NaB alone. The effects of NaB are likely mediated by epigenetic mechanisms related to chromatin relaxation, in addition to many non-histone targets including hormone receptors, cytoplasmic signaling proteins, and transcription factors [6].

Conclusions

In summary, this report indicates that the HDACi NaB reduces the viability of D283 cells. However, the findings also provide preliminary evidence supporting the possibility that combinations with NMBR or GRPR receptor antagonists are not likely to improve the efficacy of HDACi.

Acknowledgments This research was supported by the National Council for Scientific and Technological Development (CNPq; grant numbers 484185/2012-8 and 303276/2013-4 to R.R.); PRONON/Ministry of Health, Brazil (number 25000.162.034/2014-21 to C.B.F); the Rafael Koff Acordi Research Fund, Children's Cancer Institute (ICI); the South American Office for Anticancer Drug Development; and the Clinical Hospital institutional research fund (FIPE/HCPA).

Compliance with ethical standards All experimental procedures were approved by the institutional research ethics committee (GPPG-HCPA). The present study does not involve the use of experimental animals or materials obtained from patients.

Conflict of interest The authors declare that they have no conflict of interest.

References

1. Polkinghorn WR, Tarbell NJ (2007) Medulloblastoma: tumorigenesis, current clinical paradigm, and efforts to improve risk stratification. Nat Clin Pract Oncol 4:295–304
2. Taylor MD, Northcott PA, Korshunov A, Remke M, Cho YJ, Clifford SC, Eberhart CG, Parsons DW, Rutkowski S, Gajjar A, Ellison DW, Lichter P, Gilbertson RJ, Pomeroy SL, Kool M, Pfister SM (2012) Molecular subgroups of medulloblastoma: the current consensus. Acta Neuropathol 123:465–472
3. Cho YJ, Tsherniak A, Tamayo P, Santagata S, Ligon A, Greulich H, Berhoukim R, Amani V, Goumnerova L, Eberhart CG, Lau CC, Olson JM, Gilbertson RJ, Gajjar A, Delattre O, Kool M, Ligon K, Meyerson M, Mesirov JP, Pomeroy SL (2011) Integrative genomic analysis of medulloblastoma identifies a molecular subgroup that drives poor clinical outcome. J Clin Oncol 29:1424–1430
4. Friedman HS, Burger PC, Bigner SH, Trojanowski JQ, Wikstrand CJ, Halperin EC, Bigner DD (1985) Establishment and characterization of the human medulloblastoma cell line and transplantable xenograft D283 Med. J Neuropathol Exp Neurol 44:592–605
5. Xu J, Margol A, Asgharzadeh S, Erdreich-Epstein A (2015) Pediatric brain tumor cell lines. J Cell Biochem 116:218–224
6. Xu WS, Parmigiani RB, Marks PA (2007) Histone deacetylase inhibitors: molecular mechanisms of action. Oncogene 26:5541–5552
7. Northcott PA, Nakahara Y, Wu X, Feuk L, Ellison DW, Croul S, Mack S, Kongkham PN, Peacock J, Dubuc A, Ra YS, Zilberberg K, McLeod J, Scherer SW, Sunil Rao J, Eberhart CG, Grajkowska W, Gillespie Y, Lach B, Grundy R, Pollack IF, Hamilton RL, Van Meter T, Carlotti CG, Boop F, Bigner D, Gilbertson RJ, Rutka JT, Taylor MD (2009) Multiple recurrent genetic events converge on control of histone lysine methylation in medulloblastoma. Nat Genet 41:465–472

8. Dubuc AM, Remke M, Korshunov A, Northcott PA, Zhan SH, Mendez-Lago M, Kool M, Jones DT, Unterberger A, Morrissy AS, Shih D, Peacock J, Ramaswamy V, Rolider A, Wang X, Witt H, Hielscher T, Hawkins C, Vibhakar R, Croul S, Rutka JT, Weiss WA, Jones SJ, Eberhart CG, Marra MA, Pfister SM, Taylor MD (2013) Aberrant patterns of H3K4 and H3K27 histone lysine methylation occur across subgroups in medulloblastoma. Acta Neuropathol 125:373–384
9. Ecker J, Oehme I, Mazitschek R, Korshunov A, Kool M, Hielscher T, Kiss J, Selt F, Konrad C, Lodrini M, Deubzer HE, von Deimling A, Kulozik AE, Pfister SM, Witt O, Milde T (2015) Targeting class I histone deacetylase 2 in MYC amplified group 3 medulloblastoma. Acta Neuropathol Commun 3:22
10. Sonnemann J, Kumar KS, Heesch S, Müller C, Hartwig C, Maass M, Bader P, Beck JF (2006) Histone deacetylase inhibitors induce cell death and enhance the susceptibility to ionizing radiation, etoposide, and TRAIL in medulloblastoma cells. Int J Oncol 28: 755–766
11. Nör C, Sassi FA, de Farias CB, Schwartsmann G, Abujamra AL, Lenz G, Brunetto AL, Roesler R (2013) The histone deacetylase inhibitor sodium butyrate promotes cell death and differentiation and reduces neurosphere formation in human medulloblastoma cells. Mol Neurobiol 48:533–543
12. Li XN, Shu Q, Su JM, Perlaky L, Blaney SM, Lau CC (2005) Valproic acid induces growth arrest, apoptosis, and senescence in medulloblastomas by increasing histone hyperacetylation and regulating expression of p21Cip1, CDK4, and CMYC. Mol Cancer Ther 4:1912–1922
13. Schmidt AL, Brunetto AL, Schwartsmann G, Roesler R, Abujamra AL (2010) Recent therapeutic advances for treating medulloblastoma: focus on new molecular targets. CNS Neurol Disord Drug Targets 9:335–348
14. Jensen RT, Battey JF, Spindel ER, Benya RV (2008) International union of pharmacology. LXVIII. Mammalian bombesin receptors: nomenclature, distribution, pharmacology, signaling, and functions in normal and disease states. Pharmacol Rev 60:1–42
15. Cornelio DB, Roesler R, Schwartsmann G (2007) Gastrin-releasing peptide receptor as a molecular target in experimental anticancer therapy. Ann Oncol 18:1457–1466
16. Moody TW, Nakagawa T, Kang Y, Jakowlew S, Chan D, Jensen RT (2006) Bombesin/gastrin-releasing peptide receptor antagonists increase the ability of histone deacetylase inhibitors to reduce lung cancer proliferation. J Mol Neurosci 28:231–238
17. Abujamra AL, Almeida VR, Brunetto AL, Schwartsmann G, Roesler R (2009) A gastrin-releasing peptide receptor antagonist stimulates Neuro2a neuroblastoma cell growth: prevention by a histone deacetylase inhibitor. Cell Biol Int 33:899–903
18. Jaeger M, Nör C, de Farias CB, Abujamra AL, Schwartsmann G, Brunetto AL, Roesler R (2013) Anti-EGFR therapy combined with neuromedin B receptor blockade induces the death of DAOY medulloblastoma cells. Childs Nerv Syst 29:2145–2150
19. Schmidt AL, de Farias CB, Abujamra AL, Kapczinski F, Schwartsmann G, Brunetto AL, Roesler R (2010) BDNF and PDE4, but not the GRPR, regulate viability of human medulloblastoma cells. J Mol Neurosci 40:303–310
20. Pinski J, Schally AV, Halmos G, Szepeshazi K, Groot K (1994) Somatostatin analogues and bombesin/gastrin-releasing peptide antagonist RC-3095 inhibit the growth of human glioblastomas in vitro and in vivo. Cancer Res 54:5895–5901

CAPÍTULO II: Convergence of BMI1 and CHD7 on ERK signalling in medulloblastoma.

Os resultados apresentados nas figuras 3D, 3F, 4A, 5A e 6B foram desenvolvidos principalmente pela autora da tese e o artigo resultante constitui capítulo da tese.

Article

Cell Reports

Convergence of BMI1 and CHD7 on ERK Signaling in Medulloblastoma

Graphical Abstract

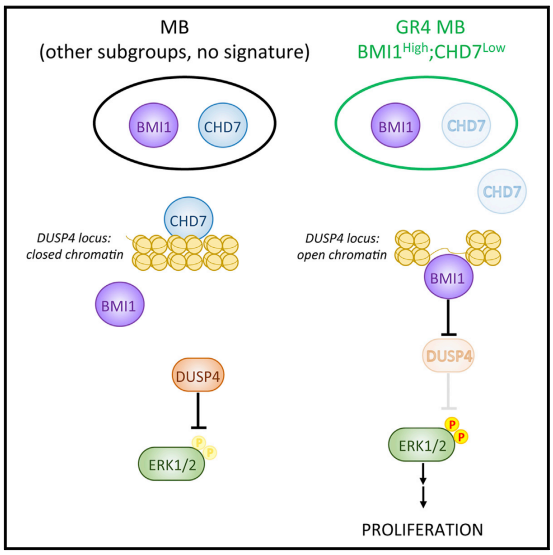

Highlights

- CHD7 inactivation induces MB in a forward genetic screen in Bmi1-overexpressing mice
- A BMI1^{High};CHD7^{Low} signature is found in MB patients with poor overall survival
- CHD7^{Low} favors chromatin accessibility at PcG target genes
- ERK overactivity increases proliferation and tumor burden in BMI1^{High};CHD7^{Low} MB

Authors

Sara Badodi, Adrian Dubuc, Xinyu Zhang, ..., M. Albert Basson, Michael D. Taylor, Silvia Marino

Correspondence

s.marino@qmul.ac.uk

In Brief

Badodi et al. find convergence of the chromatin modifiers BMI1 and CHD7 in medulloblastoma pathogenesis, and they show that this pathway regulates tumor proliferation and growth via ERK signaling.

Badodi et al., 2017, Cell Reports *21*, 2772–2784
December 5, 2017
https://doi.org/10.1016/j.celrep.2017.11.021

CellPress

OPEN ACCESS
CellPress

Cell Reports
Article

Convergence of BMI1 and CHD7 on ERK Signaling in Medulloblastoma

Sara Badodi,[1,9] Adrian Dubuc,[2,9] Xinyu Zhang,[1] Gabriel Rosser,[1] Mariane Da Cunha Jaeger,[1] Michelle M. Kameda-Smith,[3] Anca Sorana Morrissy,[2] Paul Guilhamon,[4,5,6] Philipp Suetterlin,[7] Xiao-Nan Li,[8] Loredana Guglielmi,[1] Ashirwad Merve,[1] Hamza Farooq,[2] Mathieu Lupien,[4,5,6] Sheila K. Singh,[3] M. Albert Basson,[7] Michael D. Taylor,[2,10] and Silvia Marino[1,10,11,*]

[1]Blizard Institute, Barts and The London School of Medicine and Dentistry, Queen Mary University of London, 4 Newark Street, London E1 2AT, UK

[2]Program in Developmental & Stem Cell Biology, The Hospital for Sick Children, 101 College Street, TMDT-11-401M, Toronto, ON M5G 1L7, Canada

[3]Pediatric Neurosurgery, Department of Surgery, McMaster Children's Hospital and McMaster Stem Cell & Cancer Research Institute, MDCL 5027, 1280 Main Street West, Hamilton, ON L8S 4K1, Canada

[4]Princess Margaret Cancer Centre, University Health Network, Toronto, ON, Canada

[5]Department of Medical Biophysics, University of Toronto, Toronto, ON, Canada

[6]Ontario Institute for Cancer Research, Toronto, ON, Canada

[7]Department of Craniofacial Development and Stem Cell Biology, King's College London, Floor 27, Guy's Hospital Tower Wing, London SE1 9RT, UK

[8]Texas Children's Cancer Centre, Texas Children's Hospital, Baylor College of Medicine, 6621 Fannin Street, MC-3-3320, Houston, TX 77479, USA

[9]These authors contributed equally

[10]Senior author

[11]Lead Contact

*Correspondence: s.marino@qmul.ac.uk

https://doi.org/10.1016/j.celrep.2017.11.021

SUMMARY

We describe molecular convergence between BMI1 and CHD7 in the initiation of medulloblastoma. Identified in a functional genomic screen in mouse models, a BMI1^{High};CHD7^{Low} expression signature within medulloblastoma characterizes patients with poor overall survival. We show that BMI1-mediated repression of the ERK1/2 pathway leads to increased proliferation and tumor burden in primary human MB cells and in a xenograft model, respectively. We provide evidence that repression of the ERK inhibitor DUSP4 by BMI1 is dependent on a more accessible chromatin configuration in G4 MB cells with low CHD7 expression. These findings extend current knowledge of the role of BMI1 and CHD7 in medulloblastoma pathogenesis, and they raise the possibility that pharmacological targeting of BMI1 or ERK may be particularly indicated in a subgroup of MB with low expression levels of CHD7.

INTRODUCTION

Medulloblastomas (MBs) are the most common malignant brain tumors of childhood. Current standard of care consists of multimodal therapy (surgery with radio- and/or chemotherapy) that does not take into account the specific molecular mechanisms driving tumor growth. Despite a good overall survival rate, long-term survivors face significant treatment-related morbidity and reduced quality of life. Risk stratification of patients based on molecular subtyping and targeted therapies are essential to reduce secondary effects and improve overall prognosis.

Gene expression profiling of large cohorts of MBs has dissected this historically monomorphous tumor entity into four distinct molecular subgroups (WNT, SHH, group 3, and group 4) with divergent prognoses and responses to therapy (Taylor et al., 2012). Recently, heterogeneity within these subgroups has been reduced by two independent studies that have defined additional subtypes (Cavalli et al., 2017; Schwalbe et al., 2017). While WNT, SHH, and group (G)3 MBs are well characterized molecularly and have been shown to arise from topographically distinct neural progenitor cells (reviewed in Leto et al., 2016), little is known about the molecular and cellular mechanisms underpinning the formation of G4 MB, although it is the most frequent (Ramaswamy et al., 2016).

Oncogenic events affecting chromatin-modifying genes have been described across the subgroups (Dubuc et al., 2013), although different modifications are found in the specific subgroups and their frequency varies (Jones et al., 2013). Inactivating mutations in the histone demethylase *KDM6A* and loss-of-function mutations in the Trithorax gene *MLL3* (Northcott et al., 2012) as well as elevated expression of the Polycomb proteins EZH2 (Robinson et al., 2012) and BMI1 (Behesti et al., 2013) were identified particularly in G4 MBs, raising the possibility that increased Polycomb repression is an important step in the pathogenesis of MBs and in particular of G4 tumors.

The Polycomb group protein BMI1 is a potent inducer of neural stem cell self-renewal and neural progenitor cell proliferation during development and in adult tissue homeostasis (Leung et al., 2004). Numerous studies have demonstrated that BMI1, which is upregulated in a variety of cancers, has a positive correlation with clinical grade/stage and poor prognosis (Glinsky

et al., 2005). BMI1 is overexpressed across all MB subgroups, with the highest levels of expression detected in G4 tumors, followed by G3, SHH, and WNT (Behesti et al., 2013). The growth of G4 MBs is dependent on BMI1 expression, as BMI1 knockdown results in reduced tumor growth and invasion in a xenograft model (Merve et al., 2014). Also SHH MB growth is dependent on BMI1 expression, as demonstrated by experimental genetic approaches where crossing a mouse model of SHH MB onto a *Bmi1*$^{-/-}$ background neutralized tumor formation (Michael et al., 2008). Intriguingly, we recently found that overexpression of Bmi1 alone in cerebellar granule cell progenitors (GCPs), a cell of origin of MB, is not sufficient to induce MB formation (Behesti et al., 2013). As overexpression of Bmi1 driven by the pan-neural Cre line Nestin-Cre did not yield MB formation (Yadirgi et al., 2011), it is conceivable that additional oncogenic events are required to collaborate with BMI1 to induce MB formation.

Here we used a Sleeping Beauty forward genetic approach in the mouse to identify oncogenic events collaborating with Bmi1 overexpression to induce MB formation. We identify a molecular convergence between Bmi1 and Chd7, an ATP-dependent chromatin remodeler that fine-tunes developmental gene expression through modulating chromatin structure (reviewed in Basson and van Ravenswaaij-Arts, 2015). Importantly, somatic mutations in *CHD7* have been described in G4 MBs (Robinson et al., 2012), although their tumorigenicity *in vivo* has not been proven. Here we show that CHD7 controls the proliferation of G4 MB cells and its silencing renders them susceptible to BMI1-mediated ERK1/2-induced proliferation control, raising the possibility that BMI1 and/or ERK may be promising druggable targets in this MB subgroup.

RESULTS

A Forward Genetic Screen Identifies *Chd7* as a Frequent Insertion Site in MB Arising in Mice Overexpressing Bmi1 in Cerebellar Progenitors

The Sleeping Beauty (SB) transposon-based mutagenesis system, which uses a transposase and mutagenic transposon alleles to target mutagenesis to somatic cells of a given tissue in mice, was used to identify random mutations capable of driving tumor development. Mice overexpressing Bmi1 in glutamatergic progenitors (*Math1-Bmi1* transgenic line; Figures S1A and S1B) were crossed to *SB11;T2Onc2* (Copeland and Jenkins, 2010). Triple-mutant mice as well as double-mutant controls were generated and kept on tumor watch for 12 months. Ten of 53 *Math1Bmi1;SB11;T2Onc2* mice developed MBs (18.9% incidence), while only 3 MBs were detected in 47 *SB11;T2Onc2* mice (6.4% incidence), in keeping with an increased tumorigenicity in the triple-mutant mice of 12.5% (Figure 1A). All tumors had morphological and immunohistochemical characteristics of MBs, as assessed by H&E stain and synaptophysin immunostaining (Figure 1B), and histological features were similar irrespective of their genotype.

Next, the tumors were analyzed for common transposon insertion sites in genes (gCIS) to identify candidates that could cooperate with Bmi1 in MB development (Data S1). A total of 41 recurrent clonal insertions were identified in MBs originating in *Math1Bmi1;SB11;T2Onc2*, of which 7 were shared with a published dataset of Sleeping Beauty-induced insertion sites in MBs occurring in *Ptch1*$^{+/-}$ mice (Morrissy et al., 2016; Wu et al., 2012) (Figure 1C). Among the 41 gCISs identified in *Math1Bmi1;SB11;T2Onc2*, 27 were found to be significantly ($p < 0.05$) enriched following Bmi1 overexpression and 3 of these were shared between the two Sleeping Beauty-induced MB models (Figure 1D). Sleeping Beauty insertions in Chromodomain helicase DNA-binding factor 7 (*Chd7*) were inactivating insertions and so were the majority of insertions in *Ptprd*, while the majority of insertions in *Zcchc7* were activating (Figure 1E). *Chd7* is an ATP-dependent chromatin remodeling factor (Bajpai et al., 2010); *Ptprd* is a member of the protein tyrosine phosphatase (PTP) family (Pulido et al., 1995); and *Zcchc7* is a component of a nucleolar TRAMP-like complex, an ATP-dependent exosome regulatory complex (Lubas et al., 2011). Notably, inactivating insertions in *Chd7* were significantly enriched in the *Math1Bmi1;SB11;T2Onc2* MB model (3/6) as compared to the *Ptch1*$^{+/-}$*;SB11;T2Onc2* MB model (1/36) ($p < 0.023$) (Figure 1F). Immunostaining for Bmi1 and Chd7 in the Sleeping Beauty-induced MBs with *Chd7* insertions as compared to those without revealed similar and reduced expression, respectively (Figures S1C and S1D).

Taken together, our data suggest that Bmi1 and Chd7 cooperate to induce MB in a mouse model.

A BMI1^{High};CHD7^{Low} Molecular Signature Identifies a Subgroup of G4 MBs with Reduced Overall Survival

Next, we screened primary human medulloblastoma samples for *CHD7* mutations. A collection of 830 primary human MBs profiled on Affymetrix SNP6.0 copy number arrays and subgrouped using Nanostring technology (Northcott et al., 2012) and 281 primary MBs subgrouped using next-generation sequencing (NGS) across three independent cohorts (Jones et al., 2012; Pugh et al., 2012; Robinson et al., 2012) were interrogated. Intriguingly, this analysis identified a molecular convergence on single-copy loss of *CHD7* via hemizygous deletion (Figure 2A) or hemizygous mutations (Figure 2B) in G4 MBs, while no significant enrichment for *CHD7* mutations was found in the SHH and WNT subgroups. A graphical representation of the mutational inactivating events that affect *CHD7* is shown in Figure 2C.

Next, we examined the subgroup-specific expression levels of *BMI1* and *CHD7* in a large transcriptomic dataset from primary human MBs (n = 187, run on Affymetrix HT-HG-U133A arrays) (Cho et al., 2011). While *CHD7* was most highly expressed in SHH MBs with relatively reduced expression in G3 and G4 MBs, the opposite patterns were observed for *BMI1* (Figures S2A and S2B). A Kaplan-Meier survival analysis demonstrated that tumors with a *BMI1*^{High} *CHD7*^{Low} expression profile had a significantly reduced overall survival as compared to MBs lacking this profile (Figure 2D; $p = 0.03028$). When we examined this relationship in a molecular subgroup-specific manner, a reduced overall survival was observed, particularly in G4 MBs with this signature (Figure 2E; $p = 0.00154$). No significant contribution to patients' survival was observed when the relative contribution of *BMI1*^{High} or *CHD7*^{Low} was considered (Figure S2C).

These data support the notion that the Bmi1/Chd7 molecular convergence identified in mouse models reflects a potentially pathogenically relevant mechanism underpinning a subgroup of G4 MBs.

OPEN ACCESS
CellPress

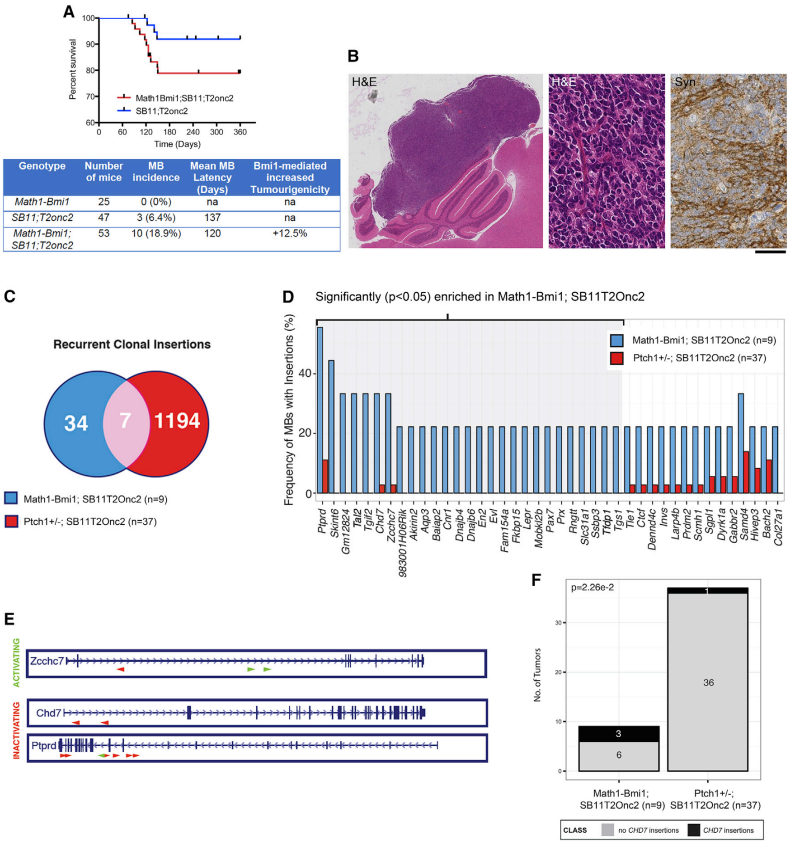

Genotype	Number of mice	MB incidence	Mean MB Latency (Days)	Bmi1-mediated increased Tumourigenicity
Math1-Bmi1	25	0 (0%)	na	na
SB11;T2onc2	47	3 (6.4%)	137	na
Math1-Bmi1; SB11;T2onc2	53	10 (18.9%)	120	+12.5%

Figure 1. Identification of Oncogenic Events Cooperating with Bmi1 to Promote MB Development Using the Sleeping Beauty Transposon System

(A) Kaplan-Meier survival analysis and summary of animal models used to assess the contributions of Bmi1 to MB development. The addition of Bmi1 overexpression to SB11;T2Onc2 led to increased MB formation.

(B) Histology shows morphological (H&E) and immunohistochemical (Synaptophysin) features of MB in Math1-Bmi1;SB11;T2Onc2.

(C) Comparison of recurrent Sleeping Beauty insertions identified in Math1-Bmi1;SB11;T2Onc2 with those identified in Ptch1$^{+/-}$;SB11;T2Onc2 mice (Morrissy et al., 2016) highlighted *Chd7* as a recurrent clonal insertion.

(D) Bar graph representation of recurrent Sleeping Beauty insertions in Math1-Bmi1;SB11;T2Onc2 versus Ptch$^{+/-}$;SB11;T2Onc2 mice, highlighting events significantly ($p < 0.05$) enriched following Bmi1 overexpression.

(E) Sleeping Beauty insertion maps for candidate genes identified in Math1-Bmi1;SB11;T2Onc2 mice, including *Zcchc7* (activating and inactivating insertions), *Chd7* (inactivating insertions), and *Ptprd* (inactivating and activating insertions).

(F) Statistically significant enrichment of *Chd7* insertions identified in the Math1-Bmi1;SB11;T2Onc2 MB model versus the Ptch1$^{+/-}$;SB11;T2Onc2 MB model. Scale bar represents 2 mm (B, left) and 125 μm (B, center and right).

See also Figure S1.

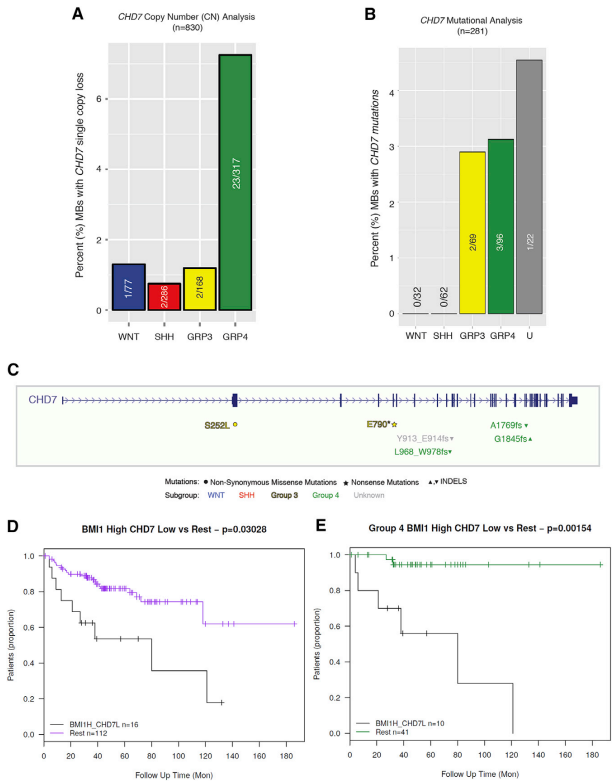

Figure 2. A BMI1^{High};CHD7^{Low} Signature in MB with Poor Prognosis

(A) Graphical representation of the percentage of MB with *CHD7* single-copy loss across subgroups with enrichment in G4.

(B) *CHD7* mutational analysis across molecular subgroups.

(C) Graphical representation of the mutational inactivating events that affect *CHD7*.

(D and E) Kaplan-Meier survival analysis demonstrates that tumors with a *BMI1*^{High};*CHD7*^{Low} signature have a significantly (p = 0.03028) reduced overall survival (D). When we examine this relationship in a subgroup-specific manner, the same trend (p = 0.00154) holds true for G4 MB (E). See also Figure S2.

CHD7 Controls Proliferation of G4 MB Cells *In Vitro* in a BMI1-Dependent Fashion

Patient-derived MB lines, some of which have been maintained as orthotopic xenografts (Zhao et al., 2012), were chosen to further dissect this molecular signature. First, we confirmed the subgroup affiliation by analyzing their gene espression against a classifier (Robinson et al., 2012). Principal-component analysis (PCA) of data obtained from RNA sequencing (RNA-seq) analysis confirmed that ICb1299, a line we have recently shown to be dependent on BMI1 for growth and intraparenchymal invasion in a xenograft model (Merve et al., 2014), and CHLA-01-Med belong to G4 with a significant overlap with G3, while ICb1595 belongs to G3 (Figure 3A). These lines were chosen for further analysis, and they were expanded and shortly maintained *in vitro* to perform functional studies. Hierarchical clustering of RNA-seq datasets of the cultured cells and the original datasets obtained from the patient's tumor (Zhao et al., 2012) confirmed that, although some shift in gene expression did occur after *in vitro* culturing, they remained reasonably similar to the cells isolated from the xenografts and retained their subgroup affiliation (Figure S3A). Validation on independent cultures confirmed very high expression of *OTX2*, a transcription factor overexpressed in the majority of G4 MBs (Bunt et al., 2010) in all three lines, with concomitant high expression levels of the G3/G4 markers (Lin et al., 2016) *LMX1A* and *LHX2* in CHLA-01-Med and *EOMEOS* and *LHX2* in ICb1595 (Figure 3B). The expression of *MATH1*, *GLI1*, and *GAB1*, markers of granule cell progenitors and SHH MBs (Ayrault et al., 2010), was negligible in these lines compared to two patient-derived SHH MB lines, ICb984 and ICb1338 (Figure 3B).

Next, we compared the expression of *BMI1* and *CHD7* in these lines with human cerebellum, and we found similar expression levels for both genes in all MB lines and human cerebellum of early postnatal time points (newborn and 2 months of age). In contrast, the expression of *BMI1* was higher in all lines compared to adult cerebellum, while it was similar for CHD7 (Figure 3C). These findings verified that ICb1299 and CHLA-01-Med are suitable models to test the contribution of CHD7 to G4 MB pathogenesis in the context of BMI1 overexpression. Line ICb1595 was also analyzed further to dissect the specificity of the BMI1/CHD7 molecular convergence to G4 MBs.

Lentivirus-mediated CHD7 knockdown (Figure S3B) resulted in increased proliferation of all lines (Figure 3D), an effect that was BMI1 dependent as it was neutralized by concomitant BMI1 knockdown (Figure S3B; Figure 3D). Importantly, reconstitution of CHD7 expression in ICb1299 after silencing (Figure S3D) brought proliferation back to basal level (Figures S3E and S3F).

Together, these data indicate that CHD7 represses proliferation in G4 and G3 MB cells that overexpress BMI1.

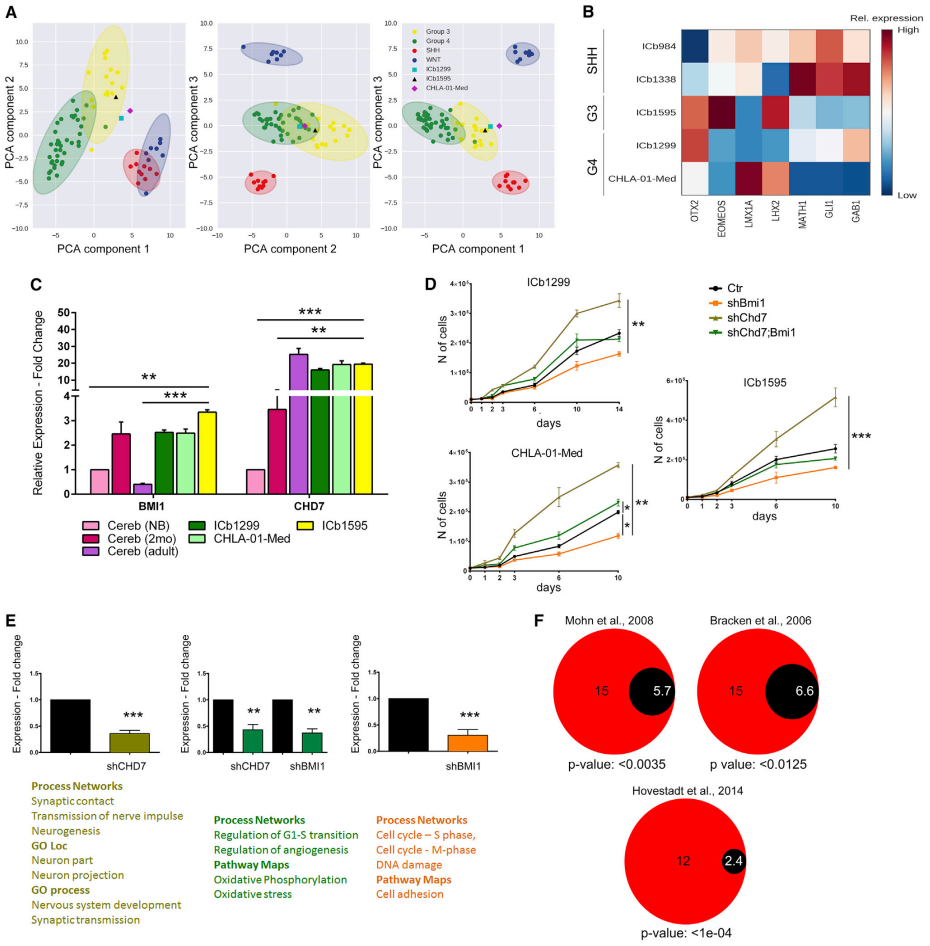

Figure 3. Increased Proliferation upon CHD7 Silencing Is BMI1-Dependent in Non-WNT, Non-SHH MB Patient-Derived Cell Models

(A) Scatterplots of the first 3 principal components of the Robinson dataset (Robinson et al., 2012). Points are shaded based on their subgroup. Ellipses represent the 99% confidence intervals of each subgroup, computed using the covariance matrix of each subset. RNA-seq data of G4 (ICb1299 and CHLA-01-Med) and G3 primary MB cells were subjected to the same PCA transformation and are shown in cyan, magenta, and black respectively.

(B) Heatmap representation of relative expression of selected MB markers in patient-derived cells (ICb1299 and CHLA-01-Med, G4; ICb1595, G3; and ICb1338 and ICb984, SHH). *OTX2*, *EOMEOS*, *LMX1A*, and *LHX2* are mainly expressed by G4 and G3 cells, while *GAB1*, *GLI1*, and *MATH1* are specifically expressed by SHH cells.

(C) Expression of *BMI1* and *CHD7* in ICb1299, CHLA-01-Med, and ICb1595 patient-derived MB lines is comparable to their expression in the early postnatal cerebellum (*BMI1*) and adult cerebellum (*CHD7*).

(D) Increased proliferation upon CHD7 silencing is BMI1 dependent (n = 3).

(E) Pathway analysis reveals different processes and pathways affected by silencing CHD7 and BMI1 individually or concomitantly.

(legend continued on next page)

Genome-wide Expression Analysis Identifies CHD7 and BMI1 as Key Regulators of Neuronal Differentiation and Proliferation of G4 MB Primary Cells

To clarify the molecular mechanism mediating the synergistic effect between CHD7 and BMI1 in MB differentiation and proliferation, we carried out a genome-wide analysis of gene expression in the ICb1299 MB line. In particular, we set out to assess the impact of silencing CHD7 in a BMI1-overexpressing G4 MB primary cell line (shCHD7) compared with the same primary cell line treated with scrambled small hairpin RNA (shRNA) as a control (Ctr versus shCHD7). The impact of silencing BMI1 in shCHD7 cultures compared to silencing only CHD7 was also assessed (shCHD7 versus shCHD7;shBMI1), in addition to an evaluation of the impact of silencing BMI1 in the context of CHD7 expression (Ctr versus shBMI1). 360 genes were differentially expressed in Ctr versus shCHD7 (277 upregulated and 83 downregulated), 1,175 in shCHD7 versus shCHD7;shBMI1 (406 upregulated and 769 downregulated), and 584 in Ctr versus shBMI1 (224 upregulated and 360 downregulated) when thresholds of 0.05 for statistical significance and 0.6 for absolute log2 expression change were applied. First, we confirmed that no changes in the subgroup-defining marker expression were noted upon silencing CHD7 or BMI1 or both (Figure S3C). Pathway analysis carried out on the MetaCore platform highlighted different functions and pathways for these three comparisons. Interestingly, different terms and pathways were impacted in the different conditions tested. In the Ctr versus shCHD7 comparison, nervous system development, synaptic transmission (gene ontology [GO] process), neuron part, neuron projection (GO location), synaptic contact, transmission of nerve impulse, neurogenesis, and chromatin condensation in prometaphase (process networks) were significantly enriched. Regulation of G1-S transition, regulation of angiogenesis (process networks), oxidative phosphorylation, and oxidative stress (pathway maps) were highlighted for the comparison shCHD7 versus shCHD7;shBMI1; and cell adhesion (pathways maps) and cell cycle S phase and M phase as well as DNA damage were impacted in the Ctr versus shBMI1 comparison (Figure 3E).

Assessment of enrichment for Polycomb-group (PcG) targets among the differentially expressed (DE) genes in CHD7-depleted cells (using the statistical significant cutoff of $p < 0.01$) revealed that 15 of the 68 DE genes were previously reported to possess H3K27me3 on their promoters in mouse neural progenitor cells (Mohn et al., 2008), representing a 2.62-fold enrichment ($p = 0.0035$) (Figure 3F). Enrichments of 2.25-fold ($p = 0.012$) and 4.8-fold (p value < 1e−04) were found when the data were compared with the proportion of PcG target genes in human fibroblasts (Bracken et al., 2006) and in an MB dataset (Hovestadt et al., 2014), respectively (Figure 3F). These results support the notion that CHD7 functionally relates to the Polycomb complex in MB.

Taken together, these data suggest that the differentiation potential of MB G4 is controlled by CHD7 via direct or indirect interplay with genes repressed by the Polycomb complex in neural progenitors.

Comparative Analysis with G4 MB Datasets Reveals Activation of ERK Pathway upon CHD7 Silencing via BMI1-Mediated Repression of DUSP4

To identify the genes mediating the pro-proliferative effect of CHD7 silencing in a BMI1-overexpressing context and to ensure we were focusing on those relevant for MB patients, a comparative analysis with the expression data of the G4 MB subgroup of patients with a $BMI1^{High};CHD7^{Low}$ signature (Figure 2E) was carried out. Five genes that were upregulated upon BMI1 knockdown in the shCHD7 cell model were also expressed at a lower level in the $BMI1^{High};CHD7^{Low}$ patient group compared to the remaining patients, while 15 genes were downregulated in the shCHD7;shBMI1 cell model and expressed at higher levels in the $BMI1^{High};CHD7^{Low}$ patient group (Figure 4A; Figure S4A). Pathway analysis carried out on the MetaCore platform for all 20 genes indicated ERK signal transduction as the most significant pathway affected (Figure S4B). A literature review identified *DUSP4*, *HIF-1α*, and *COL8A2* as being linked to ERK signaling, and analysis of a published dataset of chromatin immunoprecipitation sequencing (ChIP-seq) data for Bmi1 in neural stem cells and glioblastoma cells identified *Dusp4* as a direct Bmi1 target gene (Gargiulo et al., 2013). Moreover, several members of the DUSP gene family were upregulated in an RNA-seq dataset comparing neural stem cells lacking Bmi1 versus control in the mouse (Gargiulo et al., 2013). Upregulation of DUSP4 was confirmed in both G4 MB lines upon silencing of BMI1 (Figure 4B), and a lower expression level of *DUSP4* was confirmed in the G4 MB subgroup with a $BMI1^{High};CHD7^{Low}$ signature (Figure 4C). Interestingly, no upregulation of DUSP4 expression was noted in the G3 MB line upon CHD7 silencing (Figure S4C). Next, we assessed chromatin accessibility in the vicinity of the *DUSP4* transcription start site (TSS) using the assay for transposase-accessible chromatin (ATAC) method (Buenrostro et al., 2013). Silencing of CHD7 increased DNA accessibility around the *DUSP4* TSS and the *DUSP4* promoter (Figures 4D and 4E), a configuration that was lost upon concomitant silencing of BMI1 (Figure 4E).

Western blot analysis for pERK1/2 and ERK1/2 demonstrated pathway activation under conditions where BMI1 was expressed and in a more pronounced fashion when CHD7 was silenced (Figures 5A and 5B), in keeping with *DUSP4* gene repression by BMI1. Indeed, knockdown of BMI1 significantly reduced ERK1/2 pathway activation in G4 MB lines (Figures 5A and 5B), as predicted and in line with the upregulation of *DUSP4* observed in the genome-wide comparative expression analysis. Importantly, no overactivity of ERK signaling was found in the G3 MB line (Figure S5A), in keeping with no evidence of DUSP4

(F) Diagram representing the fold enrichment of PcG target genes in the cohort of genes deregulated in CHD7-depleted cells, as compared to the expected values in murine NPCs (Mohn et al., 2008), in human fibroblasts (Bracken et al., 2006), and in human MBs (Hovestadt et al., 2014), as previously reported. Data are represented as mean ± SEM.
See also Figure S3.

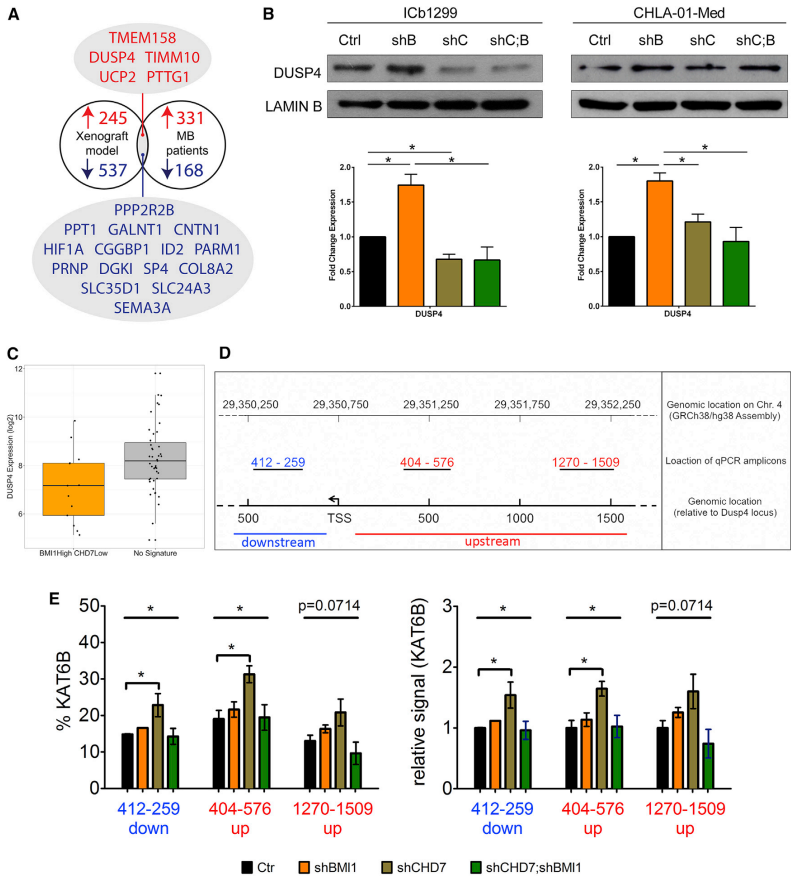

Figure 4. Molecular Convergence on Activation of ERK-Signaling Pathway upon CHD7 Silencing Is Mediated by the Repression of DUSP4 by BMI1

(A) Comparative analysis with human MB datasets identified conserved DE genes in G4 MB cells upon BMI1 knockdown in a CHD7-silenced context and in G4 MB with a BMI^{High};$CHD7^{Low}$ signature. Venn diagram represents the analysis.

(B) Western blot analysis (top) and quantification (bottom) show CHD7 dependency of BMI1-mediated repression of DUSP4 in G4 MB cells. Histograms show mean ± SEM (n = 3).

(C) Boxplot showing lower expression of *DUSP4* in $BMI1^{High}$;$CHD7^{Low}$ G4 MB.

(D) Assessment of DNA accessibility in the vicinity of the *DUSP4* TSS by assay for transposase-accessible chromatin (ATAC). Schematic representation of the promoter region of *DUSP4* with primer locations is shown.

(E) Increased accessibility in CHD7-silenced cells is lost upon concomitant silencing of BMI1. Data are represented as mean ± SEM.

See also Figure S4.

upregulation (Figure S4C). These data suggest a model where CHD7 silencing increases chromatin accessibility at the *DUSP4* locus to facilitate BMI1-mediated repression and consequent ERK pathway activation in G4 MB. Under conditions where both BMI1 and CHD7 are silenced, ERK pathway activation is down to baseline levels, a finding that is unlikely to be

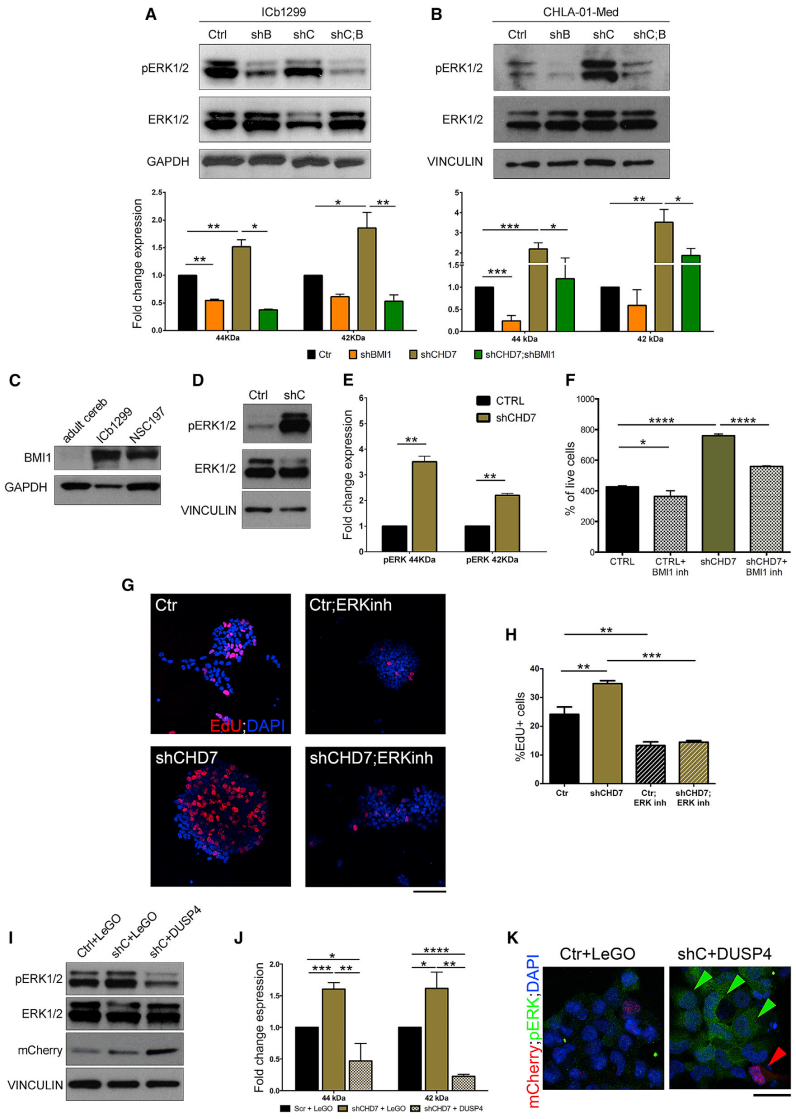

Figure 5. The Pro-proliferative State of the G4 MB Cells upon Silencing of CHD7 Is Mediated by ERK1/2

(A) Overactivity of the ERK1/2-signaling pathway in ICb1299 CHD7-silenced cells is neutralized by concomitant BMI1 silencing.

(B) Similar effects are seen in CHLA-01-Med.

(legend continued on next page)

mediated by DUSP4, as BMI1 and CHD7 are silenced and the chromatin configuration at the locus is closed (Figure 4E).

To determine whether this BMI1-CHD7 connection also applied to freshly isolated cells and is not a feature of cells maintained through several *in vitro* passages, we obtained neural progenitor cells (NPCs) from human fetal brains. These cells expressed high levels of BMI1 as compared to adult cerebellum, albeit not as high as G4 MB cells (Figure 5C; Figure S5C). We found that the ERK1/2 pathway activity was increased (Figures 5D and 5E) upon CHD7 silencing (Figure S5D), which led to increased proliferation in a BMI1-dependent fashion also in these cells (Figure 5F).

Next, we assessed whether activation of ERK signaling was an essential mediator of the pro-proliferative phenotype observed upon silencing of CHD7 in G4 MB cells. Treatment of ICb1299 cells with an ERK inhibitor effectively inhibited the pathway (Figure S5E) and led to neutralization of the increased proliferation observed upon silencing of CHD7, an effect that was also observed in control cells (Figures 5G and 5H). Re-expression of CHD7 in ICb1299 rescued the pro-proliferative phenotype induced by CHD7 knockdown (Figures S3D–S3F), and it neutralized the ERK pathway overactivity in these cells (Figure S5B).

Finally lentiviral-mediated overexpression of mCherry-DUSP4 (Figure S5F) in ICb1299 abolished the ERK overactivation mediated by CHD7 silencing (Figures 5I–5K).

In conclusion, these data highlight a mechanism mediating a pro-proliferative role for BMI1/CHD7 in MB G4, which impacts ERK and is regulated by DUSP4.

CHD7 Controls Tumor Volume in a BMI1/pERK-Dependent Fashion in Xenograft Models

To evaluate the *in vivo* relevance of these findings, we injected shCHD7 ICb1299 cells, as well as shCHD7;shBMI1 and shBMI1 cells, into the cerebellum of newborn mice. Xenografted mice were kept on tumor watch until symptoms of increased intracranial pressure developed, when they were culled. Histological analysis of the tumors did not reveal morphological differences between MBs originating from the different conditions, including the expression of markers such as Synaptophysin (Figure 6A) and *OTX2* (Figure S6A) and the lack of expression of *GAB1* (Figure S6B) and *GLI1* (Figure S6C). Stereological assessment of tumor volume revealed larger MBs in mice engrafted with shCHD7 cells, an effect that was lost upon concomitant silencing of BMI1 in the engrafted cells (Figure 6B). Increased proliferation in shCHD7 tumors was confirmed with immunohistochemical detection of Ki67 (Figures 6C and 6D). Silencing of CHD7 did not affect intraparenchymal invasion, while silencing of BMI1 alone significantly hampered tumor cell invasion (Figure S6D), in keeping with previous reports (Merve et al., 2014). Overactivity of the ERK pathway was confirmed in the shCHD7 xenografts (Figure 6E).

Together, these data support the conclusion that CHD7 depletion enhances proliferation of G4 MB cells via a BMI1/pERK mechanism.

DISCUSSION

The PcG gene *BMI1* is upregulated in a variety of cancers, where it correlates with clinical grade/stage and a poor prognosis. Importantly, it is a highly druggable molecule; hence, understanding its mechanism of action in tumorigenesis will be essential to guide the further development and clinical testing of BMI1 pharmacological inhibitors.

Here we show that genome-wide *in vivo* insertional mutagenesis (T2Onc2) driven by the Sleeping Beauty (SB11) transposase in glutamatergic progenitor cells engineered to overexpress Bmi1 results in MB formation. In a Bmi1-overexpressing background, we observe frequent *T2Onc2*-inactivating insertions in the chromatin remodeling factor *Chd7* (Bajpai et al., 2010; Whittaker et al., 2017), suggesting that Bmi1 overexpression and Chd7 loss of function cooperate to induce MB. Importantly, we show the relevance of this molecular convergence for human MB. In fact, high expression of BMI1 in combination with low expression of CHD7 was found to be associated with a poor prognosis in human MBs, particularly those of the G4 subgroup, and loss-of-function mutations of *CHD7* are significantly enriched for in this subgroup.

The Sleeping Beauty transposon mutagenesis is a powerful *in vivo* screening tool for cancer gene discovery. In the context of MB, this tool has been successfully used to identify candidate genes, particularly in the context of SHH MB as expected when using Math1 drivers; however, many of the candidate genes identified with this tool are known to be overexpressed or silenced in non-SHH models of the human disease (Dey et al., 2013; Genovesi et al., 2013; Mumert et al., 2012; Wu et al., 2012). We have studied the molecular convergence of BMI1/CHD7 in G4 MB because of the results of mutation analysis in human tumors indicating that genetic lesions leading to reduced CHD7 expression are found almost exclusively in G4 MB—and never in SHH MB—and because of the negative prognostic correlation of the $BMI1^{High}$;$CHD7^{Low}$ signature found exclusively in G4 MB. Thus, while we initially sought to model the effects and

(C) BMI1 expression in G4 MB cells and in NSC197 is higher than adult cerebellum, as shown by western blot analysis.
(D and E) Silencing of CHD7 in NPCs leads to ERK1/2 pathway overactivation, as shown by western blot analysis (D) and quantification (E) (n = 2).
(F) Increased proliferation is seen upon CHD7 silencing in NPCs, a finding that is neutralized by incubation with a BMI1 inhibitor (n = 3).
(G) Increased proliferation as assessed by EdU pulse/chase is dependent on ERK1/2 overactivity, as demonstrated by its reduction upon pharmacological inhibition of ERK in ICb1299.
(H) Quantification of the findings.
(I and J) Overexpression of exogenous mCherry-DUSP4 abolishes ERK signaling overactivation mediated by CHD7 silencing. Western blot analysis (I) of ICb1299 transduced with empty LeGO control or LeGO-mCherry-DUSP4 and quantification (J) (n = 3).
(K) Immunofluorescence of ICb1299 transduced as described in (I). Green arrows indicate CHD7-silenced cells with ERK overactivation, while red arrow indicates a cell overexpressing DUSP4 and devoid of ERK phosphorylation. Scale bar represents 25 μm. Data are represented as mean ± SEM.
See also Figure S5.

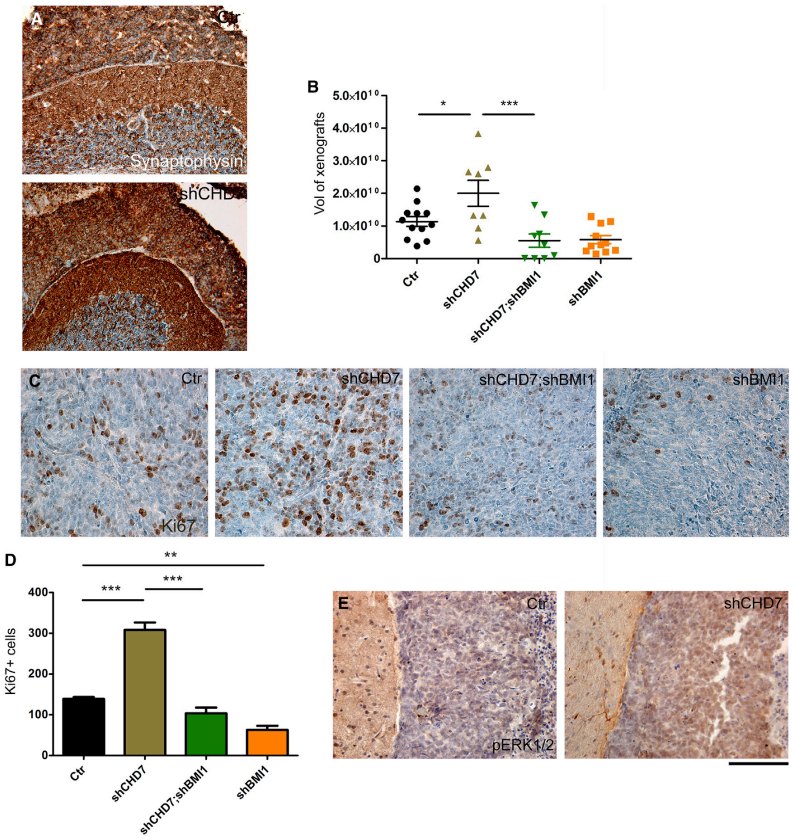

Figure 6. Increased Tumor Volume in CHD7-Silenced Xenografts of G4 MB Is BMI1 Dependent

(A) Orthotopic xenografts of G4 MB cells silenced for CHD7 or CHD7;BMI1 or BMI1 show similar morphology, and they express Synaptophysin.

(B) Increased tumor volume upon injection of shCHD7 G4 MB cells, which is neutralized by concomitant silencing of BMI1.

(C) Increased proliferation, as assessed by Ki67 staining, in shCHD7 xenografts is shown together with its BMI1 dependency.

(D) Quantification of the findings.

(E) Overactivation of the ERK pathway is seen in shCHD7 xenografts. Scale bar represents 2 mm (A) and 125 μm (C and E).

Data are represented as mean ± SEM. See also Figure S6.

consequences of BMI1 overexpression in an SHH model of MB, this forward genetic screen uncovered a molecular axis whose signaling modulates the pathogenesis of a proportion of human G4 MBs instead. Interestingly, there is mounting evidence of a glutamatergic cell of origin for at least a proportion of G4 MBs, as recently suggested by a computational reconstruction of core regulatory circuitry that identified subgroup-specific transcription factors (Lin et al., 2016), hence highlighting a potential ontogeny link between the discovery tool we used and the molecular signature we have identified. Further studies in genetically engineered mouse models will confirm or dispute this hypothesis.

We have used primary G4 MB cells to dissect the contribution of CHD7 to tumorigenesis, both *in vitro* and *in vivo* in a xenograft model. We show deregulated expression of neural differentiation markers upon silencing of CHD7, an effect that is in keeping with a pro-neurogenic role of CHD7 as previously described (Feng et al., 2013; Jones et al., 2015). Genome-wide analysis of gene

expression upon CHD7 silencing reveals many more upregulated genes as compared to downregulated genes, in keeping with CHD7 functioning as a repressor in our experimental setting. This is in agreement with a reported role of CHD7 as a repressive modulator of embryonic stem cell (ESC)-specific gene expression via targeting enhancer regions (Schnetz et al., 2010). In keeping with CHD7 functioning as a repressor in our experimental setup, no synergism between CHD7 and SOX2 was observed, an interaction known to lead to gene activation (Engelen et al., 2011). SOX4 and 11 are also unlikely to mediate CHD7 function in our setting, because CHD7 promotes an open chromatin configuration at their promoters (Feng et al., 2013).

We show increased proliferation of G4 MB cells upon CHD7 silencing *in vitro* as well as increased tumor volume upon orthotopic xenografting of these cells into NOD/SCID mice, an effect that is dependent on BMI1 expression. Bioinformatic analysis of the deregulated genes identified in a comparative gene expression analysis with human MB datasets revealed a BMI1-dependent convergence on modulation of ERK signaling via repression of DUSP4 in CHD7-depleted cells. Meta-analysis of publicly available ChIP-seq and RNA-seq datasets (Gargiulo et al., 2013) confirmed that DUSP family members are direct target genes of Bmi1. We provide evidence of altered chromatin accessibility at the promoter of *DUSP4* upon CHD7 silencing. This is in keeping with the recently reported ability of CHD7 to alter chromatin accessibility in primary cerebellar granule neuron progenitors (Feng et al., 2017; Whittaker et al., 2017), and it provides support to the notion that PcG-mediated gene repression is counteracted by a compacted chromatin configuration induced by CHD7 in G4 MB cells. Our findings are in good agreement with a previously reported role for DUSP4 in promoting neuronal differentiation and repressing proliferation via repression of the ERK pathway (Kim et al., 2015). Furthermore, activation of ERK signaling has been shown to control a proneural genetic program during cortical development and to activate an Ascl1-controlled neuronal differentiation program (Li et al., 2014). Overactivity of the pathway was found to exert a pro-proliferative role in SHH MBs (Brechbiel et al., 2014; Sengupta et al., 2012) and in other brain tumors, pilocytic astrocytomas, and glioneuronal tumors (Li et al., 2014). We show that activation of ERK signaling via the repression of DUSP4 by BMI1 is not found in a G3 MB line, lending additional support to the conclusion that this molecular convergence is functionally relevant only in a subset of G4 MBs. Pharmacological inhibition of ERK signaling confirmed the functional relevance of this regulatory loop in the G4 MB lines analyzed. Finally, silencing CHD7 in human neural progenitor cells expressing high levels of BMI1 induced overactivation of the ERK pathway and increased proliferation of these cells *in vitro*. These data raise the possibility that a $BMI1^{High}$;$CHD7^{Low}$ signature is oncogenic in human progenitor cells; genetically engineered models recapitulating this signature in a spatiotemporally controlled fashion will be essential to test this hypothesis.

The reversible nature of epigenetic modifications makes them attractive therapeutic targets, and pharmacological agents that can potentially reverse altered chromatin states are undergoing trials. Our findings extend the current knowledge of the role of two essential chromatin modifiers, BMI1 and CHD7, in MB pathogenesis, and they raise the possibility that pharmacological targeting of BMI1 may be particularly indicated in a subgroup of MB with low expression level of CHD7. Alternatively, the use of ERK inhibitors could also be further explored for MB treatment, and we provide here essential preclinical evidence that BMI1 and CHD7 could be useful biomarkers to define the patient subgroup that could benefit from this approach.

EXPERIMENTAL PROCEDURES

Detailed methods are available in the Supplemental Experimental Procedures.

Sleeping Beauty Mutagenesis

Male and female Math1-Bmi1, Math1-Bmi1;SB11;T2Onc2, or T2Onc2 mice (12 to 20 weeks of age; at the time they developed signs of MB) were used. We did not perform a formal sample size estimate for the study but based our experimental plan on our previous experience with Sleeping Beauty mutagenesis screening. When mice showed clinical signs of increased intracranial pressure, they were culled, the brains were removed, and they were either fixed in formalin for histological assessment or used for genomic DNA extraction. All the procedures involving animals have been approved by the institutional Animal Care Committee and in no case were tumor-bearing animals allowed to reach a tumor burden compromising normal behavior, food and water intake, or exceeding the approved volume of 1,700 mm^3.

Culture Conditions for Patient-Derived MB Lines

Patient-derived MB lines were obtained from Dr Xiao-Nan Li, Baylor College of Medicine, Texas Children Cancer Centre, USA (Shu et al., 2008; Zhao et al., 2012). ICb1299 was cultured in DMEM (high glucose, GlutaMAX, Thermo Fisher Scientific) supplemented with 10% fetal bovine serum and 1% penicillin-streptomycin. ICb1595, ICb984, and ICb1338 were cultured in NeuroCult NS-A Basal Medium (human) (STEMCELL Technologies) supplemented with NeuroCult Proliferation Supplement (human) (STEMCELL Technologies), 1% penicillin-streptomycin, 2 μg/mL heparin (STEMCELL Technologies), 20 ng/mL epidermal growth factor (EGF) (recombinant mouse, PeproTech), and 10 ng/mL basic fibroblast growth factor (bFGF) (human recombinant, PeproTech). ICb1595, ICb984, and ICb1338 were cultured on plates coated with Poly-L-ornithine and Laminin (Sigma). CHLA-01-Med was purchased from ATCC (CRL3021) and grown in DMEM-F12 (Gibco) supplemented with B27 (Gibco), 20 ng/mL EGF, and 10 ng/mL bFGF. Cells were maintained at 37°C and were sub-cultured every 3 days once they reached confluence.

Proliferation Assay

Patient-derived cells infected with lentiviral constructs coding for shBMI1 and/or shCHD7 were analyzed with cell growth curve and EdU staining to assess their proliferation potential compared to scramble control.

In Vivo Orthotopic Xenografts

All procedures had Home Office approval (Animals Scientific Procedures Act 1986, PPL 70/7275) and were carried out as previously reported (Merve et al., 2014). Mice were killed when developing neurological signs and brains were removed and placed in 10% formalin for 24 hr and then transferred to PBS.

Inhibition of MEK/ERK Activity

Patient-derived cells were treated with the MEK inhibitors PD98059 (Cell Signaling Technology) or U0126 (Cell Guidance Systems) at different concentrations. After 1 hr of treatment, cells were harvested and lysed for protein analysis. Alternatively, to assess proliferation potential, cells were treated twice with U0126 (50 μM) before pulsing with EdU or collecting them for western blot analysis.

Western Blot Analysis

Total protein extracts were prepared with radioimmunoprecipitation assay (RIPA) buffer supplemented with protease inhibitors. Nuclear protein extracts were obtained as previously described (Badodi et al., 2015). Equal amounts of protein extracts were separated by SDS-PAGE and analyzed by western blot analysis.

Statistical Analysis

Differences between groups were determined by one-way ANOVA, followed by Dunnett's post hoc test (ATAC experiments) or Tukey's multiple comparison test (all other experiments) to determine which groups differed significantly from control. Any p values < 0.05 were considered significant (*p < 0.05, **p < 0.01, ***p < 0.001, and ****p < 0.0001).

SUPPLEMENTAL INFORMATION

Supplemental Information includes Supplemental Experimental Procedures, six figures, and two data files and can be found with this article online at https://doi.org/10.1016/j.celrep.2017.11.021.

AUTHOR CONTRIBUTIONS

S.M. and M.D.T. conceived the project. S.B., P.G., M.L., M.A.B., M.D.T., and S.M. designed the experiments. S.B., X.Z., A.D., A.M., P.S., M.D.C.J., M.M.K.-S., and M.A.B. conducted the wet lab experiments. S.B., X.Z., A.D., A.M., P.S., L.G., M.D.C.J., M.A.B., M.D.T., M.M.K.-S., S.K.S., and S.M. analyzed the data. X.-N.L. provided molecularly characterized primary MB lines. A.S.M., H.F., and G.R. conducted and analyzed the computational experiments. S.B. and S.M. wrote the paper with contributions from all authors.

ACKNOWLEDGMENTS

We are grateful to the BSU staff for help in the daily care of our mouse colony and to the Blizard Core Facilities (Imaging and FACS) and UCL IQPath for technical support and advice. This work is supported by grants from the Medical Research Council UK (MR/N000528/1) to S.M. and M.A.B., the Brain Tumour Research Centre of Excellence to S.M., the Pathological Society of Great Britain and Ireland (SGS 2013/04/03) to A.M., Barts and the London Charity (527/2087) to A.M., and a CAPES Foundation scholarship, Ministry of Education of Brazil to M.D.C.J.

Received: September 23, 2016
Revised: October 9, 2017
Accepted: November 3, 2017
Published: December 5, 2017

REFERENCES

Ayrault, O., Zhao, H., Zindy, F., Qu, C., Sherr, C.J., and Roussel, M.F. (2010). Atoh1 inhibits neuronal differentiation and collaborates with Gli1 to generate medulloblastoma-initiating cells. Cancer Res. *70*, 5618–5627.

Badodi, S., Baruffaldi, F., Ganassi, M., Battini, R., and Molinari, S. (2015). Phosphorylation-dependent degradation of MEF2C contributes to regulate G2/M transition. Cell Cycle *14*, 1517–1528.

Bajpai, R., Chen, D.A., Rada-Iglesias, A., Zhang, J., Xiong, Y., Helms, J., Chang, C.P., Zhao, Y., Swigut, T., and Wysocka, J. (2010). CHD7 cooperates with PBAF to control multipotent neural crest formation. Nature *463*, 958–962.

Basson, M.A., and van Ravenswaaij-Arts, C. (2015). Functional insights into chromatin remodelling from studies on CHARGE syndrome. Trends Genet. *31*, 600–611.

Behesti, H., Bhagat, H., Dubuc, A.M., Taylor, M.D., and Marino, S. (2013). Bmi1 overexpression in the cerebellar granule cell lineage of mice affects cell proliferation and survival without initiating medulloblastoma formation. Dis. Model. Mech. *6*, 49–63.

Bracken, A.P., Dietrich, N., Pasini, D., Hansen, K.H., and Helin, K. (2006). Genome-wide mapping of Polycomb target genes unravels their roles in cell fate transitions. Genes Dev. *20*, 1123–1136.

Brechbiel, J., Miller-Moslin, K., and Adjei, A.A. (2014). Crosstalk between hedgehog and other signaling pathways as a basis for combination therapies in cancer. Cancer Treat. Rev. *40*, 750–759.

Buenrostro, J.D., Giresi, P.G., Zaba, L.C., Chang, H.Y., and Greenleaf, W.J. (2013). Transposition of native chromatin for fast and sensitive epigenomic profiling of open chromatin, DNA-binding proteins and nucleosome position. Nat. Methods *10*, 1213–1218.

Bunt, J., de Haas, T.G., Hasselt, N.E., Zwijnenburg, D.A., Koster, J., Versteeg, R., and Kool, M. (2010). Regulation of cell cycle genes and induction of senescence by overexpression of OTX2 in medulloblastoma cell lines. Mol. Cancer Res. *8*, 1344–1357.

Cavalli, F.M.G., Remke, M., Rampasek, L., Peacock, J., Shih, D.J.H., Luu, B., Garzia, L., Torchia, J., Nor, C., Morrissy, A.S., et al. (2017). Intertumoral Heterogeneity within Medulloblastoma Subgroups. Cancer Cell *31*, 737–754.e6.

Cho, Y.J., Tsherniak, A., Tamayo, P., Santagata, S., Ligon, A., Greulich, H., Berhoukim, R., Amani, V., Goumnerova, L., Eberhart, C.G., et al. (2011). Integrative genomic analysis of medulloblastoma identifies a molecular subgroup that drives poor clinical outcome. J. Clin. Oncol. *29*, 1424–1430.

Copeland, N.G., and Jenkins, N.A. (2010). Harnessing transposons for cancer gene discovery. Nat. Rev. Cancer *10*, 696–706.

Dey, J., Dubuc, A.M., Pedro, K.D., Thirstrup, D., Mecham, B., Northcott, P.A., Wu, X., Shih, D., Tapscott, S.J., LeBlanc, M., et al. (2013). MyoD is a tumor suppressor gene in medulloblastoma. Cancer Res. *73*, 6828–6837.

Dubuc, A.M., Remke, M., Korshunov, A., Northcott, P.A., Zhan, S.H., Mendez-Lago, M., Kool, M., Jones, D.T., Unterberger, A., Morrissy, A.S., et al. (2013). Aberrant patterns of H3K4 and H3K27 histone lysine methylation occur across subgroups in medulloblastoma. Acta Neuropathol. *125*, 373–384.

Engelen, E., Akinci, U., Bryne, J.C., Hou, J., Gontan, C., Moen, M., Szumska, D., Kockx, C., van Ijcken, W., Dekkers, D.H., et al. (2011). Sox2 cooperates with Chd7 to regulate genes that are mutated in human syndromes. Nat. Genet. *43*, 607–611.

Feng, W., Khan, M.A., Bellvis, P., Zhu, Z., Bernhardt, O., Herold-Mende, C., and Liu, H.K. (2013). The chromatin remodeler CHD7 regulates adult neurogenesis via activation of SoxC transcription factors. Cell Stem Cell *13*, 62–72.

Feng, W., Kawauchi, D., Körkel-Qu, H., Deng, H., Serger, E., Sieber, L., Lieberman, J.A., Jimeno-González, S., Lambo, S., Hanna, B.S., et al. (2017). Chd7 is indispensable for mammalian brain development through activation of a neuronal differentiation programme. Nat. Commun. *8*, 14758.

Gargiulo, G., Cesaroni, M., Serresi, M., de Vries, N., Hulsman, D., Bruggeman, S.W., Lancini, C., and van Lohuizen, M. (2013). In vivo RNAi screen for BMI1 targets identifies TGF-β/BMP-ER stress pathways as key regulators of neural- and malignant glioma-stem cell homeostasis. Cancer Cell *23*, 660–676.

Genovesi, L.A., Ng, C.G., Davis, M.J., Remke, M., Taylor, M.D., Adams, D.J., Rust, A.G., Ward, J.M., Ban, K.H., Jenkins, N.A., et al. (2013). Sleeping Beauty mutagenesis in a mouse medulloblastoma model defines networks that discriminate between human molecular subgroups. Proc. Natl. Acad. Sci. USA *110*, E4325–E4334.

Glinsky, G.V., Berezovska, O., and Glinskii, A.B. (2005). Microarray analysis identifies a death-from-cancer signature predicting therapy failure in patients with multiple types of cancer. J. Clin. Invest. *115*, 1503–1521.

Hovestadt, V., Jones, D.T., Picelli, S., Wang, W., Kool, M., Northcott, P.A., Sultan, M., Stachurski, K., Ryzhova, M., Warnatz, H.J., et al. (2014). Decoding the regulatory landscape of medulloblastoma using DNA methylation sequencing. Nature *510*, 537–541.

Jones, D.T., Jäger, N., Kool, M., Zichner, T., Hutter, B., Sultan, M., Cho, Y.J., Pugh, T.J., Hovestadt, V., Stütz, A.M., et al. (2012). Dissecting the genomic complexity underlying medulloblastoma. Nature *488*, 100–105.

Jones, D.T., Northcott, P.A., Kool, M., and Pfister, S.M. (2013). The role of chromatin remodeling in medulloblastoma. Brain Pathol. *23*, 193–199.

Jones, K.M., Sarić, N., Russell, J.P., Andoniadou, C.L., Scambler, P.J., and Basson, M.A. (2015). CHD7 maintains neural stem cell quiescence and prevents premature stem cell depletion in the adult hippocampus. Stem Cells *33*, 196–210.

Kim, S.Y., Han, Y.M., Oh, M., Kim, W.K., Oh, K.J., Lee, S.C., Bae, K.H., and Han, B.S. (2015). DUSP4 regulates neuronal differentiation and calcium homeostasis by modulating ERK1/2 phosphorylation. Stem Cells Dev. *24*, 686–700.

Leto, K., Arancillo, M., Becker, E.B., Buffo, A., Chiang, C., Ding, B., Dobyns, W.B., Dusart, I., Haldipur, P., Hatten, M.E., et al. (2016). Consensus Paper: Cerebellar Development. Cerebellum *15*, 789–828.

Leung, C., Lingbeek, M., Shakhova, O., Liu, J., Tanger, E., Saremaslani, P., Van Lohuizen, M., and Marino, S. (2004). Bmi1 is essential for cerebellar development and is overexpressed in human medulloblastomas. Nature *428*, 337–341.

Li, S., Mattar, P., Dixit, R., Lawn, S.O., Wilkinson, G., Kinch, C., Eisenstat, D., Kurrasch, D.M., Chan, J.A., and Schuurmans, C. (2014). RAS/ERK signaling controls proneural genetic programs in cortical development and gliomagenesis. J. Neurosci. *34*, 2169–2190.

Lin, C.Y., Erkek, S., Tong, Y., Yin, L., Federation, A.J., Zapatka, M., Haldipur, P., Kawauchi, D., Risch, T., Warnatz, H.J., et al. (2016). Active medulloblastoma enhancers reveal subgroup-specific cellular origins. Nature *530*, 57–62.

Lubas, M., Christensen, M.S., Kristiansen, M.S., Domanski, M., Falkenby, L.G., Lykke-Andersen, S., Andersen, J.S., Dziembowski, A., and Jensen, T.H. (2011). Interaction profiling identifies the human nuclear exosome targeting complex. Mol. Cell *43*, 624–637.

Merve, A., Dubuc, A.M., Zhang, X., Remke, M., Baxter, P.A., Li, X.N., Taylor, M.D., and Marino, S. (2014). Polycomb group gene BMI1 controls invasion of medulloblastoma cells and inhibits BMP-regulated cell adhesion. Acta Neuropathol. Commun. *2*, 10.

Michael, L.E., Westerman, B.A., Ermilov, A.N., Wang, A., Ferris, J., Liu, J., Blom, M., Ellison, D.W., van Lohuizen, M., and Dlugosz, A.A. (2008). Bmi1 is required for Hedgehog pathway-driven medulloblastoma expansion. Neoplasia *10*, 1343–1349.

Mohn, F., Weber, M., Rebhan, M., Roloff, T.C., Richter, J., Stadler, M.B., Bibel, M., and Schübeler, D. (2008). Lineage-specific polycomb targets and de novo DNA methylation define restriction and potential of neuronal progenitors. Mol. Cell *30*, 755–766.

Morrissy, A.S., Garzia, L., Shih, D.J., Zuyderduyn, S., Huang, X., Skowron, P., Remke, M., Cavalli, F.M., Ramaswamy, V., Lindsay, P.E., et al. (2016). Divergent clonal selection dominates medulloblastoma at recurrence. Nature *529*, 351–357.

Mumert, M., Dubuc, A., Wu, X., Northcott, P.A., Chin, S.S., Pedone, C.A., Taylor, M.D., and Fults, D.W. (2012). Functional genomics identifies drivers of medulloblastoma dissemination. Cancer Res. *72*, 4944–4953.

Northcott, P.A., Shih, D.J., Peacock, J., Garzia, L., Morrissy, A.S., Zichner, T., Stütz, A.M., Korshunov, A., Reimand, J., Schumacher, S.E., et al. (2012). Subgroup-specific structural variation across 1,000 medulloblastoma genomes. Nature *488*, 49–56.

Pugh, T.J., Weeraratne, S.D., Archer, T.C., Pomeranz Krummel, D.A., Auclair, D., Bochicchio, J., Carneiro, M.O., Carter, S.L., Cibulskis, K., Erlich, R.L., et al. (2012). Medulloblastoma exome sequencing uncovers subtype-specific somatic mutations. Nature *488*, 106–110.

Pulido, R., Krueger, N.X., Serra-Pagès, C., Saito, H., and Streuli, M. (1995). Molecular characterization of the human transmembrane protein-tyrosine phosphatase delta. Evidence for tissue-specific expression of alternative human transmembrane protein-tyrosine phosphatase delta isoforms. J. Biol. Chem. *270*, 6722–6728.

Ramaswamy, V., Remke, M., Bouffet, E., Bailey, S., Clifford, S.C., Doz, F., Kool, M., Dufour, C., Vassal, G., Milde, T., et al. (2016). Risk stratification of childhood medulloblastoma in the molecular era: the current consensus. Acta Neuropathol. *131*, 821–831.

Robinson, G., Parker, M., Kranenburg, T.A., Lu, C., Chen, X., Ding, L., Phoenix, T.N., Hedlund, E., Wei, L., Zhu, X., et al. (2012). Novel mutations target distinct subgroups of medulloblastoma. Nature *488*, 43–48.

Schnetz, M.P., Handoko, L., Akhtar-Zaidi, B., Bartels, C.F., Pereira, C.F., Fisher, A.G., Adams, D.J., Flicek, P., Crawford, G.E., Laframboise, T., et al. (2010). CHD7 targets active gene enhancer elements to modulate ES cell-specific gene expression. PLoS Genet. *6*, e1001023.

Schwalbe, E.C., Lindsey, J.C., Nakjang, S., Crosier, S., Smith, A.J., Hicks, D., Rafiee, G., Hill, R.M., Iliasova, A., Stone, T., et al. (2017). Novel molecular subgroups for clinical classification and outcome prediction in childhood medulloblastoma: a cohort study. Lancet Oncol. *18*, 958–971.

Sengupta, R., Dubuc, A., Ward, S., Yang, L., Northcott, P., Woerner, B.M., Kroll, K., Luo, J., Taylor, M.D., Wechsler-Reya, R.J., and Rubin, J.B. (2012). CXCR4 activation defines a new subgroup of Sonic hedgehog-driven medulloblastoma. Cancer Res. *72*, 122–132.

Shu, Q., Wong, K.K., Su, J.M., Adesina, A.M., Yu, L.T., Tsang, Y.T., Antalffy, B.C., Baxter, P., Perlaky, L., Yang, J., et al. (2008). Direct orthotopic transplantation of fresh surgical specimen preserves CD133+ tumor cells in clinically relevant mouse models of medulloblastoma and glioma. Stem Cells *26*, 1414–1424.

Taylor, M.D., Northcott, P.A., Korshunov, A., Remke, M., Cho, Y.J., Clifford, S.C., Eberhart, C.G., Parsons, D.W., Rutkowski, S., Gajjar, A., et al. (2012). Molecular subgroups of medulloblastoma: the current consensus. Acta Neuropathol. *123*, 465–472.

Whittaker, D.E., Riegman, K.L., Kasah, S., Mohan, C., Yu, T., Sala, B.P., Hebaishi, H., Caruso, A., Marques, A.C., Michetti, C., et al. (2017). The chromatin remodeling factor CHD7 controls cerebellar development by regulating reelin expression. J. Clin. Invest. *127*, 874–887.

Wu, X., Northcott, P.A., Dubuc, A., Dupuy, A.J., Shih, D.J., Witt, H., Croul, S., Bouffet, E., Fults, D.W., Eberhart, C.G., et al. (2012). Clonal selection drives genetic divergence of metastatic medulloblastoma. Nature *482*, 529–533.

Yadirgi, G., Leinster, V., Acquati, S., Bhagat, H., Shakhova, O., and Marino, S. (2011). Conditional activation of Bmi1 expression regulates self-renewal, apoptosis, and differentiation of neural stem/progenitor cells in vitro and in vivo. Stem Cells *29*, 700–712.

Zhao, X., Liu, Z., Yu, L., Zhang, Y., Baxter, P., Voicu, H., Gurusiddappa, S., Luan, J., Su, J.M., Leung, H.C., and Li, X.N. (2012). Global gene expression profiling confirms the molecular fidelity of primary tumor-based orthotopic xenograft mouse models of medulloblastoma. Neuro-oncol. *14*, 574–583.

CAPÍTULO II: Resultados Adicionais

Math1, an early marker of cerebellar granule cell progenitors, is upregulated in BMI^{high}/CHD7^{low} cells compare to control (BMI1^{high}/CHD7^{high}). Importantly, silencing of BMI1 together with CHD7 prevented Match1 upregulation, in keeping with the dramatic reduction in cell proliferation of shCHD7 cell upon concomitant BMI1 silencing (Fig. 1A,B).

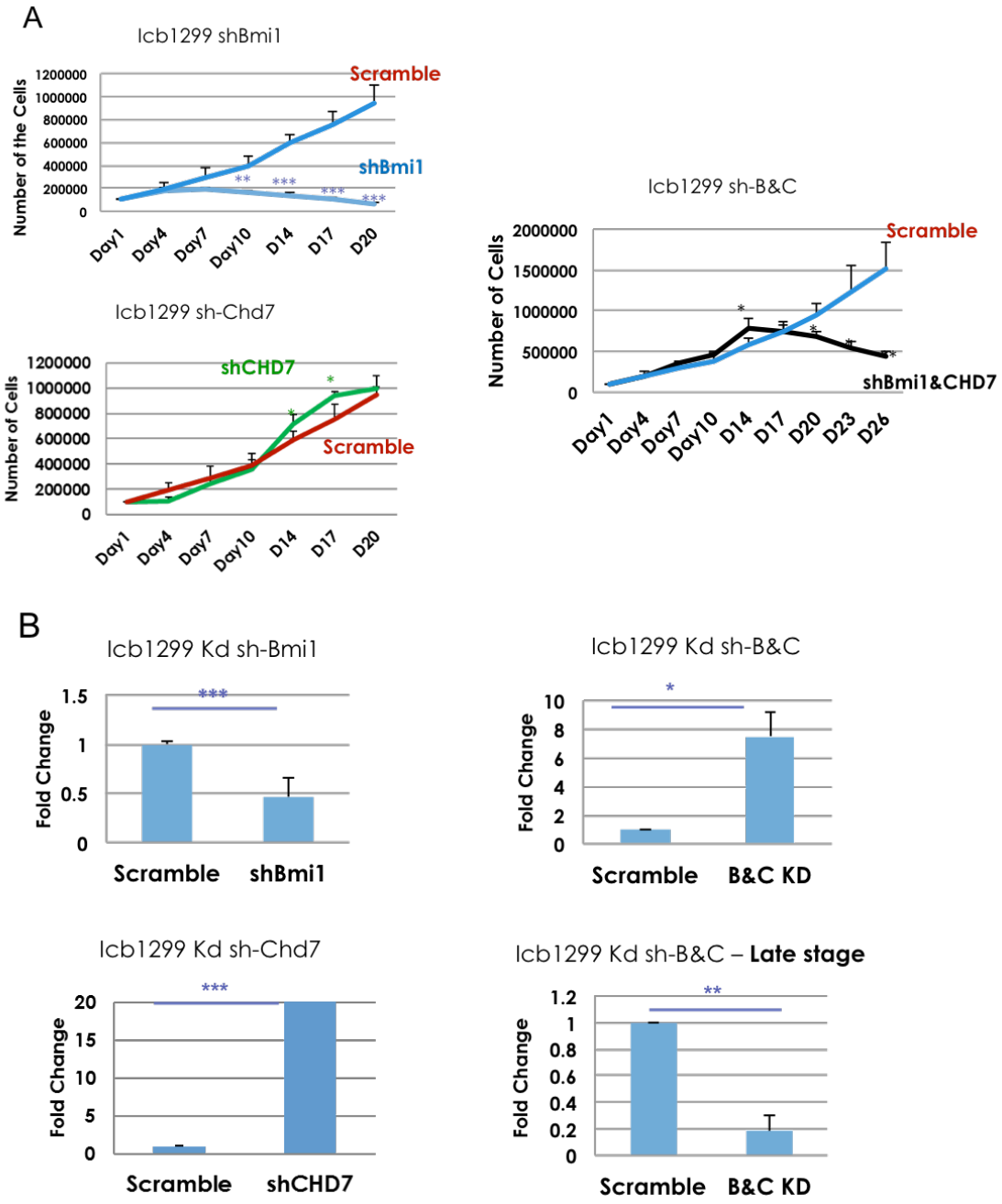

Fig. 1. Growth Curve and *Math1* expression in Icb1299 cells. Cell counting (A) and *Math1* expression (B) after puromicyn selection of silenced Icb1299 cells. *p<0.05; **p<0.01; ***p<0.001.

The protein level analysis of cells by immunocytochemistry confirmed the upregulation of Math1 (Fig.2).

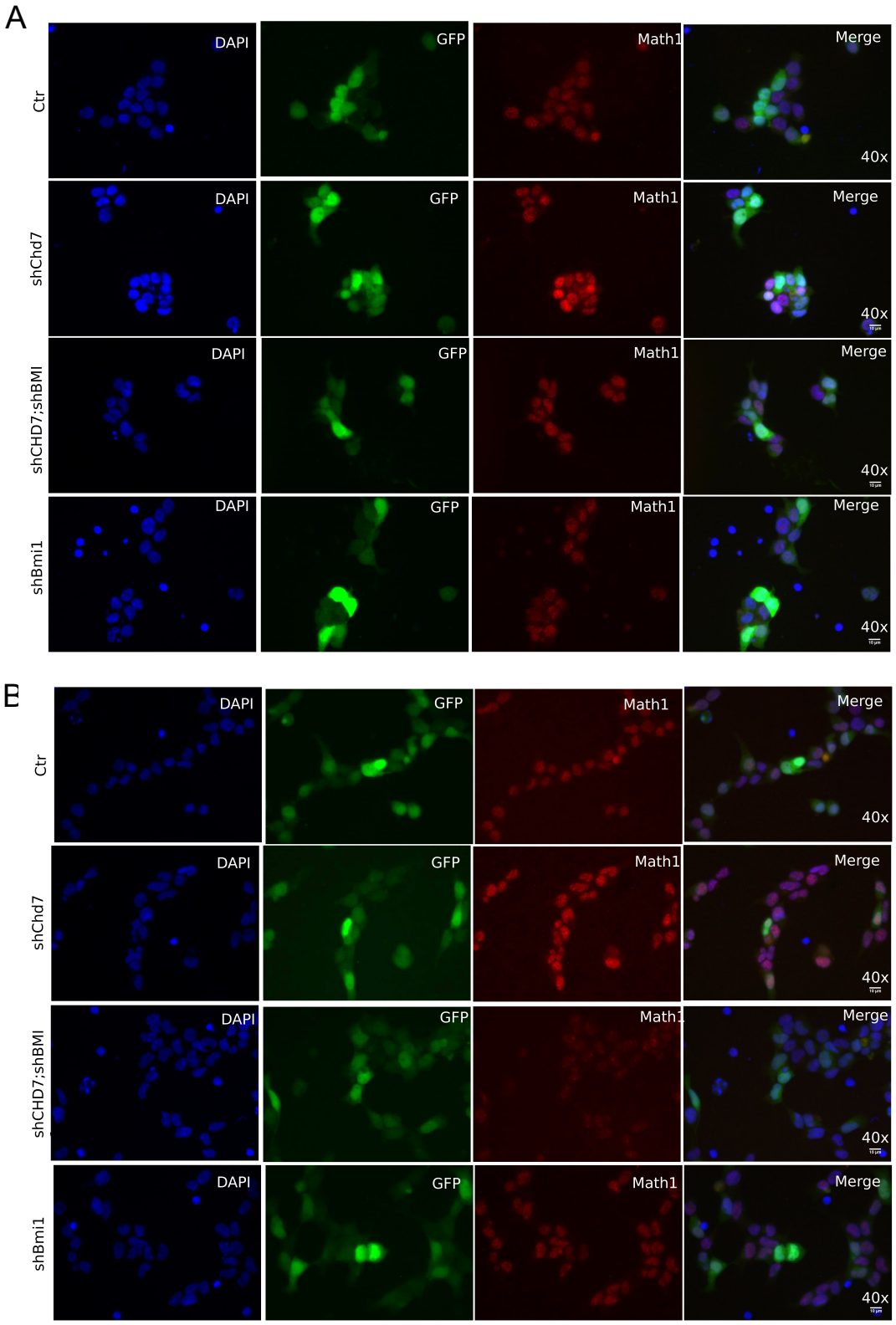

Fig. 2. Math1 protein expression in Icb1299. Math1 imunocitochemistry at 6 (A) or 15 (B) days after puromicyn selection of silenced Icb1299 cells

Expression analysis on RNA extracted from the xenografts tumors confirmed upregulation of *Math1* (Fig.3B), a finding also validated at protein level (Fig.3A).

Together, these data raise the possibility that CHD7 depletion shifts the differentiation state of G4 MB cells towards an undifferentiated pro-proliferative state, which is dependent on BMI1 overexpression.

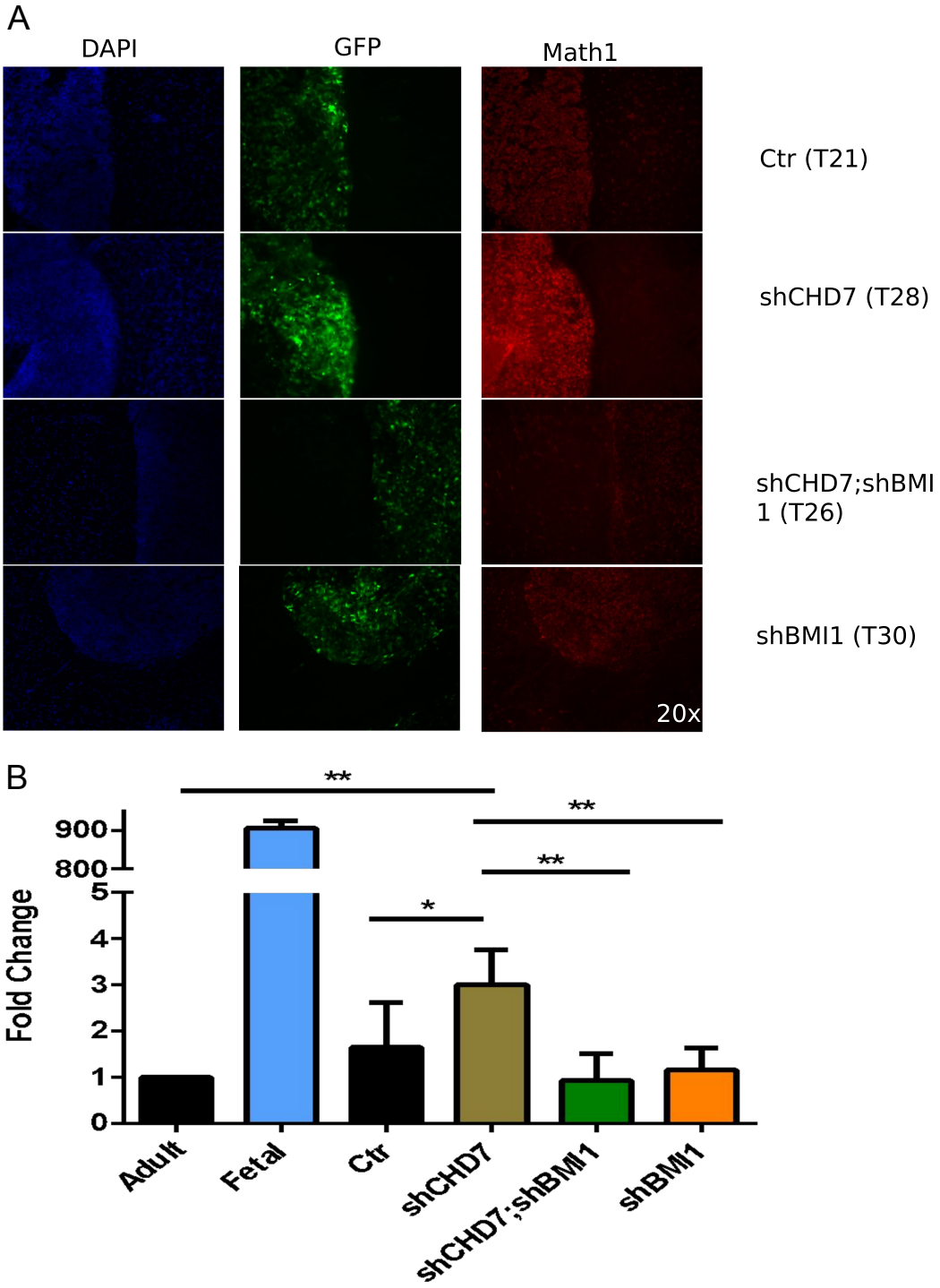

Fig. 3. Math1 levels in xenograft tumors. Protein (A) and mRNA (B) expression of Math1 in xenografts tumors of silenced Icb1299 cells *p<0.05; **p<0.01.

Additional Material & Methods

RNA extraction and qRT-PCR analysis

Cell pellets were lysed in RLT buffer from the RNeasy Micro purification kit (Qiagen). Total RNA was isolated using the same kit and the extra On-column DNase. 8-12 frozen sections of xenografts were used to extract RNA by proteinase K/acid phenol method (Khodosevich et al., 2007). Digestion was carried out to remove genomic DNA. The cDNA synthesis was carried out with SuperScript III Reverse Transcriptase Kit (Invitrogen). Analysis of gene expression was performed with the Applied Biosystems 7500 Real-Time PCR System using TaqMan gene expression assay (Thermo Fisher Scientific) according to standard protocols. Technical duplicates for each samples and $\geq$3 independently derived cultures were analyzed. The Ct values of all the genes analyzed were normalized to GAPDH and fold changes were calculated.

The primers used are listed as below:

Bmi1	Hs00180411_m1
CHD7	Hs00215010_m1
GAPDH (as housekeeping gene)	Hs02758991_g1
MATH1 (ATOH1)	Hs00245453_s1

Immunofluorescence analyses

Immunofluorescence analyses were conducted on Icb1299 cells and frozen tissue sections from xenograft tumours. Icb1299 cells, cultured on Poly-lysine (PLL) coated coverslips, were fixed using 4% PFA. Cells and freshly frozen tissue sections (xenografts fixed with

4% PFA and embedded in OCT) were treated with 10% Normal Goat Serum, followed by incubation with Math1 primary antibodies overnight at 4^{o}C (Millipore AB5692 to cells and Abcam Ab85513 to cryosections). Appropriate secondary antibody labeled with Alexa Fluor® 546 (Invitrogen) was used. The samples were counterstained with DAPI. At least 5 representative images (high power field, 40x) of each sample were captured using Leica DFC350 microscope and analyzed using Image J software.

DISCUSSÃO GERAL

Stemness é definido como o conjunto de programas moleculares que governam e mantem as propriedades de células tronco, incluindo seu estado indiferencido e capacidade de auto-renovação, e tem sido associado à uma população específica de células de câncer com potencial altamente tumorigênico, as CSC (KRESO & DICK, 2014). A manutenção do fenótipo agressivo de muitos tumores depende desses mecanismos que definem o estado celular mais indiferenciado característico de células tronco. Mecanismos epigenéticos modulam a expressão e a ativação de vias de sinalização de células tronco e podem promover *stemness* em células de câncer que são responsáveis pela formação, propagação, resistência e maior malignidade tumoral. (Lytle *et al.*, 2018; Bao *et al*., 2013). Nesse trabalho, nós demostramos que a modulação epigenética altera o fenótipo *stemness* de células de MB humano, contribuindo não só para a manutenção, mas também para a formação desse tumor.

No capítulo I, mostramos que o aumento da acetilação de histona induzida pelo inibidor de HDAC butirato de sódio altera dois mecanismos reguladores do fenótipo *stemness*: o regulador epigenético BMI1 e a via de sinalização de ERK. A redução nos níveis de BMI1 e da ativação de ERK impedem a formação de CSC e diminuem a proliferação celular em MB. No capítulo II, esses dois mecanismos aparecem envolvidos na formação de MB-Grupo 4; a alta expresssão de BMI1 combinada com um aumento na ativação da via de ERK (devida ao *background* genético $BMI^{high}/CHD7^{low}$) forma tumores com maiores taxas proliferativas e que apresentam manutenção de um estado mais indiferenciado.

A alta expressão de BMI1 e a ativação de ERK são componentes envolvidos no desenvolvimento cerebelar e na patogênese de MB. Durante o desenvolvimento cerebelar normal, BMI1 apresenta alta expressão em células indiferenciadas (Zhang et al, 2011). Como citado anteriormente nessa tese, BMI1 integra o complexo repressor PRC1 envolvido na regulação da transcrição de diferentes genes associados a células tronco neurais (BHATTACHARYA *et al*., 2015). Devido a essa regulação e sua influencia em diferentes processos relacionados a CSC, BMI1 pode ser importante para a modulação de *stemness* em células de câncer, particularmente MB (XU *et al*., 2018). De fato, CSC de

MB definidas pela expressão de marcadores de células tronco neurais como *CD133* ou pela habilidade de formarem esferas quando cultivadas em meio específico para células tronco apresentam expressão aumentada de *BMI1* (SINGH *et al.*, 2004; YU *et al.*, 2010; WANG *et al.*, 2012; MANORANJAN *et al.*, 2013). Além disso, inibição de *BMI1* em células de MB impede processos relacionados a CSC como crescimento, radioresistência e invasão (CHEN et al., 2010; VENKATARAMAN et al., 2010; MERVE *et al.*, 2014).

Apesar de essencial para a manutenção de MB, BMI1 é capaz de induzir a formação desse tumor apenas quando eventos oncogênicos adicionais ocorrem (BEHESTI *et al*., 2013). A inativação de *CHD7* pode ser um desses eventos por aumentar a ativação de ERK. CHD7 é um remodelador da cromatina altamente expresso durante o processo de diferenciação de células granulares do cerebelo que mantem a cromatina aberta para a ativação de genes envolvidos na diferenciação de neurônios, incluindo *DUSP4*, um repressor da via de ERK (FENG et al., 2017; KIM *et al.,* 2014). Mutações sem sentido ou de mudança de fase de leitura em *CHD7* foram descritas em MB do Grupo 3 e Grupo 4 (ROBINSON *et al.*, 2012). Esses dois subgrupos de MB apresentam alta frequência de metástase (Northcott et al., 2012a), capacidade associada ao aumento de expressão de membros da sinalização de ERK (MACDONALD *et al.*, 2001). Similar aos resultados desta tese, um estudo recente mostrou que inibição da sinalização de ERK diminui a proliferação de células e a formação de esferas de células de MB-SHH (Liang et al., 2018). Apesar desse trabalho não avaliar expressão de *BMI1* ou *CD133*, amplamente descritos na literatura como marcadores de *stemness*, o bloqueio de ERK reduziu a expressão de *CD271*, identificado pelos autores como marcador de CSC de MB-SHH. Inibição de ERK foi ainda capaz de reduzir invasão celular *in vitro* e aumentar sobrevida em modelo *in vivo* de MB (Liang *et al*., 2018).

Mecanismos epigenéticos podem influenciar a expressão e ativação de vias de sinalização associadas ao status *stemness* e, assim, colaborar com o crescimento e manutenção tumoral (TOH *et al.*, 2017). Nessa tese, mostramos que alterações no código de histonas, por modulação do *eraser* HDAC ou do modelador da cromatina CHD7, alteram a expressão/atividade de BMI1 e a ativação da sinalização de ERK e, assim, contribuem para fenótipo *stemness* de células de MB.

CONCLUSÃO

> "*(…), if you cure an adult with a carcinoma, we extend their median lifespan by three years, whereas if we cure a six-years-old kid with leukemia, we give them another 70-plus years.*"
>
> Peter Houghton [2]

CAPÍTULO I: A inibição de HDAC e consequente aumento na acetilação de histonas é capaz de diminuir marcadores de *stemness* de células de MB. A ativação da via de ERK contribui para esse efeito e a inibição combinada desses dois processos moduladores da capacidade *stemness* (acetilação de histonas e ativação de ERK) deve ser considerada como potencial terapia para MB.

CAPÍTULO II: MB-Grupo 4 com alterações em modificadores epigenéticos da cromatina com alta expressão de BMI1 e baixa expressão de CHD7 tem proliferação celular aumentada e manutenção da expressão do marcador de indiferenciação *Math1*. O fenótipo dessas células está relacionado com uma expressão aumentada da via de sinalização de ERK.

Os resultados apresentados nesta tese, em conjunto com o conhecimento existente e crescente da literatura, mostram que o FATOR EPIGENÉTICO BMI1 E A ATIVAÇÃO DA VIA DE SINALIZAÇÃO DE ERK, MECANISMOS ASSOCIADOS AO FENÓTIPO DE CÉLULAS INDIFERENCIADAS, SÃO RESPONSÁVEIS PELA CAPACIDADE TUMORAL DE MB e devem ser considerados potenciais alvos terapêuticos.

REFERÊNCIAS BIBLIOGRÁFICAS

Adamson PC, Houghton PJ, Perilongo G, Pritchard-Jones K (2014) Drug discovery in paediatric oncology: roadblocks to progress. Nat Rev Clin Oncol 11: 732-739.

Al-Hajj M, Wicha MS, Benito-Hernandez A, Morrison SJ, Clarke MF (2003) Prospective identification of tumorigenic breast cancer cells. Proc Natl Acad Sci U S A, 100: 3983–3988.

Allis CD, Jenuwein T (2016) The molecular hallmarks of epigenetic control. Nat Rev Genet 17: 487-500.

Annabi B, Rojas-Sutterlin S, Laflamme C, Lachambre MP, Rolland Y et al. (2008) Tumor environment dictates medulloblastoma cancer stem cell expression and invasive phenotype. Mol Cancer Res 6: 907-916.

Baccelli I, Trumpp A (2012) The evolving concept of cancer and metastasis stem cells. J Cell Biol 198: 281-293.

Bakhshinyan D, Adile AA, Venugopal C, Singh k (2017) Bmi1 – A Path to Targeting Cancer Stem Cells. Eur Oncol Haematol 13: 147-151.

Bao B, Ahmad A, Azmi AS, Ali S, Sarkar FH (2013) Cancer Stem Cells (CSCs) and Mechanisms of Their Regulation: Implications for Cancer Therapy. Current Protocols in Pharmacology. SJ Enna et al. (eds.), 0 14, Unit–14.25.

Bartlett F, Kortmann R, Saran F (2013) Medulloblastoma. Clin Oncol (R Coll Radiol) 25: 36-45.

Bautista F, Fioravante V, Rojas T, Carceller F, Madero L et al. (2017) Medulloblastoma in children and adolescents: a systematic review of contemporary phase I and II clinical trials and biology update. Cancer Med 6: 2606-2624.

Begicevic RR, Falasca M (2017) ABC transporters in cancer stem cells: beyond chemoresistance. Int J Mol Sci 18: E2362.

Behesti H, Bhagat H, Dubuc AM, Taylor MD, Marino S (2013) Bmi1 overexpression in the cerebellar granule cell lineage of mice affects cell proliferation and survival without initiating medulloblastoma formation. Dis Model Mech 6: 49-63.

Berger SL, Kouzarides T, Shiekhattar R, Shilatifard A (2009) An operational definition of epigenetics. Genes Dev 23: 781-783.

Berni Canani R, Di Costanzo M, Leone L (2012) The epigenetic effects of butyrate: potential therapeutic implications for clinical practice. Clin Epigenetics 4: 4.

Bhattacharya R, Mustafi SB, Street M, Dey A, Dwivedi SK (2015) Bmi-1: at the crossroads of physiological and pathological biology. Gene Dis 2:225-239.

Biswas S, Rao CM (2017) Epigenetics in cancer: Fundamentals and Beyond. Pharmacol Ther 173: 118-134.

Blank M (2015) Regulação epigenética na formação da memória aversiva : modulação via inibidores de histona desacetilases. 130 pp. Tese de Doutorado apresentada ao Programa de Pós-Graduação em Biologia Celular e Molecular - Universidade Federal do Rio Grande do Sul. Porto Alegre.

Bolden JE, Peart MJ, Johnstone RW (2006) Anticancer activities of histone deacetylase inhibitors. Nat Rev Drug Discov 5: 769-784.

Bommi PV, Dimri M, Sahasrabuddhe AA, Khandekar JD, Dimri GP (2010) The polycomb group protein BMI1 is a transcriptional target of HDAC inhibitors. Cell Cycle 9: 2663-2673.

Bracken AP, Kleine-Kohlbrecher D, Dietrich N, Pasini D, Gargiulo G et al. (2007) The Polycomb group proteins bind throughout the INK4A-ARF locus and are disassociated in senescent cells. Genes Dev 21: 525-530.

Brien GL, Valerio DG, Armstrong SA (2016) Exploiting the Epigenome to Control Cancer-Promoting Gene-Expression Programs. Cancer Cell 29: 464-476.

Bruggeman SW, Hulsman D, Tanger E, Buckle T, Blom M et al. (2007) Bmi1 controls tumor development in an Ink4a/Arf-independent manner in a mouse model for glioma. Cancer Cell 12: 328-341.

Cao R, Tsukada Y, Zhang Y (2005) Role of Bmi-1 and Ring1A in H2A ubiquitylation and Hox gene silencing. Mol Cell. 20: 845-854.

Cavalli FMG, Remke M, Rampasek L, Peacock J, Shih DJH et al. (2017) Intertumoral Heterogeneity within Medulloblastoma Subgroups. Cancer Cell 31: 737-754 e736.

Chang CJ1, Chiang CH, Song WS, Tsai SK, Woung LC et al. (2012) Inhibition of phosphorylated STAT3 by cucurbitacin I enhances chemoradiosensitivity in medulloblastoma-derived cancer stem cells. Childs Nerv Syst 28:363-373.

Chen KH, Hsu CC, Song WS, Huang CS, Tsai CC et al. (2010) Celecoxib enhances radiosensitivity in medulloblastoma-derived CD133-positive cells. Childs Nerv Syst 26: 1605-1612.

Chow KH, Shin DM, Jenkins MH, Miller EE, Shih DJ et al. (2014) Epigenetic states of cells of origin and tumor evolution drive tumor-initiating cell phenotype and tumor heterogeneity. Cancer Res 74: 4864-4874.

Cohen I, Poreba E, Kamieniarz K, Schneider R (2011) Histone modifiers in cancer: friends or foes? Genes Cancer 2: 631-647.

Cojoc M, Mäbert K, Muders MH, Dubrovska A (2015) A role for cancer stem cells in therapy resistance: cellular and molecular mechanisms. Semin Cancer Biol 31:16-27.

Collins AT, Berry PA, Hyde C, Stower MJ, Maitland NJ (2005)Prospective identification of tumorigenic prostate cancer stem cells. Cancer Res 65:10946-10951.

de Robles P, Fiest KM, Frolkis AD, Pringsheim T, Atta C et al. (2015) The worldwide incidence and prevalence of primary brain tumors: a systematic review and meta-analysis. Neuro Oncol 17: 776-783.

Delcuve GP, Khan DH, Davie JR (2012) Roles of histone deacetylases in epigenetic regulation: emerging paradigms from studies with inhibitors. Clin Epigenetics 4: 5.

Di Cerbo V, Schneider R (2013) Cancers with wrong HATs: the impact of acetylation. Brief Funct Genomics 12: 231-243.

Downing JR, Wilson RK, Zhang J, Mardis ER, Pui CH et al. (2012) The Pediatric Cancer Genome Project. Nat Genet 44: 619-622.

Eckschlager T, Plch J, Stiborova M, Hrabeta J (2017) Histone Deacetylase Inhibitors as Anticancer Drugs. Int J Mol Sci 18.

Ellison DW, Onilude OE, Lindsey JC, Lusher ME, Weston CL et al. (2005) beta-Catenin status predicts a favorable outcome in childhood medulloblastoma: the United Kingdom Children's Cancer Study Group Brain Tumour Committee. J Clin Oncol 23: 7951-7957.

Eramo A, Lotti F, Sette G, Pilozzi E, Biffoni M et al. (2008) Identification and expansion of the tumorigenic lung cancer stem cell population. Cell Death Differ 15: 504-514.

Fairley L, Picton SV, McNally RJ, Bailey S, McCabe MG et al. (2016) Incidence and survival of children and young people with central nervous system embryonal tumours in the North of England, 1990-2013. Eur J Cancer 61: 36-43.

Fang D, Nguyen TK, Leishear K, Finko R, Kulp AN et al. (2005) A tumorigenic subpopulation with stem cell properties in melanomas. Cancer Res 65:9328-9337.

Feng W, Kawauchi D, Körkel-Qu H, Deng H, Serger E et al. (2017) Chd7 is indispensable for mammalian brain development through activation of a neuronal differentiation programme. Nat Commun 8: 14758.

Fraga MF, Ballestar E, Villar-Garea A, Boix-Chornet M, Espada J et al. (2005) Loss of acetylation at Lys16 and trimethylation at Lys20 of histone H4 is a common hallmark of human cancer. Nat Genet 37: 391-400.

Frumm SM, Fan ZP, Ross KN, Duvall JR, Gupta S et al. (2013) Selective HDAC1/HDAC2 inhibitors induce neuroblastoma differentiation. Chem Biol 20: 713-725.

Genua MI, Giraldez J, Rocha E, Monge A (1980) Effects of antibiotics on platelet functions in human plasma in vitro and dog plasma in vivo. J Pharm Sci 69: 1282-1284.

Glinsky GV, Berezovska O, Glinskii AB (2005) Microarray analysis identifies a death-from-cancer signature predicting therapy failure in patients with multiple types of cancer. J Clin Invest 115: 1503-1521.

Gong C, Valduga J, Chateau A, Richard M, Pellegrini-Moïse N et al. (2018) Stimulation of medulloblastoma stem cells differentiation by a peptidomimetic targeting neuropilin-1. Oncotarget 9: 15312-15325.

Gottlicher M, Minucci S, Zhu P, Kramer OH, Schimpf A et al. (2001) Valproic acid defines a novel class of HDAC inhibitors inducing differentiation of transformed cells. EMBO J 20: 6969-6978.

Grob ST, Levy JMM (2018) Improving Diagnostic and Therapeutic Outcomes in Pediatric Brain Tumors. Mol Diagn Ther 22: 25-39.

Hemmati HD, Nakano I, Lazareff JA, Masterman-Smith M, Geschwind DH et al. (2003) Cancerous stem cells can arise from pediatric brain tumors. Proc Natl Acad Sci U S A 100: 15178-15183.

Holgado BL, Guerreiro Stucklin A, Garzia L, Daniels C, Taylor MD (2017) Tailoring Medulloblastoma Treatment Through Genomics: Making a Change, One Subgroup at a Time. Annu Rev Genomics Hum Genet 18: 143-166.

Huang GH, Xu QF, Cui YH, Li N, Bian XW et al. (2016) Medulloblastoma stem cells: Promising targets in medulloblastoma therapy. Cancer Sci 107: 583-589.

Huether R., Dong L, Chen X, Wu G, Parker M, et al. (2014) The landscape of somatic mutations in epigenetic regulators across 1,000 paediatric cancer genomes. Nat Commun 8: 3630.

INCA (Insituto Nacional do Câncer José Alencar Gomes da Silva / Coordenação de Prevenção e Vigilância) (2015) Estimativa 2016: incidência de câncer no Brasil / Instituto Nacional de Câncer José Alencar Gomes da Silva. Rio de Janeiro: INCA.

Ingram WJ, Crowther LM, Little EB, Freeman R, Harliwong I et al. (2013) ABC transporter activity linked to radiation resistance and molecular subtype in pediatric medulloblastoma. Exp Hematol Oncol 2: 26.

Jacobs JJ, Kieboom K, Marino S, DePinho RA, van Lohuizen M (1999) The oncogene and Polycomb-group gene bmi-1 regulates cell proliferation and senescence through the ink4a locus. Nature 397: 164-168.

Jenuwein T, Allis CD (2001) Translating the histone code. Science 293: 1074-1080.

Johnstone RW (2002) Histone-deacetylase inhibitors: novel drugs for the treatment of cancer. Nat Rev Drug Discov 1: 287-299.

Kenney AM, Rowitch DH (2000) Sonic hedgehog promotes G(1) cyclin expression and sustained cell cycle progression in mammalian neuronal precursors. Mol Cell Biol 20: 9055-9067.

Khanna V, Achey RL, Ostrom QT, Block-Beach H, Kruchko C et al. (2017) Incidence and survival trends for medulloblastomas in the United States from 2001 to 2013. J Neurooncol 135: 433-441.

Kim SY, Han YM, Oh M, Kim WK, Oh KJ et al. (2015) DUSP4 regulates neuronal differentiation and calcium homeostasis by modulating ERK1/2 phosphorylation. Stem Cells Dev 24: 686-700.

Kimura A, Matsubara K, Horikoshi M (2005) A decade of histone acetylation: marking eukaryotic chromosomes with specific codes. J Biochem 138: 647-662.

Kool M, Korshunov A, Remke M, Jones DT, Schlanstein M et al. (2012) Molecular subgroups of medulloblastoma: an international meta-analysis of transcriptome, genetic aberrations, and clinical data of WNT, SHH, Group 3, and Group 4 medulloblastomas. Acta Neuropathol 123: 473-484.

Kouzarides T (2007) Chromatin modifications and their function. Cell 128: 693-705.

67. Kreso A, Dick JE (2014). Evolution of the cancer stem cell model. Cell Stem Cell 14: 275-291.

Kretsovali A, Hadjimichael C, Charmpilas N (2012) Histone deacetylase inhibitors in cell pluripotency, differentiation, and reprogramming. Stem Cells Int 2012: 184154.

Lapidot T, Sirard C, Vormoor J, Murdoch B, Hoang T et al. (1994) A cell initiating human acute myeloid leukaemia after transplantation into SCID mice. Nature 367: 645–648.

Lawson DA, Bhakta NR, Kessenbrock K, Prummel KD, Yu Y et al. (2015) Single-cell analysis reveals a stem-cell program in human metastatic breast cancer cells. Nature 526: 131–135.

Lee KK, Workman JL (2007) Histone acetyltransferase complexes: one size doesn't fit all. Nat Rev Mol Cell Biol 8: 284-295.

Leece R, Xu J, Ostrom QT, Chen Y, Kruchko C et al. (2017) Global incidence of malignant brain and other central nervous system tumors by histology, 2003-2007. Neuro Oncol 19: 1553-1564.

Leung C, Lingbeek M, Shakhova O, Liu J, Tanger E et al. (2004) Bmi1 is essential for cerebellar development and is overexpressed in human medulloblastomas. Nature 428: 337-341.

Li XN, Parikh S, Shu Q, Jung HL, Chow CW et al. (2004) Phenylbutyrate and phenylacetate induce differentiation and inhibit proliferation of human medulloblastoma cells. Clin Cancer Res 10: 1150-1159.

Li Z, Cao R, Wang M, Myers MP, Zhang Y et al. (2006) Structure of a Bmi-1-Ring1B polycomb group ubiquitin ligase complex. J Biol Chem 281: 20643–20649.
Li C, Heidt DG, Dalerba P, Burant CF, Zhang L et al (2007) Identification of pancreatic cancer stem cells. Cancer Res 67:1030-1037.

Li DW, Tang HM, Fan JW, Yan DW, Zhou CZ et al. (2010) Expression level of Bmi-1 oncoprotein is associated with progression and prognosis in colon cancer. J Cancer Res Clin Oncol 136: 997-1006.

Li Y, Laterra J (2012) Cancer stem cells: distinct entities or dynamically regulated phenotypes?. Cancer Res 72: 576-580.

Li X, Yang Z, Song W, Zhou L, Li Q et al. (2013) Overexpression of Bmi-1 contributes to the invasion and metastasis of hepatocellular carcinoma by increasing the expression of matrix metalloproteinase (MMP)-2, MMP-9 and vascular endothelial growth factor via the PTEN/PI3K/Akt pathway. Int J Oncol 43: 793-902.

Liang L, Coudière-Morrison L, Tatari N, Stromecki M, Fresnoza A et al. (2018) $CD271^{+}$ Cells are diagnostic and prognostic and exhibit elevated MAPK activity in SHH medulloblastoma. Cancer Res 78: 4745-4759.

Louis DN, Ohgaki H, Wiestler OD, Cavenee WK, Burger PC et al. (2007) The 2007 WHO classification of tumours of the central nervous system. Acta Neuropathol 114: 97-109.

Louis DN, Perry A, Reifenberger G, von Deimling A, Figarella-Branger D et al. (2016) The 2016 World Health Organization classification of tumors of the central nervous system: a summary. Acta Neuropathol 131: 803-820.

Luger K, Dechassa ML, Tremethick DJ (2012) New insights into nucleosome and chromatin structure: an ordered state or a disordered affair? Nat Rev Mol Cell Biol 13: 436-447.

Lytle NK, Barber AG, Reya T (2018) Stem cell fate in cancer growth, progression and therapy resistance. Nat Rev Cancer doi: 10.1038/s41568-018-0056-x .

Ma S, Chan KW, Hu L, Lee TKW, Wo JYH et al. (2007) Identification and characterization of tumorigenic liver cancer stem/progenitor cells. Gastroenterology 132:2542-2556.

MacDonald TJ, Brown KM, LaFleur B, Peterson K, Lawlor C et al. (2001) Expression profiling of medulloblastoma: PDGFRA and the RAS/MAPK pathway as therapeutic targets for metastatic disease. Nat Genet 29: 143-152.

Manoranjan B, Wang X, Hallett RM, Venugopal C, Mack SC et al. (2013) FoxG1 interacts with Bmi1 to regulate self-renewal and tumorigenicity of medulloblastoma stem cells. Stem Cells 31: 1266-1277.

Marks PA, Richon VM, Rifkind RA (2000) Histone deacetylase inhibitors: inducers of differentiation or apoptosis of transformed cells. J Natl Cancer Inst 92: 1210-1216.

Merve A, Dubuc AM, Zhang X, Remke M, Baxter PA et al. (2014) Polycomb group gene BMI1 controls invasion of medulloblastoma cells and inhibits BMP-regulated cell adhesion. Acta Neuropathol Commun 2: 10.

Michael LE, Westerman BA, Ermilov AN, Wang A, Ferris J et al. (2008) Bmi1 is required for Hedgehog pathway-driven medulloblastoma expansion. Neoplasia 10: 1343-1349.

Milde T, Oehme I, Korshunov A, Kopp-Schneider A, Remke M et al. (2010) HDAC5 and HDAC9 in medulloblastoma: novel markers for risk stratification and role in tumor cell growth. Clin Cancer Res 16: 3240-3252.

Millard NE, De Braganca KC (2016) Medulloblastoma. J Child Neurol 31: 1341-1353.

Mitra A, Mishra L, Li S (2015) EMT, CTCs and CSCs in tumor relapse and drug-resistance. Oncotarget 6:10697-10711.

Munster PN, Troso-Sandoval T, Rosen N, Rifkind R, Marks PA et al. (2001) The histone deacetylase inhibitor suberoylanilide hydroxamic acid induces differentiation of human breast cancer cells. Cancer Res 61: 8492-8497.

Nightingale KP, Gendreizig S, White DA, Bradbury C, Hollfelder F et al. (2007) Cross-talk between histone modifications in response to histone deacetylase inhibitors. J Biol Chem 282: 4408-4418.

Nör C, Sassi FA, Farias CB, Schartsmann G, Abujamra AL et al. (2013) The histone deacetylase inhibitor sodium butyrate promotes cell death and differentiation and reduces neurosphere formation in human medulloblastoma cells. Mol Neurobiol 48: 533-543.

Northcott PA, Buchhalter I, Morrissy AS, Hovestadt V, Weischenfeldt J et al. (2017) The whole-genome landscape of medulloblastoma subtypes. Nature 547: 311-317.

Northcott PA, Korshunov A, Pfister SM, Taylor MD (2012a) The clinical implications of medulloblastoma subgroups. Nat Rev Neurol 8: 340-351.

Northcott PA, Shih DJ, Peacock J, Garzia L, Morrissy AS et al. (2012b) Subgroup-specific structural variation across 1,000 medulloblastoma genomes. Nature 488: 49-56.

O'Brien CA, Pollett A, Gallinger S, Dick JE (2006). A human colon cancer cell capable of initiating tumour growth in immunodeficient mice. Nature 445: 106-110.

Packer RJ, Zhou T, Holmes E, Vezina G, Gajjar A (2013) Survival and secondary tumors in children with medulloblastoma receiving radiotherapy and adjuvant chemotherapy: results of Children's Oncology Group trial A9961. Neuro Oncol 15: 97-103.

Peitzsch C, Tyutyunnykova A, Pantel K, Dubrovska A (2017) Cancer stem cells: the root of tumor recurrence and metastases. Semin Cancer Biol 44: 10-24.

Phillips DM (1963) The presence of acetyl groups of histones. Biochem J 87: 258-263.

Pickles JC, Howkins C, Pietsch T, Jacques TS (2018) CNS embryonal tumours: WHO 2016 and beyond. Neuropathol Appl Neurobiol 44: 151-162.

Prasetyanti PR, Medema JP (2017) Intra-tumor heterogeneity from a cancer stem cell perspective. Mol Cancer 16: 41.

Qureshi IA, Mehler MF (2013) Understanding neurological disease mechanisms in the era of epigenetics. JAMA Neurol 70: 703-710.

Ramaswamy V, Taylor MD (2017) Medulloblastoma: from myth to molecular. J Clin Oncol 35: 2355-2363.

Reya T, Morison SJ, Clarke MF, Weissman IL (2001) Stem cells, cancer, and cancer stem cells. Nature 414: 105-111.

Robinson G, Parker M, Kranenburg TA, Lu C, Chen X et al. (2012) Novel mutations target distinct subgroups of medulloblastoma. Nature 488: 43-48.

Roth SY, Denu JM, Allis CD (2001) Histone acetyltransferases. Annu Rev Biochem 70: 81-120.

Sauvageau M, Sauvageau G (2010) Polycomb group proteins: multi-faceted regulators of somatic stem cells and cancer. Cell Stem Cell 7: 299-313.

Schneider A, Chatterjee S, Bousiges O, Selvi BR, Swaminathan A et al. (2013) Acetyltransferases (HATs) as targets for neurological therapeutics. Neurotherapeutics 10: 568-588.

Schwalbe EC, Lindsey JC, Nakjang S, Crosier S, Smith AJ et al. (2017) Novel molecular subgroups for clinical classification and outcome prediction in childhood medulloblastoma: a cohort study. Lancet Oncol 18: 958-971.

Seto E, Yoshida M (2014) Erasers of histone acetylation: the histone deacetylase enzymes. Cold Spring Harb Perspect Biol 6: a018713.

Sharma S, Kelly TK, Jones PA (2010) Epigenetics in cancer. Carcinogenesis 31: 27-36.

Shiozawa Y, Nie B, Pienta KJ, Morgan TM, Taichman RS (2013) Cancer stem cells and their role in metastasis. Pharmacol Ther 138:285-293.

Simon JA, Kingston RE (2009) Mechanisms of polycomb gene silencing: knowns and unknowns. Nat Rev Mol Cell Biol 10: 697-708.

Singh SK, Clarke ID, Terasaki M, Bonn VE, Hawkins C et al. (2003) Identification of a cancer stem cell in human brain tumors. Cancer Res 63:5821-5828.

Singh SK, Hawkins C, Clarke ID, Squire JA, Bayani J et al. (2004) Identification of human brain tumour initiating cells. Nature 432: 396-401.

Souza BK, Lopez PLC, Menegotto PR, Vieira IA, Kersting N et al. (2018) Targeting histone deacetylase activity to arrest cell growth and promote neural differentiation in Ewing sarcoma. Mol Neurobiol 55: 7242:7258.

Steliarova-Foucher E, Colombet M, Ries LAG, Moreno F, Dolya A et al. (2017) International incidence of childhood cancer, 2001-10: a population-based registry study. Lancet Oncol 18: 719-731.

Strahl BD, Allis CD (2000) The language of covalent histone modifications. Nature 403: 41-45.

Su J, Wu S, Tang W, Qian H, Zhou H et al. (2016) Reduced SLC27A2 induces cisplatin resistance in lung cancer stem cells by negatively regulating Bmi1-ABCG2 signaling. Mol Carcinog 55: 1822-1832.

Sutter R, Shakhova O, Bhagat H, Behesti H, Sutter C et al. (2010) Cerebellar stem cells act as medulloblastoma-initiating cells in a mouse model and a neural stem cell signature characterizes a subset of human medulloblastomas. Oncogene 29: 1845-1856.

Taylor MD, Northcott PA, Korshunov A, Remke M, Cho YJ et al. (2012) Molecular subgroups of medulloblastoma: the current consensus. Acta Neuropathol 123: 465-472.

Toh TB, Lim JJ, Chow EK (2017) Epigenetics in cancer stem cells. Mol Cancer 16: 29.

Tulla M, Berthold F, Graf N, Rutkowski S, von Schweinitz D et al. (2015) Incidence, Trends, and Survival of Children With Embryonal Tumors. Pediatrics 136: e623-632.

Turner BM (2002) Cellular memory and the histone code. Cell 111: 285-291.

Venkataraman S, Alimova I, Fan R, Harris P, Foreman N et al. (2010) MicroRNA 128a increases intracellular ROS level by targeting Bmi-1 and inhibits medulloblastoma cancer cell growth by promoting senescence. PLoS One 5:e10748.

Wang JY, Del Valle L, Gordon J, Rubini M, Romano G et al. (2001) Activation of the IGF-IR system contributes to malignant growth of human and mouse medulloblastomas. Oncogene 20: 3857-3868.

Wang E, Bhattacharyya S, Szabolcs A, Rodriguez-Aguayo C, Jennings NB et al. (2011) Enhancing chemotherapy response with Bmi-1 silencing in ovarian cancer. PLoS One 6: e17918.

Wang X, Venugopal C, Manoranjan B, McFarlane N, O'Farrell E et al. (2012) Sonic hedgehog regulates Bmi1 in human medulloblastoma brain tumor-initiating cells. Oncogene 31: 187-199.

Wang LT, Liou JP, Li YH, Liu YM, Pan SL et al. (2014) A novel class I HDAC inhibitor, MPT0G030, induces cell apoptosis and differentiation in human colorectal cancer cells via HDAC1/PKCdelta and E-cadherin. Oncotarget 5: 5651-5662.

Wang MC, Li CL, Cui J, Jiao M, Wu T (2015) BMI-1, a promising therapeutic target for human cancer. Oncol Lett 10: 583-588.

West AC, Johnstone RW (2014) New and emerging HDAC inhibitors for cancer treatment. J Clin Invest 124: 30-39.

Witt O, Deubzer HE, Milde T, Oehme I (2009) HDAC family: What are the cancer relevant targets? Cancer Lett 277: 8-21.

Włodarski P, Grajkowska W, Łojek M, Rainko K, Jóźwiak J (2006) Activation of Akt and Erk pathways in medulloblastoma. Folia Neuropathol 44:214-220.

Xu X, Wang Z, Liu N, Zhang P, Liu H et al. (2018) The mechanism of BMI1 in regulating cancer stemness maintenance, metastasis, chemo- and radiation resistance. Cancer Transl Med 4: 59-63.

Yadirgi G, Leinster V, Acquati S, Bhagat H, Shakhova O et al. (2011). Conditional activation of Bmi1 expression regulates self-renewal, apoptosis, and differentiation of neural stem/progenitor cells in vitro and in vivo. Stem Cells 29: 700-712.

Yang MH, Hsu DS, Wang HW, Wang HJ, Lan HY et al. (2010) Bmi1 is essential in Twist1-induced epithelial-mesenchymal transition. Nat Cell Biol 12: 982-992.

Yu CC, Chiou GY, Lee YY, Chang YL, Huang PI et al. (2010) Medulloblastoma-derived tumor stem-like cells acquired resistance to TRAIL-induced apoptosis and radiosensitivity. Childs Nerv Syst 26: 897-904.

Yuan L, Santi M, Rushing EJ, Cornelison R, MacDonald TJ (2010) ERK activation of p21 activated kinase-1 (Pak1) is critical for medulloblastoma cell migration. Clin Exp Metastasis 27: 481-491.

Zakrzewska M, Zakrzewski K, Grešner SM, Piaskowski S, Zalewska-Szewczyk B et al. (2011) Polycomb genes expression as a predictor of poor clinical outcome in children with medulloblastoma. Childs Nerv Syst 27: 79-86.

Zhang S, Balch C, Chan MW, Lai HC, Matei D et al. (2008) Identification and characterization of ovarian cancer-initiating cells from primary human tumors. Cancer Res 68: 4311-4320.

Zhang X, Santuccione A, Leung C, Marino S (2011) Differentiation of postnatal cerebellar glial progenitors is controlled by Bmi1 through BMP pathway inhibition. Glia 59: 1118-1131.

Zhukova N, Ramaswamy V, Remke M, Pfaff E, Shih DJ et al. (2013) Subgroup-specific prognostic implications of TP53 mutation in medulloblastoma. J Clin Oncol 31: 2927-2935.

REFERÊNCIAS CITAÇÕES

[1] Children in the New Millennium; Environmental Impact on Health. UNEP/UNICEF/WHO (2002) (www.who.int/water_sanitation_health/hygiene/settings/millennium/en/). Acesso em: 21 de setembro de 2018. Disponível em: <http://www.who.int/ceh/capacity/Children_are_not_little_adults.pdf>.

[2] Morgan B (2011) The search for child cancer drugs grows up. Nat Med 17: 267.